

2  
DTIC FILE COPY



Defense Nuclear Agency  
Alexandria, VA 22310-3398



DNA-TR-89-242

## Electron Spin Resonance and Radiation Effects in MOS Devices

P. M. Lenahan  
M. A. Jupina  
Pennsylvania State University  
Department of Engineering Science & Mechanics  
133 Hammond Building  
University Park, PA 16802

October 1990

Technical Report

DTIC  
S E L E C T E D  
OCT 30 1990  
S B D  
fb

CONTRACT No. DNA 001-86-C-0055

Approved for public release;  
distribution is unlimited.

90 10 33 08 9

Destroy this report when it is no longer needed. Do not return to sender.

PLEASE NOTIFY THE DEFENSE NUCLEAR AGENCY,  
ATTN: CSTI, 6801 TELEGRAPH ROAD, ALEXANDRIA, VA  
22310-3398, IF YOUR ADDRESS IS INCORRECT, IF YOU  
WISH IT DELETED FROM THE DISTRIBUTION LIST, OR  
IF THE ADDRESSEE IS NO LONGER EMPLOYED BY YOUR  
ORGANIZATION.



REPORT DOCUMENTATION PAGE			Form Approved OMB No. 0704-0188
<p>Public reporting burden for this collection of information is estimated to average 1 hour per response, including the time for reviewing instructions, searching existing data sources, gathering and maintaining the data needed, and completing and reviewing the collection of information. Send comments regarding this burden estimate or any other aspect of this collection of information, including suggestions for reducing this burden, to Washington Headquarters Services, Directorate for Information Operations and Reports, 1215 Jefferson Davis Highway Suite 1204 Arlington VA 22202 4302 and to the Office of Management and Budget, Paperwork Reduction Project (0704 0188) Washington, DC 20503</p>			
1. AGENCY USE ONLY (Leave blank)	2. REPORT DATE	3. REPORT TYPE AND DATES COVERED	
	901001	Technical	860601 to 890630
4. TITLE AND SUBTITLE		5. FUNDING NUMBERS	
Electron Spin Resonance and Radiation Effects in MOS Devices		C - DNA 001-86-C-0055 PE - 62715H PR - RV TA - RA WU - DH012430	
6. AUTHOR(S)			
P.M. Lenahan and M.A. Jupina			
7. PERFORMING ORGANIZATION NAME(S) AND ADDRESS(ES)		8. PERFORMING ORGANIZATION REPORT NUMBER	
Pennsylvania State University Department of Engineering Science & Mechanics 133 Hammond Building University Park, PA 16802			
9. SPONSORING/MONITORING AGENCY NAME(S) AND ADDRESS(ES)		10. SPONSORING/MONITORING AGENCY REPORT NUMBER	
Defense Nuclear Agency 6801 Telegraph Road Alexandria, VA 22310-3398 RAEE/Cohn		DNA-TR-89-242	
11. SUPPLEMENTARY NOTES This work was sponsored by the Defense Nuclear Agency under RDT&E RMC Code B3230864662 RV RA 00141 25904D.			
12a. DISTRIBUTION/AVAILABILITY STATEMENT		12b. DISTRIBUTION CODE	
Approved for public release; distribution is unlimited.		explored were	
13. ABSTRACT (Maximum 200 words)			
<p>For the past 3 years we have explored the basic mechanisms of radiation damage in metal/oxide/silicon (MOS) field effect transistors (MOSFET's) with a combination of electron spin resonance (ESR) and electrical measurements. The major focus of our work has been to develop a new and much more sensitive ESR technique called spin dependent recombination (SDR) to study radiation damage in MOSFET's.</p> <p><i>Keywords: Metal oxide semiconductors; Field effect transistors; Electron spin resonance; Radiation effects. (RH)</i></p>			
14. SUBJECT TERMS		15. NUMBER OF PAGES	
Spin Dependent Recombination (SDR) Metal-Oxide-Semiconductor Field-Effect Transistors (MOSFET's)		88	
		16. PRICE CODE	
17. SECURITY CLASSIFICATION OF REPORT		18. SECURITY CLASSIFICATION OF THIS PAGE	
UNCLASSIFIED		UNCLASSIFIED	
19. SECURITY CLASSIFICATION OF ABSTRACT		20. LIMITATION OF ABSTRACT	
UNCLASSIFIED		SAR	

UNCLASSIFIED

SECURITY CLASSIFICATION OF THIS PAGE

CLASSIFIED BY

N/A since Unclassified.

DECLASSIFY ON

N/A since Unclassified.

14. SUBJECT TERMS (Continued)

P<sub>b</sub> Center

Electron Spin Resonance (ESR)

Accession For	
NTIS	GRA&I <input checked="" type="checkbox"/>
DTIC TAB	<input type="checkbox"/>
Unannounced	<input type="checkbox"/>
Justification	
By _____	
Distribution/	
Availability Codes	
Dist	Avail and/or Special
1	



SECURITY CLASSIFICATION OF THIS PAGE

## CONVERSION TABLE

Conversion factors for U.S. Customary to metric (SI) units of measurement

MULTIPLY TO GET	BY	TO GET DIVIDE
angstrom	1.000 000 X E -10	meters (m)
atmosphere (normal)	1.013 25 X E +2	kilo pascal (kPa)
bar	1.000 000 X E +2	kilo pascal (kPa)
barn	1.000 000 X E -28	meter <sup>2</sup> (m <sup>2</sup> )
British thermal unit (thermochemical)	1.054 350 X E +3	joule (J)
calorie (thermochemical)	4.194 000	joule (J)
cal (thermochemical)/cm <sup>2</sup>	4.184 000 X E -2	mega joule/m <sup>2</sup> (MJ/m <sup>2</sup> )
curie	3.100 000 X E +1	giga becquerel (GBq)
degree (angle)	1.745 329 X E -2	radian (rad)
degree Fahrenheit	$t_K = (t^{\circ}F + 459.67)/1.8$	degree kelvin (K)
electron volt	1.602 19 X E -1	joule (J)
erg	1.000 000 X E -7	joule (J)
erg/second	1.000 000 X E -7	watt (W)
foot	3.048 000 X E -1	meter (m)
foot-pound-force	1.355 818	joule (J)
gallon (U. S. liquid)	3.785 412 X E -3	meter <sup>3</sup> (m <sup>3</sup> )
inch	2.540 000 X E -2	meter (m)
jerk	1.000 000 X E +9	joule (J)
joule/kilogram (J/kg) (radiation dose absorbed)	1.000 000	Gray (Gy)
kilotons	4.183	terajoules
kip (1000 lbf)	4.448 222 X E +3	newton (N)
kip/inch <sup>2</sup> (ksi)	6.894 757 X E +3	kilo pascal (kPa)
kip	1.000 000 X E +2	newton-second/m <sup>2</sup> (N-s/m <sup>2</sup> )
micron	1.000 000 X E -6	meter (m)
mil	2.540 000 X E -5	meter (m)
mile (international)	1.609 344 X E +3	meter (m)
ounce	2.834 952 X E -2	kilogram (kg)
pound-force (lbs avoirdupois)	4.448 222	newton (N)
pound-force inch	1.129 848 X E -1	newton-meter (N·m)
pound-force/inch	1.751 268 X E +2	newton/meter (N/m)
pound-force/foot <sup>2</sup>	4.788 026 X E -2	kilo pascal (kPa)
pound-force/inch <sup>2</sup> (psi)	6.894 757	kilo pascal (kPa)
pound-mass (lbm avoirdupois)	4.535 924 X E -1	kilogram (kg)
pound-mass-foot <sup>2</sup> (moment of inertia)	4.214 011 X E -2	kilogram-meter <sup>2</sup> (kg·m <sup>2</sup> )
pound-mass/foot <sup>3</sup>	1.601 846 X E +1	kilogram/meter <sup>3</sup> (kg/m <sup>3</sup> )
rad (radiation dose absorbed)	1.000 000 X E -2	**Gray (Gy)
roentgen	2.579 760 X E -4	coulomb/kilogram (C/kg)
shake	1.000 000 X E -8	second (s)
slug	1.459 390 X E +1	kilogram (kg)
torr (mm Hg, 0° C)	1.333 22 X E -1	kilo pascal (kPa)

\*The becquerel (Bq) is the SI unit of radioactivity; 1 Bq = 1 event/s.

\*\*The Gray (Gy) is the SI unit of absorbed radiation.

## TABLE OF CONTENTS

Section	Page
Summary.....	v
1 Introduction.....	1
2 Background.....	4
2.1 Earlier ESR Studies.....	4
2.1.1 General ESR Observations in MOS Devices.....	4
2.1.2 ESR Studies of Radiation Effects in MOS Devices.....	5
2.2 Need for a Much More Sensitive Detection System.....	6
3 Spin Dependent Recombination.....	8
3.1 Basic Theory.....	8
3.2. Spin Dependent Recombination Spectrometer Design.....	9
3.3 Spin Dependent Recombination in MOSFETs in Integrated Circuits.....	10
4 List of References.....	11

### Appendices

A A Spin Dependent Recombination Study of Radiation Induced Defects at and Near the Si/SiO <sub>2</sub> Interface .....	13
B Spin Dependent Recombination at the Silicon/Silicon Dioxide Interface.....	23
C Related Studies.....	45

## SUMMARY

For the past three years we have explored the basic mechanisms of radiation damage in metal/oxide/silicon (MOS) field effect transistors (MOSFET's) with a combination of electron spin resonance (ESR) and electrical measurements. The major focus of our work has been to develop a new and much more sensitive ESR technique called spin dependent recombination (SDR) to study radiation damage in MOSFET's.

We have designed, constructed, and evaluated the performance of an SDR system built to study radiation damage in MOS devices. We have demonstrated that SDR permits extremely rapid, high signal to noise ratio ESR measurements of electrically active radiation damage centers in (relatively) hard MOS transistors in integrated circuits.

Using our SDR spectrometer we have observed the radiation induced buildup of  $P_{bo}$  and E' centers at relatively low concentration in individual MOSFETs in integrated circuits with (100) silicon surface orientation. To the best of our knowledge, our measurements represent the most sensitive electron spin resonance measurements ever made on any system.

Earlier ESR studies of extremely large ( $\sim 1 \text{ cm}^2$ ) capacitor structures identified  $P_{bo}$  and E' centers as the dominant radiation induced defects in MOS devices. Our results extend and confirm these earlier studies and at least qualitatively answer objections to the earlier work related to the relevance of large capacitor studies to transistors in an integrated circuit.

By varying the biases applied to source, drain, gate, and substrate we can (to some extent) directly identify the electronic role of the defects from the SDR measurements. Varying the frequency at which the SDR measurements are made, we can obtain electronic relaxation time behaviour.

Our measurements have involved a comparison of relatively hard and relatively soft MOSFETs. Our results suggest that E' centers are closer to the Si/SiO<sub>2</sub> interface in the hard oxides. (This result is consistent with and supports earlier work done at HDL which indicates that the trapped positive charge distribution is closer to the Si/SiO<sub>2</sub> interface in hard oxides.

The SDR technique allows measurements of devices in integrated circuits in a period of seconds using a spectrometer which, with effort, may be made portable. The rapid data acquisition and (marginal) portability open up many possibilities. The higher data acquisition rate means that, with signal averaging, quite high signal to noise ratios are now possible. The rapid data acquisition rate coupled with the still somewhat marginal portability open up the possibility of studying the effects of a LINAC pulse on the ESR response of an MOS device. Studies of electrical measurements of devices seconds to minutes after a LINAC pulse have recently provided considerable insight into the kinetics of the radiation damage process. SDR studies in the same time scale may provide insights into the process by which the interface states are formed.

In addition to our DNA sponsored SDR work, we have made substantial progress in other areas of ESR study of irradiated MOS devices. We have made progress in identifying the fundamental nature of the deep hole trap in the oxide, identifying differences between radiation damage and high field stressing damage, in identifying the defects involved in radiation damage of (100) silicon substrate devices and in studying the interactions of hydrogen with radiation induced point defects.

## SECTION 1

### INTRODUCTION

Exposure to ionizing radiation substantially degrades the performance of metal oxide silicon field effect transistors (MOSFET's)<sup>1-17</sup> Studies of the electronic properties of irradiated devices have demonstrated that the irradiation leads to MOSFET transconductance and channel conductance losses as well as to threshold voltage shifts. The damage involves primarily the generation of interface states at the Si/SiO<sub>2</sub> boundary and a buildup of trapped holes in the SiO<sub>2</sub>.<sup>6,8,18</sup> Extensive studies at Harry Diamond Laboratory have established that the interface state buildup is field and temperature dependent. It has also been established that the extent to which radiation damages a device is strongly upon device processing.<sup>19-21</sup> Although the first significant work on radiation damage in MOSFET's took place twenty-five years ago,<sup>1</sup> and although enormous effort has been expended in radiation damage studies,<sup>1-21</sup> a complete atomic scale picture c.f the radiation damage process has yet to emerge. Such an atomic scale understanding would be extremely useful to process engineers involved in the development of radiation hard technologies.

The technique of electron spin resonance (ESR)<sup>22</sup> is uniquely well suited to studies of the atomic scale processes involved in the radiation damage process in MOSFET's. The radiation damage process involves the capture of holes in deep trapping centers and the creation of interface state defects at the Si/SiO<sub>2</sub> boundary. These radiation induced imperfections are point defects. Electron spin resonance is sensitive to point defects with unpaired electrons. Since we can change the number of electrons at interface traps and at hole traps, at least under some circumstances, these centers should be amenable to ESR studies. ESR is sensitive to relatively small numbers of point defects; under ideal circumstances the technique may be sensitive to as few as  $\sim 10^{11}$  defects in a sample with

$\sim 10^{23}$  atomic sites. ESR can provide a detailed identification of defect structure and (often) a fairly precise determination of defect concentration.

In fact ESR, in combination with a variety of electrical measurements, has been quite powerful in studies of very large area  $\sim 1 \text{ cm}^2$  irradiated MOS capacitors<sup>23-30</sup>. These ESR studies have identified both the dominant radiation induced interface state defect<sup>24-29</sup> and the dominant deep hole trap.<sup>25-30</sup> Unfortunately, the sensitivity of standard ESR detection is not sufficiently high to permit many very useful measurements.

One would like to be able to explore a wide variety of processing steps with ESR. If measurements are restricted to  $\sim 1 \text{ cm}^2$  capacitors, many steps in device processing are simply not amenable to ESR studies. Although standard ESR is quite sensitive to defects in large area ( $\sim 1 \text{ cm}^2$ ) capacitors, the acquisition of a single trace-in effect a single data point-may require several days of continuous signal averaging if the defect density approaches  $1 \times 10^{11}/\text{cm}^2$ . Some of the most interesting studies of radiation damage in the past few years have probed the evolution of radiation damage process in a period of hundreds of seconds after exposure to a burst of (for example) LINAC electrons. In order to study such a transient response one would need to be able to acquire ESR data in a period of seconds.

The major focus of our efforts in the past three years has been to develop a type of ESR spectrometer which would allow extremely rapid acquisition of ESR data from very small MOS structures "on a chip". We have utilized the technique of spin dependent recombination (SDR) in this program. We have designed, constructed, and tested an SDR spectrometer which is many orders of magnitude more sensitive than (even the most expensive) "state of the art" standard ESR spectrometers. We have demonstrated that this system is extremely sensitive to radiation damage centers in an MOS device on a "chip". We have also demonstrated that the SDR system has the ability to acquire MOS spectra in a

period of less than 100 seconds. In order to place SDR's potential in appropriate perspective, we briefly review earlier ESR work which utilized standard detection techniques.

## SECTION 2

### BACKGROUND

#### 2.1 EARLIER ESR STUDIES.

##### 2.1.1 GENERAL ESR OBSERVATIONS IN MOS DEVICES.

An extensive ESR study of radiation effects in MOS devices was initiated in 1979 by Lenahan, Dressendorfer, and coworkers<sup>24-30</sup>. However they were not first to explore an MOS device problem with ESR. Y. Nishi and coworkers<sup>31-33</sup> and later E. H. Poindexter, P. Caplan and their coworkers<sup>34-36</sup> had earlier explored the effects of high temperature processing on the silicon-dioxide interface.

Y. Nishi and coworkers<sup>31-33</sup> identified an MOS point defect, which they termed the  $P_b$  center, as a trivalent silicon defect at or very near the  $Si/SiO_2$  interface<sup>33</sup>. Nishi et al<sup>33</sup> were also able to establish that the presence of this  $P_b$  center was strongly correlated with variations in interface state density induced by a variety of high temperature processing steps and they also successfully modeled n-channel electron mobility in terms of negatively charged  $P_b$  centers at the  $Si/SiO_2$  interface.

In the late 1970's, E. H. Poindexter, P. J. Caplan and several collaborators extended and refined the pioneering results of Nishi's group<sup>34-36</sup>. They refined the Nishi identification of  $P_b$  as a trivalent silicon at or near the  $Si/SiO_2$  interface by demonstrating that (at least for the (111) silicon case)  $P_b$  is a trivalent silicon bonded to three other silicons at the  $Si/SiO_2$  interface<sup>34</sup>. They also somewhat extended and refined the observations of Nishi's group regarding the correlation between  $P_b$  and high temperature processing induced variations in interface state density<sup>34,35</sup>. Poindexter et al<sup>36</sup> additionally established that  $P_b$  spin lattice relaxation time is strongly dependent upon bias<sup>36</sup>, but were unable to establish whether or not the  $P_b$  levels are themselves interface states.

Lenahan and Dressendorfer provided the first conclusive evidence that  $P_b$  is indeed a defect giving rise to interface state levels<sup>25-29</sup> and that the  $P_b$  level distribution in the gap approximately matches the distribution of interface state levels throughout the gap<sup>25-29</sup>. They measured the amplitude of (unsaturated)  $P_b$  absorption spectra as a function of the Si/SiO<sub>2</sub> interface Fermi level using a TE<sub>104</sub> microwave resonant cavity and a calibrated spin standard. They showed that the distribution of  $P_b$  levels was very broadly distributed throughout the bandgap<sup>25-29</sup>. When the Fermi level is near the valence band, most  $P_b$  centers accept an electron becoming paramagnetic and neutral. As the Fermi level moves from the vicinity of midgap towards the conduction band edge most  $P_b$  centers accept a second electron, becoming diamagnetic and negatively charged.

### 2.1.2 ESR STUDIES OF RADIATION EFFECTS IN MOS DEVICES.

Lenahan and Dressendorfer used large area ( $\sim 1$  cm<sup>2</sup>) MOS capacitors with (111) silicon substrates in their ESR study of radiation damage. They established that  $P_b$  centers were generated by ionizing radiation in numbers approximately equal to the number of radiation induced interface states<sup>25-29</sup>. They further showed that  $P_b$  centers and the radiation induced interface states had the same annealing behavior. As mentioned previously they also showed that the  $P_b$  centers are amphoteric interface state defects<sup>25-29</sup>. Their observations established that  $P_b$  is the dominant radiation induced interface state and strongly suggest that since  $P_b$  is neutral when the Fermi level is about at midgap, one can measure space charge in the oxide by measuring the CV shift corresponding to the Fermi level at midgap. They also observed a second center in irradiated MOS devices, an oxygen deficient silicon defect in the oxide termed 'E'. The E' center is one of many defects which have been studied in irradiated bulk SiO<sub>2</sub>. The E' center is a silicon bonded to three oxygens in the oxide<sup>37-40</sup>. It is almost certainly a simple oxygen vacancy in MOS oxides;<sup>28-30</sup> however, its structure may be somewhat different in bulk glasses. Lenahan and Dressendorfer showed that E' centers are generated in numbers about equal to the

numbers of trapped holes in irradiated oxides<sup>28,29</sup>. They further showed that these E' centers are distributed in the oxide in a pattern identical to that of the trapped holes and that E' and trapped holes have identical annealing characteristics. These observations collectively establish that two "trivalent silicon" defects are primarily responsible for the radiation damage process in MOS devices: the P<sub>b</sub> center is primarily responsible for the radiation induced interface states and the E' centers are primarily responsible for the trapped holes.

## 2.2 NEED FOR A MUCH MORE SENSITIVE DETECTION SYSTEM.

The technique of electron spin resonance has been and will continue to be an extremely powerful tool in the study of radiation damage in MOS devices. However, it has serious sensitivity limitations. By stacking several  $\sim 1\text{cm}^2$  capacitors in the microwave resonant cavity we may, with considerable difficulty, observe a defect density of about  $1 \times 10^{11}/\text{cm}^2$ . This takes about two days of signal averaging! Since signal to noise ratio improvement scales with the square root of signal averaging time, an additional improvement of a factor of two in sensitivity would require about eight days of signal averaging time.

A variety of quite useful observations could be made if ESR sensitivity could be increased by several orders of magnitude. We would very much like to study the radiation response of quite hard oxides. With standard ESR sensitivity, this is possible but the acquisition of data proceeds very slowly. We would like to explore the effects of a number of device processing steps which cannot be studied with large area capacitors but which could be studied with ESR measurements on a device on the "chip". With even a "large" device on a chip, standard ESR sensitivity would be many orders of magnitude too low to allow any signal to be observed.

One of the most interesting areas of possible study would be the transient response of an MOS device after a burst of LINAC irradiation. After a short burst of electron irradiation from a LINAC the radiation damage process proceeds for a period of several hundred seconds. It would be most useful if we could observe atomic scale processes taking place during this period. In order to do this we would need to be able to acquire ESR spectra in a period of about  $\sim$ 10 seconds, preferably from a device on a chip. Such a measurement would require about ten thousand times higher sensitivity than is available with standard ESR detection. As discussed in the next section, we have constructed a system which can (very nearly) provide this sensitivity. Furthermore, this system is (with considerable effort) portable; it could be transported to a LINAC.

## SECTION 3

### SPIN DEPENDENT RECOMBINATION

#### 3.1 BASIC THEORY.

Spin Dependent Recombination is an ESR detection technique in which the resonance is observed by monitoring the conductance of the sample. It is therefore sensitive only to electrically active point defects or to defects very close to electrically active centers. Since it utilizes sample conductance to detect resonance, its sensitivity is only weakly sample size dependent. It thus has an enormous advantage over the standard ESR techniques utilized in earlier studies of radiation in MOS devices.

The SDR effect is explained<sup>41-43</sup> by assuming that trapping may take place at a paramagnetic trap site only when the spin of the charge carrier is antiparallel to that of the trapping center. The application of a large magnetic field ( $H \sim 3000G$ ) will partially polarize the spin systems of both the trap centers and charge carriers. This polarization increases the probability of parallel charge carrier and trap center spin; thus the magnetic field reduces the capture cross section of the traps centers (Interface state defects).

Consider the effect of the simultaneous application of a large magnetic field and a microwave field of frequency  $n$  satisfying the ESR resonance condition  $\nu = g\mu_B H/h$  (here  $g$  is the ESR  $g$  value of the trap,  $\mu_B$  is the Bohr magneton,  $H$  is the magnetic field, and  $h$  is Planck's constant). If the microwave intensity is great enough to "saturate" the ESR resonance (heat up the trap spin system) it will randomize the trap spin orientations, thereby overcoming the capture cross section reduction caused by the polarization. If one measures the conductance of a device subjected to the slowly varying magnetic field and microwave radiation one may observe an SDR induced change in sample conductance when the resonance condition is satisfied. (This will only be the case if the device conductance is dependent upon trap capture

cross section). The SDR signal will have the same g value and line width as that of the ESR signal.

Lenahan and Schubert<sup>44-46</sup> showed that this effect is quite large for  $P_b$  interface state defects in grain boundaries. Henderson demonstrated<sup>47</sup> that it is also quite large for  $P_b$  centers at the Si/SiO<sub>2</sub> interface. For reasons which remain obscure, the technique is also sensitive to E' centers (hole traps in SiO<sub>2</sub> ).

### 3.2 THE SPIN DEPENDENT RECOMBINATION SPECTROMETER DESIGN.

During the past three years we have designed, constructed and tested a spin dependent recombination spectrometer. A block diagram is illustrated in Figure 1.

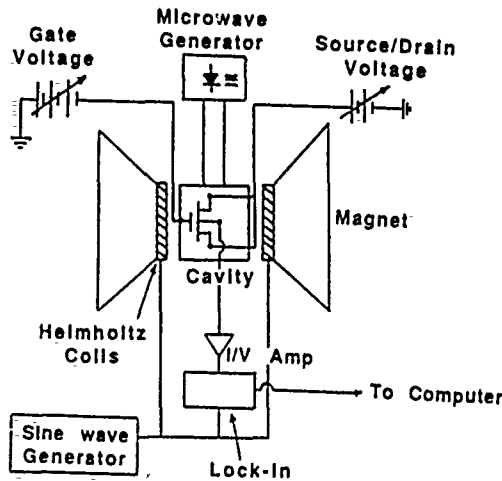


Figure 1. A block diagram of a SDR spectrometer.

The operation of the system can be readily understood through an examination of Figure 1. The SDR sample, a gate controlled diode, is placed in a TE<sub>102</sub> microwave resonant cavity. The cavity is critically coupled to a microwave generator tuned to the resonant frequency of the cavity. The cavity is placed in an electromagnet which provides large slowly varying

field. An NMR gaussmeter monitors the field amplitude quite precisely ( $\pm 0.005\%$ ). A comparison of microwave frequency (provided by the microwave/rf counter) and the NMR gaussmeter frequency, allows us to determine the  $g$  value of our SDR spectrum.

We use a lock-in amplifier to measure SDR induced changes in sample conductance. As illustrated in the figure, we monitor current change in a gate controlled diode inside the microwave resonant cavity. Helmholtz coils superimpose a small ( $\sim 4$  Gauss) magnetic field oscillating at audio frequency ( $\sim 100$  Hz to 10 KHz) on the large slowly varying field. When the large field ( $H_0$ ) reaches the resonance value, that is  $H_0^{-1} = g\mu_B/h\nu$ , the oscillating magnetic field brings the sample in and out of resonance at 150 Hz. Since the lock-in amplifier is phase and frequency locked to the current driving the Helmholtz coils, small changes in sample conductance (i.e. changes in current) are readily observable.

### 3.3 SPIN DEPENDENT RECOMBINATION IN MOSFETS IN INTEGRATED CIRCUITS.

Our most significant observations are discussed in Appendices A and B. Appendix A, "A Spin Dependent Recombination Study of Radiation Induced Defects at and Near the Si/SiO<sub>2</sub> Interface," has been accepted for publication in IEEE Transactions on Nuclear Science and will appear in the December 1989 issue. Mark Jupina presented the paper at the NSREC meeting at Marco Island in July 1989.

Appendix B, a second paper, presented as the "Plenary Lecture on Electronic Materials" at the Fifth International Symposium on Magnetic Resonance in Colloid and Interface Science, focuses on the magnetic resonance and was written for magnetic resonance specialists who are not particularly knowledgeable about MOS device physics. It will be published in the magnetic resonance conference proceedings.

SECTION 4  
LIST OF REFERENCES

1. Hughes, H.L. and R.R. Giroux, Electronics 37, 58 (1964).
2. Szedon, J. R. and J.E. Sandor, Appl. Phys. Lett. 6, 181 (1965).
3. Snow, E.H., A.S. Grove and D.J. Fitzgerald, Proc. IEEE 55, 1168 (1967).
4. Zaininger, K.H., IEEE Trans. Nucl. Sci. NS-13, 237 (1966).
5. Powell, R.J. and G.F. Derbenwick, IEEE Trans. Nucl. Sci. NS-18, 99 (1971).
6. Winokur, P.W. , H.E. Boesch, Jr., J.M. McGarrity and F.B. McLean, J. Appl. Phys. 50, 3492 (1979).
7. Hu, G.H. and W.C. Johnson, Appl. Phys. Lett. 36, 590 (1980).
8. McLean, F.B., IEEE Trans. Nucl. Sci. NS-27, 1651 (1980).
9. Winokur, P.S. and M. M. Sokoloski, Appl. Phys. Lett. 28, 627 (1976).
10. Revesz, A.G., IEEE Trans. Nucl. Sci. NS-18, 113 (1971).
11. Johnson, W.C., IEEE Trans. Nucl. Sci. NS-22, 2144 (1975).
12. Sah, C.T. , IEEE Trans. Nucl. Sci. NS-23, 1563 (1976).
13. Svensson, C.M., in The Physics of SiO<sub>2</sub> and Its Interfaces, edited by S.T. Pantelides (Pergamon, New York, 1978), p. 328.
14. Sah, C.T., IEEE Trans. Nucl. Sci. NS-23, 1563 (1976).
15. Deal, B.E., J. Electrochem. Soc. 121, 198C (1974).
16. Revesz, A.G., IEEE Trans. Nucl. Sci. NS-24, 2102 (1977).
17. Pepper, M., Thin Solid Films 14, 57 (1972).
18. Winokur, P.S., H.E. Boesch, J.N. McGarrity and F.B. McLean, IEEE Trans.. Nucl. Sci. NS-24, 2113 (1977).
19. Aubuchon, K.G., IEEE Trans. Nucl. Sci. NS-18, 117 (1971).
20. Ringel, H., M. Knoll, D. Braunig and W.H. Fehrner, J. Appl. Phys. 57, 393 (1985).
21. Derbenwick, G.F. and B.L. Gregory, IEEE Trans. NS-22, 2151 (1975).
22. Abragam, A. and B. Bleaney, Electron Paramagnetic Resonance of Transition Ions, Clarendon Press, Oxford (1970).
23. Marquardt, C.L. and G.H. Sigel, IEEE Trans. Nucl. Sci. 22, 2234 (1975).

24. Lenahan, P.M., K.L. Brower, P.V. Dressendorfer and W.C. Johnson, IEEE Trans. Nucl. Sci. NS-28, 4105 (1981).
25. Lenahan, P.M. and P.V. Dressendorfer, IEEE Trans. Nucl. Sci. NS-29, 1459 (1982).
26. Lenahan, P.M. and P.V. Dressendorfer, Appl. Phys. Lett. 41, 542 (1982).
27. Lenahan, P. M. and P.V. Dressendorfer, Appl. Phys. Lett. 54, 1457 (1983).
28. Lenahan, P.M. and P.V. Dressendorfer, Appl. Phys. Lett. 44, 96 (1984).
29. Lenahan, P.M. and P.V. Dressendorfer, J. Appl. Phys. 55, 3495 (1984).
30. Witham, H.S. and P.M. Lenahan, Appl. Phys. Lett. 51, 1007 (1987).
31. Nishi, Y., Jpn. J. Appl. Phys. 5, 333 (1966).
32. Nishi, Y., Jpn. J. Appl. Phys. 10, 52 (1971).
33. Nishi, Y., K. Tanaka, A. Ohwada, Jpn. J. Appl. Phys. 11, B5 (1972).
34. Caplan, P.J., E.H. Poindexter, B.E. Deal, and R.R. Razouk, J. Appl. Phys. 50, 5847 (1979).
35. Poindexter, E.H., P.J. Caplan, B.E. Deal and R.R. Razouk, J. Appl. Phys. 52, 879 (1981).
36. Poindexter, E.H., P.J. Caplan, J.J. Finnegan, N.M. Johnson, D.K. Biegelsen, M.D. Moyer in The Physics of MOS Insulators, edited by G. Lukovsky, S.T. Pantelides and F.L. Galeener (Pergamon, New York 1980), p. 326.
37. Weeks, R.A. J. Appl. Phys. 27, 1376 (1956).
38. Silsbee, R.H., J. Appl. Phys. 32, 1459 (1961).
39. Feigl, F., W.B. Fowler and K.L. Yip, Solid State Commun. 14, 225 (1974).
40. Griscom, D.L., Phys. Rev. 22, 4192 (1980).
41. Lepine, D., Phys. Rev. B, 6, 436 (1972).
42. Solomon, I., Solid State Commun. 20, 215 (1976).
43. Kaplan, D., I. Solomon, N.F. Mott, J. dePhysique 39, L-51 (1978).
44. Lenahan, P.M. and W.K. Schubert, Solid State Commun. 47, 423 (1983).
45. Lenahan, P.M. and W.K. Schubert, Phys. Rev. B, 30, 1544 (1984).
46. Schubert, W.K. and P.M. Lenahan, Appl. Phys. Lett. 43, 497 (1983).
47. Henderson, B., Appl. Phys. Lett. 44, 228 (1984).

APPENDIX A  
A SPIN DEPENDENT RECOMBINATION STUDY OF RADIATION  
INDUCED DEFECTS AT AND NEAR THE Si/Si<sub>0</sub><sub>2</sub> INTERFACE

# A SPIN DEPENDENT RECOMBINATION STUDY OF RADIATION INDUCED DEFECTS AT AND NEAR THE Si/SiO<sub>2</sub> INTERFACE

M. A. Jupina and P. M. Lenahan  
Pennsylvania State University  
University Park, PA 16802

## ABSTRACT

A new electron spin resonance technique, spin dependent recombination (SDR) permits extremely rapid, high signal to noise ratio Electron Spin Resonance (ESR) measurements of electrically active radiation damage centers in (relatively) hard MOS transistors in integrated circuits.

Using SDR, we observe the radiation induced buildup of P<sub>b</sub> and E' centers at relatively low concentration in individual MOSFETs in integrated circuits with (100) silicon surface orientation. Earlier ESR studies of extremely large (~1 cm<sup>2</sup>) capacitor structures have identified P<sub>b</sub> and E' centers as the dominant radiation induced defects in MOS devices. Our results extend and confirm these earlier results and at least qualitatively answer objections to the earlier work related to the relevance of large capacitor studies to transistors in an integrated circuit.

## INTRODUCTION

Since the mid-1960s when it was shown that metal-oxide-semiconductor (MOS) devices were sensitive to ionizing radiation [1], the radiation response of these devices has been an active research area. The radiation damage process results in the creation of interface states at the Si/SiO<sub>2</sub> interface and the capture of holes in deep traps near the Si/SiO<sub>2</sub> interface [2-6]. Combining electron spin resonance (ESR) and capacitance versus voltage (CV) measurements, Lenahan and Dressendorfer [7,8] showed that a trivalent silicon defect called the P<sub>b</sub> center, which is located at the Si/SiO<sub>2</sub> interface, is the dominant radiation-induced interface state, while an oxygen deficient silicon defect in the oxide, termed the E' center, is the hole trap. Their studies used large area MOS capacitors (several cm<sup>2</sup>) because standard ESR detection techniques available at that time were many orders of magnitude too insensitive to permit studies of individual metal-oxide-semiconductor field-effect transistors (MOSFETs).

In this study we use the electron spin resonance technique called spin dependent recombination (SDR). SDR has several advantages over standard ESR in the study of radiation damage in MOSFETs. It is many orders of magnitude more sensitive than standard ESR detection; it allows the rapid (a few minutes) detection of low densities (~10<sup>11</sup>/cm<sup>2</sup>) of radiation induced point defects in single MOSFETs in integrated circuits. We show that SDR is sensitive to both radiation induced P<sub>b</sub> and E' centers. We provide a semiquantitative analysis of the P<sub>b</sub> results, however we are able only to show

that SDR is sensitive to the E' centers generated by radiation and that these E' centers are "close" to the Si/SiO<sub>2</sub> interface.

Our observations collectively confirm and extend earlier ESR studies of radiation damage that used large area capacitors. Our studies qualitatively answer objections to earlier ESR work related to the relevance of very large area capacitor ESR studies to MOSFETs in integrated circuits.

Our measurements involve relatively hard and relatively soft MOSFETs. The difference in hardness in the two sets of devices involved only a high temperature post oxidation anneal. Our results suggest that E' centers are, on average, closer to the interface in the harder device.

## EARLIER ESR STUDIES INVOLVING MOS CAPACITORS

Our SDR results involve two point defects that earlier capacitor/standard ESR studies have shown to be the dominant radiation induced defects in MOS devices. P<sub>b</sub> and E' centers.

The P<sub>b</sub> center was discovered by Nishi [9]. Nishi and his coworkers studied unirradiated MOS structures. Nishi *et al* [9, 10] identified the P<sub>b</sub> center as a trivalent silicon at or very near the Si/SiO<sub>2</sub> interface. They demonstrated [10] that high temperature processing steps that yield high Si/SiO<sub>2</sub> interface state density also yield high P<sub>b</sub> density, and that high temperature processing steps that yield low interface state density, also yield low P<sub>b</sub> density.

Nishi *et al* [10] established that the Hall mobility of inversion layer electrons at the Si/SiO<sub>2</sub> interface decreases with increasing P<sub>b</sub> concentration. They showed that this correlation between processing induced P<sub>b</sub> and electron mobility could be explained in terms of coulombic scattering from negatively charged P<sub>b</sub> interface state centers at the Si/SiO<sub>2</sub> boundary. They also showed that the MOSFET's transconductance increases with decreasing P<sub>b</sub> concentration, and furthermore, specifically noted that the dependence of P<sub>b</sub> density on the partial pressure of water during oxidation is quite similar to that of the Si/SiO<sub>2</sub> interface state density. These observations convincingly established the strong correlation between interface states created by high temperature processing and P<sub>b</sub> centers. Caplan *et al* [11] while studying unirradiated devices, later provided an ingenious proof that P<sub>b</sub> is a silicon bonded to three other silicons at the Si/SiO<sub>2</sub>

interface. Poindexter *et al* [12] additionally established that  $P_b$  spin-lattice relaxation time is strongly dependent upon gate bias, but they were unable to establish whether or not the  $P_b$  center charge state and spin state are bias dependent—that is whether or not the  $P_b$  levels are themselves interface states.

Lenahan and Dressendorfer [7,8,13] established that the  $P_b$  center is an amphoteric interface state defect with levels in the band gap matching the electronic density of interface states. Their ESR work indicates that when the Fermi level is at midgap there is approximately zero net charge in the  $P_b$  center interface state defects. They furthermore demonstrated that  $P_b$  centers and radiation induced interface states [14,15] are generated in approximately equal numbers and that they exhibit the same annealing characteristics [15]. Their work, however, was restricted to (111) substrate silicon devices. Kim and Lenahan have found quite similar results for  $P_b$  centers on (100) substrates [16].

More than 30 years ago, Weeks [17] discovered the  $E'$  center in irradiated crystalline  $SiO_2$ . He proposed that  $E'$  is an electron trap with an unpaired electron residing on a silicon atom [17]. Silsbee [18] and Feigl [19] *et al* refined Week's initial assessment of  $E'$  in crystalline quartz. Feigl *et al* argued that the  $E'$  center is essentially a hole trapped in an oxygen vacancy. An asymmetric relaxation of the silicons on either side of the vacancy occurs upon hole capture; the relaxation results in the unpaired spin residing almost entirely at one of the silicons.

Marquardt and Sigel [20] were apparently the first to observe  $E'$  centers in an irradiated MOS structure. They observed a weak narrow resonance with the appropriate g value in heavily irradiated (220 Mrad), rather thick (up to 11,000 Å) oxides on silicon. Although they reported no results of electrical measurements on their devices, they suggested (correctly) that  $E'$  centers could be the trapped hole centers in the oxide.

Lenahan and Dressendorfer showed that the  $E'$  center is primarily responsible for the buildup of positive charge in irradiated oxides. They found that the densities of  $E'$  centers and holes trapped in the oxide are approximately equal, [8,16,21,22] that the  $E'$  centers and trapped holes have identical annealing characteristics, [8] and that the  $E'$  centers and trapped holes are identically distributed in the oxide [8]. Combining vacuum ultraviolet ( $hc/\lambda \approx 10.2$  eV) and ultraviolet ( $hc/\lambda \approx 5$  eV) illumination sequences with ESR and CV measurements, Witham and Lenahan [23,24] showed that the hole trapping process involving  $E'$  centers is entirely consistent with the simple oxygen vacancy model of Feigl *et al* [19].

Quite recent electron spin resonance studies of Takahashi *et al* [25] and Miki *et al* [26] also show a correspondence between  $E'$  centers and trapped holes in MOS oxides.

## SPIN DEPENDENT RECOMBINATION

The technique of spin dependent recombination (SDR) was first demonstrated by Lepine [27] in 1972. It has been applied to unoxidized silicon surfaces [27], pn junction diodes [28], amorphous hydrogenated silicon thin films [29], silicon grain boundaries [30], and the MOS system [31-33]. Vranch *et al* [33] recently demonstrated SDR in a gate controlled diode; although Vranch and coworkers provided limited information, their diode was quite large ( $0.25\text{ cm}^2$ ) and possessed an extremely high surface state density. Although the qualitative observations of Vranch *et al* did not explore the relationship between SDR signals, applied voltages, modulation frequencies, etc., it did, as does our study, provide confirmatory evidence that  $P_b$  centers play a dominant role in the radiation induced interface states at the  $Si/SiO_2$  interface. (Unlike our study, the Vranch study was unable to detect the presence of  $E'$  centers in their SDR measurements).

## THE TECHNIQUE

Just as in standard ESR, SDR detects the presence of paramagnetic point defects, that is, defects with an unpaired electron [27-36]. The technique exploits the fact that the capture cross-section of a paramagnetic trapping center is affected by its spin state. Several somewhat contradictory models [27,28,34-36] have been proposed to explain the spin dependent recombination process. Since a detailed description of these models is not appropriate for our discussion, we present only a qualitative rationalization of the phenomenon. If we apply a strong magnetic field to a semiconductor, the electron, hole, and trap spins will be polarized: they will tend to line up with the applied field. Only those electrons and holes whose spin states are anti-parallel to the spin state of the paramagnetic defect are trapped; those electrons and holes whose spin states are parallel to the spin state of the paramagnetic defect are not (or are very unlikely to be) trapped. Only electrons and holes trapped in singlet configuration at a paramagnetic center will recombine. The applied field increases the probability of triplet configurations and decreases the probability of singlet configurations. The field induced decrease in singlet configurations decreases the overall probability of capture events. The effect of the applied field is thus to decrease the capture cross-section of paramagnetic traps.

If in addition to the static field we add an oscillating (microwave frequency) field, we can flip the spins in the paramagnetic trap centers if the ESR condition is satisfied. (For a trap with  $g = g_t$ ,  $hv = g_t \beta H$ , where  $h$  is Planck's constant,  $v$  is the microwave frequency,  $\beta$  is the Bohr magneton, and  $H$  is the "static" field.) If the microwave intensity is high enough, we can completely randomize the spin orientations in the trap, significantly increasing the probability of singlet potential trapping events. The microwave radiation in turn increases the trap capture cross-section and thereby increases the recombination rate. In our experiments the microwave frequency is fixed by the resonance

frequency of our microwave cavity; the "static" field is slowly varied over tens or hundreds of seconds.

## OUR EXPERIMENT

### A. The Device

In these studies, a MOSFET is used as a gate-controlled diode [37-41] (source and drain shorted together) to study radiation-induced paramagnetic trapping centers. The p-n junction of the gated-diode is slightly forward biased ( $V_J \leq 0.3$  V), so that changes in the recombination current associated with deep trap levels can be monitored while their spin resonance condition is satisfied. For low forward biases, with the surface under the gate in accumulation, only those centers that are within the depletion region of the p-n junction contribute to the recombination current and SDR. If the surface under the gate is inverted, centers within the depletion region of the field-induced junction between the inversion layer and the underlying substrate also contribute to the total recombination current and SDR (which are, therefore, larger than in accumulation). In depletion, interface states will provide another contribution to the total recombination current, resulting in a peak in the forward current versus gate voltage characteristic. It is the SDR spectra in depletion that we are primarily concerned with in this study.

The MOSFETs used in this study were p-channel with (100) substrate orientation. Oxides were grown in dry  $O_2$  at 1000 C to a thickness of 37 nm. Annealing these oxides *in situ* in  $N_2$  at 1000 C for 25 minutes resulted in a radiation soft oxide while annealing *in situ* in  $N_2$  at 900 C for 25 minutes resulted in a radiation hard oxide. The n-well doping was  $1.5 \times 10^{16}/cm^3$  with a well depth of 6  $\mu m$ . The gate area of the devices was  $10^{-4} cm^2$  and the  $p^+$  source and drain dopings were  $3 \times 10^{19}/cm^3$ .

Since this study is primarily concerned with radiation-induced centers at the Si/SiO<sub>2</sub> boundary, the Si/SiO<sub>2</sub> interface contribution to recombination is our major concern. In our analysis we assume that the quasi-Fermi levels for electrons ( $E_{Fn}$ ) and holes ( $E_{Fp}$ ) are approximately constant throughout the depletion region underneath the gate. This assumption has been used by others [37,38] but may not always be entirely valid [41]. The band diagram (for the cross-section AA) of a gated-diode with its gate-area depleted and junction forward biased is shown in Figure 1. The spacing between the quasi-Fermi levels is determined by the forward bias  $V_J$ . The total band bending is described by the surface potential  $\psi_s$  (a function of gate bias,  $V_G$ ). The difference between the (bulk) energy levels  $E_{Fn}$  and  $E_i$  (intrinsic Fermi level) is termed  $\Phi_{Fn}$ . The rate of recombination depends on the number of interface states in the depleted surface region and on the density of carriers injected into this region under low forward bias [38,39]. The surface recombination rate will be largest when the sum of the electron and hole concentrations at the surface has its minimum value [38,39]. This happens when the concentrations are equal. The carrier concentrations are equal when the surface potential is [39]

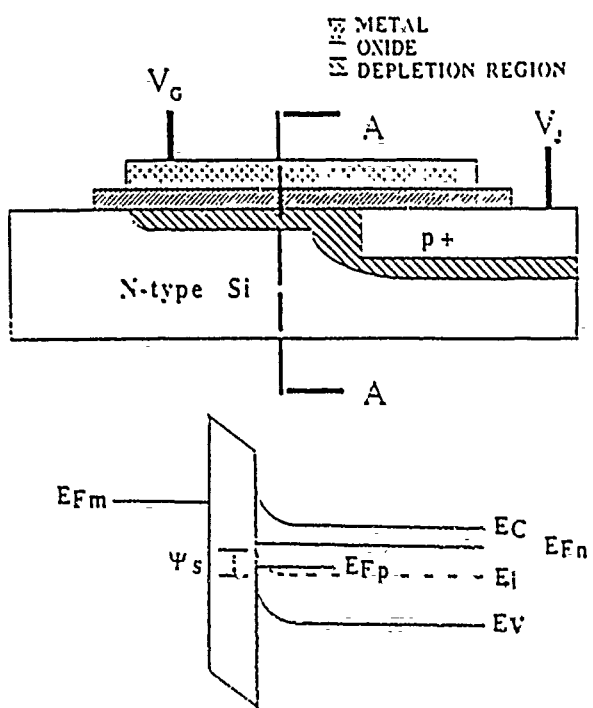


Figure 1 A gated diode (1a) forward biased and gate area depleted of carriers. An energy band diagram (1b) for the cross-section AA of the gated-diode.

$$\Psi_s = \Phi_{Fn} - V_J/2 \quad (1)$$

$$n_s = p_s = n_i \exp(qV_J/2kT) \quad (2)$$

(where  $n_s$  and  $p_s$  are the electron and hole surface concentrations and  $n_i$  is the intrinsic carrier concentration).

From simple Shockley, Read [42], Hall Theory, the surface recombination current maximum of the resulting forward current is [38]

$$I_{rec,s} \approx \left[ \frac{2}{\pi} q s_0 n_i \frac{q|V_J|}{2kT} \exp\left(\frac{q|V_J|}{2kT}\right) \right] A_G \quad (3)$$

for  $V_J \gg kT/q$ , where  $s_0 = (\pi/2) \sigma v_{th} k D_{it}$  and  $\sigma$  is taken to be the electron and hole capture cross-section,  $v_{th}$  is the thermal velocity of the charge carriers,  $k$  is the Boltzmann constant,  $T$  is the absolute temperature,  $D_{it}$  is the interface state density around the middle of the gap and  $A_G$  is the area under the gate. For  $V_J \gg kT/q$ , only the interface states whose energy lie within a band  $\sim qV_J/2$  centered around the middle of the forbidden gap contribute significantly to the surface recombination current [37,38]. (Grove and Fitzgerald have defined  $s_0$  as the surface recombination velocity of a depleted surface [37].)

## B. Experimental Technique

The SDR spectrometer employed in this study is schematically illustrated in Figure 2. The gated-diode was mounted on a rectangular quartz rod and centered inside an X band TE<sub>102</sub> microwave cavity with a resonant frequency of ~9.5 GHz. The (100) Si/SiO<sub>2</sub> interface of the device was perpendicular to the applied field. C<sub>g</sub> was taken to minimize the microwave electric field at the device, since the diode acts as a microwave detector generating an unwanted pick-up current. The loaded cavity had a Q of about 5000. The microwave source was a low noise 100 mW X-band solid state oscillator. The cavity was placed in an electromagnet (~3500 G), and Helmholtz coils were used for magnetic field modulation (audio frequencies and 4 Gpp amplitude). The microwave cavity, microwave generator, magnet, and controller were taken from a Micro-Now Model 8300 ESR spectrometer.

The gated-diode was biased at a fixed gate and junction voltage while spin dependent variations in the recombination current at resonance were monitored using a current-to-voltage pre-amplifier and lock-in amplifier (Ithaco Dynatrac Model 393). With continuous wave microwave excitation, the magnetic field was slowly ramped (~50 G in two minutes) while the SDR signal was cycled in and out resonance and monitored by the lock-in amplifier. The resulting spectra are approximately the first derivative of an "absorption-like" curve. For g-value determination of the paramagnetic recombination centers, a commercial NMR (nuclear magnetic resonance) gaussmeter (Micro-Now Model 515) was used in conjunction with a frequency meter.

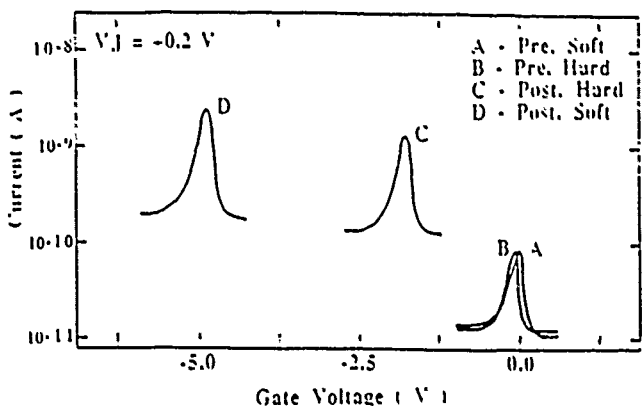


Figure 3 Pre- and post-irradiation IV curves for both hard and soft oxides.

	Pre-irradiation		Post-irradiation	
	Hard	Soft	Hard	Soft
Midgap $D_{it} (10^{11}/\text{cm}^2\text{eV})$ from CV	0.3	0.2	2.0	3.5
$s_0 (\text{cm/sec.})$	2.0	2.0	45	51
Midgap $D_{it} (10^{11}/\text{cm}^2\text{eV})$ from $s_0$ with $\sigma = 4 \times 10^{-16} \text{ cm}^2$	0.1	0.1	2.9	3.
$\Delta V_{mg}$ (volts)	----	----	-1.6	-4.8

Table 1 Summary of electrical characteristics for pre- and post-irradiated devices.

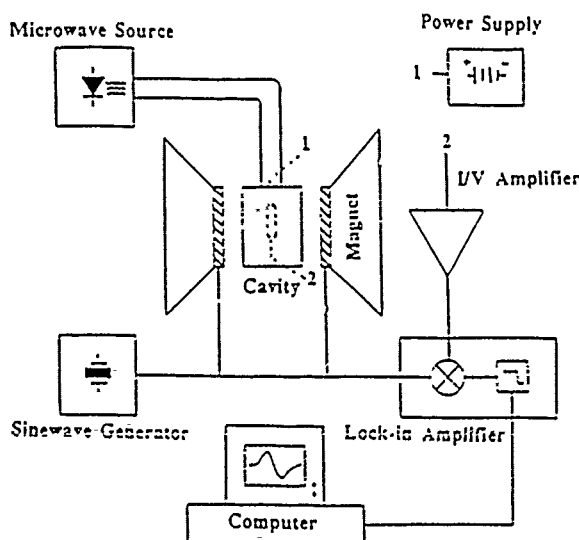


Figure 2 Block diagram of the SDR spectrometer.

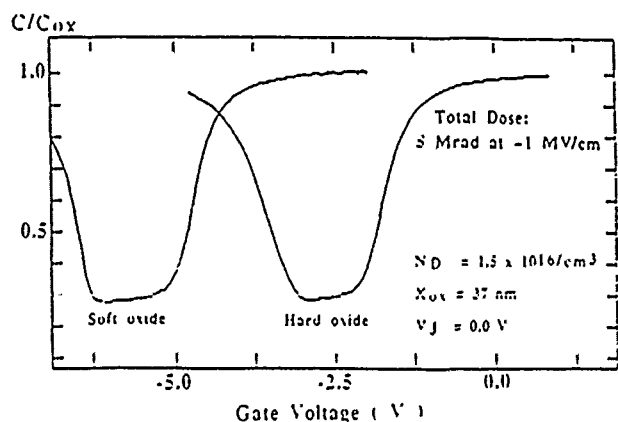


Figure 4 Post-irradiation HF CV curves for both hard and soft oxides.

## Discussion and Results

Both the relatively hard and relatively soft devices were irradiated with  $\text{Co}^{60}$   $\gamma$ -rays to a total dose of 5 Mrads. A gate bias of +5 volts was applied during irradiation. The effects of the radiation on the electrical characteristics of the devices are displayed in Figure 3 in the form of recombination current versus gate voltage for a given forward bias. Pre- and post-irradiation curves are shown for both the hard and soft devices. The radiation generated interface states in both hard and soft devices have increased the surface recombination current by about a factor of about twenty in both cases. The increase in trapped positive charge in the oxide has shifted the IV (current versus voltage) curves more negatively along the voltage axis. The MOSFETs' electrical characteristics, both before and after irradiation, are summarized in Table 1. Mid-gap interface state densities ( $D_{it}$ ) before irradiation were determined by the High-Low CV (capacitance versus voltage) technique [43] on test capacitors fabricated with the same processing steps as the MOSFETs. Mid-gap  $D_{it}$  after irradiation was determined by the Terman technique [44] on the actual MOSFETs used in this study. The post-irradiation HF (high frequency) CV curves of the MOSFETs (source and drain shorted to substrate) are shown in Figure 4. The "stretch-out" of these curves was due entirely to interface states, and no LNUs (lateral charge nonuniformities) were present as determined by a test for LNUs in MOSFETs [45]. Surface recombination velocities ( $s_0$ ) of the depleted surface both before and after irradiation, were determined from reverse bias IV curves, taking the generation current for a depleted surface as constant and given by  $I_{gen,s} = q s_0 n_i A G$  [38]. The mid-gap interface state density was also determined from the  $s_0$  values obtained from the IV curves. (In the calculation, we took the square root of the product of electron and hole capture cross-sections  $\sigma = (\sigma_n \sigma_p)^{1/2}$  to be  $4 \times 10^{-16} \text{ cm}^2$ ). Finally, the mid-gap voltage shifts are given.

In irradiated hard and soft gated diodes, we observe SDR spectra in accumulation, depletion, and inversion at low forward bias. (Attempts to observe SDR in either devices before irradiation failed. The limit of our detection was a variation  $\Delta I$  in the recombination current at resonance of approximately  $10^{-14}$  amps.) Spectra, qualitatively representative of both types of oxides, are displayed in Figure 5. In Figure 5a, the surface under the gate is in accumulation, so only those paramagnetic recombination centers in the depletion region of the p-n junction contribute to the SDR signal. This signal with a  $g$ -value of 2.0055 and a 10 Gpp width has been observed before by Solomon [28] in a depletion region of an ordinary p-n diode. In Figure 5b, the surface under the gate is in depletion, so the paramagnetic recombination centers at the Si/SiO<sub>2</sub> interface generate most of the SDR signal. In Figure 5b, both P<sub>bo</sub> ( $g = 2.006 \pm 0.0003$ ) and E' ( $g = 2.0007 \pm 0.0003$ ) centers are visible as in previous ESR studies done by Kim and Lenahan [16] on radiation-induced defects in (100) MOS structures. Just as they reported, we find that the radiation-induced interface state

buildup consists mostly of P<sub>bo</sub> centers. On (100) surfaces with process-induced interface states, Poindexter et al [46] observed two P<sub>b</sub> centers, termed P<sub>bo</sub> and P<sub>b1</sub>. The P<sub>bo</sub> defect is a silicon bonded to three other silicons at the Si/SiO<sub>2</sub> interface; the structure of P<sub>b1</sub> is not yet clearly established. Rotation of the device in the cavity revealed the P<sub>bo</sub> spectra's anisotropy. In Figure 5c, the surface under the gate is in inversion, so the paramagnetic recombination centers within the depletion region of the field-induced junction between the inversion layer and the underlying substrate contribute to the SDR signal. This SDR signal ( $g = 2.0055$  and 10 Gpp width) is very much like the resonance signal found in the depletion region of the p-n junction for accumulation.

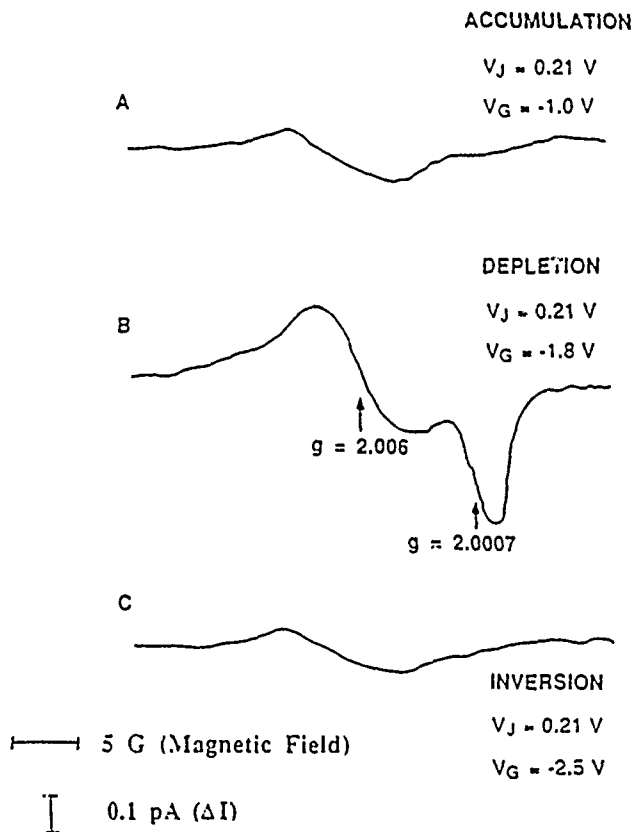


Figure 5 SDR spectra for the irradiated "hard" device in accumulation (A), depletion (B), inversion (C).

## Semiquantitative Analysis of P<sub>bo</sub> Results

Recombination current ( $I$ ) and the peak-to-peak magnitude of the P<sub>bo</sub> center's SDR signal ( $\Delta I$ ) versus gate bias are plotted in Figures 6 and 7 (hard oxide is 6 and soft oxide is 7) where the maximum  $\Delta I/I = \sim 5 \times 10^{-4}$  in both plots. Shockley-Read statistics [42] for nonequilibrium predict that the recombination current peaks in the region between the quasi Fermi levels near mid-gap ( $\psi_s = \Phi_{Fn} - V_J/2$ ). Qualitatively, the P<sub>bo</sub> signals in both the hard and the soft oxides also peak in the gate bias regime where surface recombination dominates, as one would expect for interface defects with levels near mid-gap.

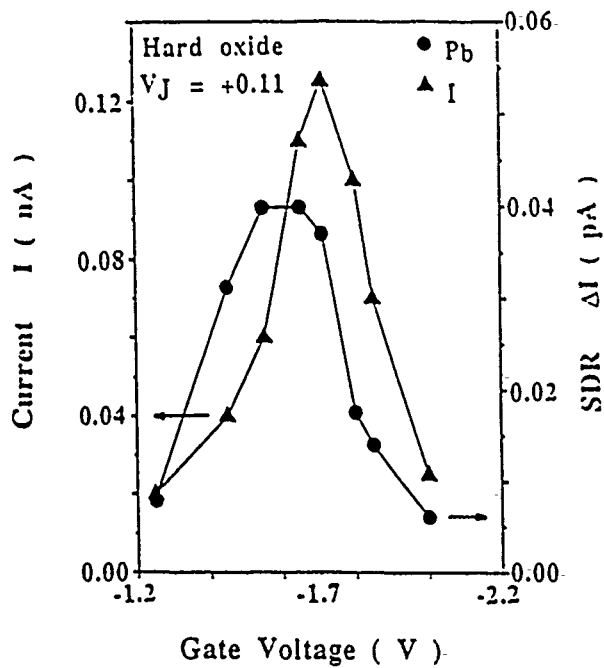


Figure 6 Recombination Current (I) and  $\text{Pb}_{\text{O}}$  center SDR signal ( $\Delta I$ ) versus gate voltage for the "hard" device.

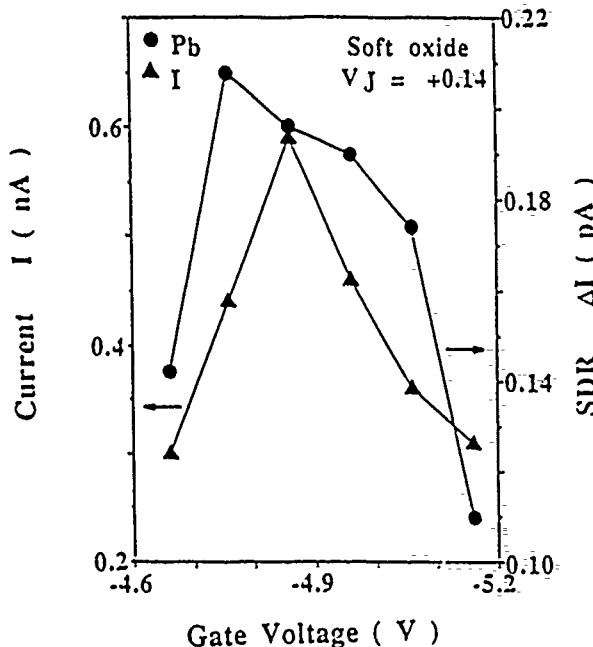


Figure 7 Recombination current (I) and  $\text{Pb}_{\text{O}}$  center SDR signal ( $\Delta I$ ) versus gate voltage for the "soft" device.

In Figure 8 the magnetic field modulation frequency dependence of the  $\text{Pb}_{\text{O}}$  center is displayed (where the  $\Delta I$ 's are normalized to their maximum values). Similar results were found in both the hard and soft oxides. (The junction was

forward biased at 0.2 V; the frequency dependence varied little with gate bias for depletion). By using a small sinusoidal magnetic field at various frequencies, the system is driven in and out of resonance about a steady state value, the result being the determination of an electronic relaxation time associated with the rate limiting process at that paramagnetic center. With a dual-phase lock-in amplifier, both the in-phase and out-of-phase SDR signal can be monitored for various modulation frequencies. The frequency response of a system in SDR normalized to steady state is [27,30]

$$\Delta I = \omega \tau \sin(\omega \tau) / ((\omega \tau)^2 + 1) + \cos(\omega \tau) / ((\omega \tau)^2 + 1) \quad (4)$$

where  $\omega$  is the angular modulation frequency,  $\tau$  is the electronic relaxation time,  $1/((\omega \tau)^2 + 1)$  is the in-phase component, and  $\omega \tau / ((\omega \tau)^2 + 1)$  is the out-of-phase component. From equation 4, the electronic relaxation times associated with the  $\text{Pb}$  center is found to be 0.3 msec. This  $\tau$  should be the average time required for a neutral paramagnetic  $\text{Pb}_{\text{O}}$  center to capture either an electron or a hole. This time is given by the inverse of the product of the number of electrons or holes times the thermal velocity ( $v_{\text{th}}$ ) times the capture cross-section of a trap. The number of electrons and holes under the gate at the maximum surface recombination rate is given by equation (2), so

$$\tau = ([n_i \exp(qV_J/2kT)] v_{\text{th}} \sigma)^{-1} \quad (5)$$

For a forward bias of  $V_J = +0.2$  V, taking  $v_{\text{th}} \approx 10^7$  cm/s, and  $\sigma = 4 \times 10^{-16}/\text{cm}^2$ , we arrive at  $\tau = 0.3$  msec, the value obtained in Figure 8 for  $\text{Pb}_{\text{O}}$  center's modulation frequency dependence.

#### Qualitative Discussion of E' Results

The  $\text{E}'$  signal observed by standard ESR in MOS structures was shown to be a hole trapped in an oxygen-vacancy very near the  $\text{Si}/\text{SiO}_2$  interface [8,13,14,22]. Whether the  $\text{E}'$  centers observed in SDR are associated with the deep hole trap can not be ascertained with absolute certainty at this time. What is certain, though, is that the  $\text{E}'$  center must reside close enough to the  $\text{Si}/\text{SiO}_2$  interface to play some role in an SDR event. In Figure 9, the  $\text{Pb}_{\text{O}}$  and  $\text{E}'$  resonances are displayed for the hard (9a) and soft (9b) devices. Although the  $\text{Pb}_{\text{O}}$  and  $\text{E}'$  amplitudes are roughly equal in the hard oxide, the  $\text{E}'$  signals are considerably smaller in the soft oxide. Simple SDR theory indicates that only  $\text{E}'$  centers that act as recombination levels near midgap could be detected; however, it is well established [47] that paramagnetic centers that are relatively close to one another may exchange energy with one another via a spin-spin interaction. The strength of the spin-spin interaction is proportional to the inverse cube of the distance between the centers [47]. Conceivably, the  $\text{E}'$  centers near the  $\text{Si}/\text{SiO}_2$  interface could be detected via some indirect spin-spin interaction of as yet unestablished origin.

Previous studies have investigated differences in radiation hard and soft oxides [48-50]. One recent study involving

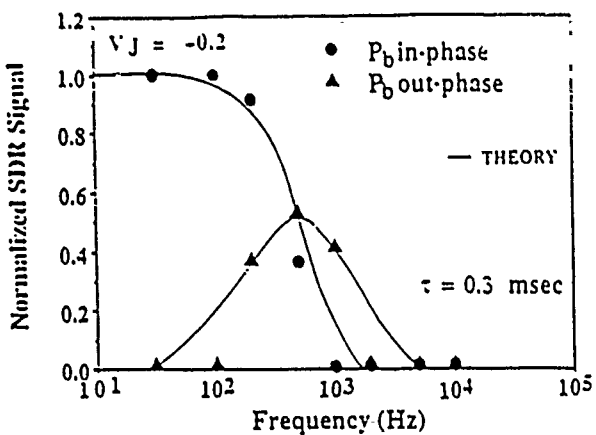


Figure 8  $P_{b0}$  center's In-phase and Out-of-phase SDR signals versus magnetic field modulation frequency.

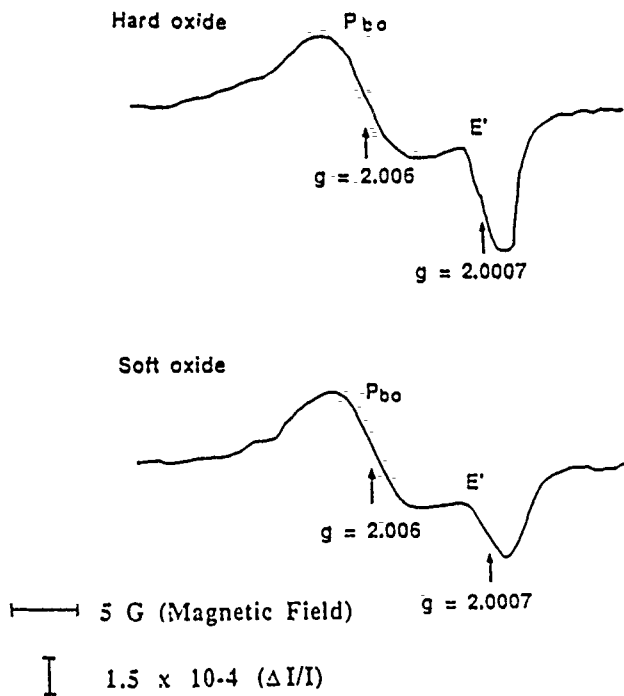


Figure 9  $P_{b0}$  and  $E'$  spectra for both hard (9a) and soft (9b) oxides.

annihilation of holes via tunneling [48] shows that quite substantial differences exist in the distribution of trapped holes in hard and soft oxides. The trapped holes are trapped very close to the  $Si/SiO_2$  interface in hard oxides; the trapped hole distribution extends well into the oxide in softer devices. Another study involving XPS (X-ray photoemission spectroscopy) revealed differences in the amount of strain at

the  $Si/SiO_2$  interface in hard and soft oxides [49,50]. The results indicated that in hard oxides the strained transition region was much narrower than in the soft oxides.

Our results regarding  $E'$  must be regarded as preliminary. The SDR technique is clearly sensitive to  $E'$ 's presence in MOSFETs; SDR shows they are not present before irradiation, but are present afterward. SDR shows that they are "close" to the  $Si/SiO_2$  interface. The SDR results suggest that the  $E'$  centers are closer to the  $Si/SiO_2$  boundary in hard oxides than in soft oxides.

## SUMMARY AND CONCLUSIONS

In this study we used SDR to observe the radiation induced buildup of  $P_{b0}$  and  $E'$  centers in relatively hard and soft oxide devices. The SDR technique allowed rapid detection of low ( $\sim 10^{11} P_{b0}/cm^2$ ) densities of radiation induced defects in individual MOSFETs in integrated circuits, where conventional ESR detection is impossible. Confirming earlier studies,  $P_{b0}$  centers were found to play a dominant role in surface recombination, as one would expect for interface defects with levels near midgap. The average capture time of the midgap interface states was found to agree quite well with the SDR's modulation frequency dependence for the  $P_{b0}$  center. Finally, differences in the magnitude of the  $E'$  spectra in both the hard and soft oxides is tentatively attributed to  $E'$  centers residing, on the average, closer to the interface in a hard oxide.

## ACKNOWLEDGMENTS

The authors would like to thank Greg Dunn of MIT Lincoln Laboratories for the MOSFETs used in this study. This work was sponsored by Sandia National Laboratories under Contract #03-3999 and the Defense Nuclear Agency under Contract #DNA002-86-0055.

## REFERENCES

- [1] H. L. Hughes and R. A. Giroux, *Electronics* 37, 58 (1964).
- [2] K. H. Zaininger, *IEEE Trans. Nucl. Sci.* NS-13, 237 (1966).
- [3] J. R. Szedon and J. E. Sandor, *Appl. Phys. Lett.* 6, 181 (1965).
- [4] R. J. Powell and G. F. Derbenwick, *IEEE Trans. Nucl. Sci.* NS-18, 99 (1971).
- [5] P. S. Winokur and M. M. Sokoloski, *Appl. Phys. Lett.* 28, 627 (1976).
- [6] F. B. McLean, *IEEE Trans. Nucl. Sci.* NS-27, 1651 (1980).
- [7] P. M. Lenahan and P. V. Dressendorfer, *Appl. Phys. Lett.* 41, 542 (1982).

[8] P. M. Lenahan and P. V. Dressendorfer, *J. Appl. Phys.* **55**, 3495 (1984).

[9] Y. Nishi, *Jpn. J. Appl. Phys.* **10**, 52 (1971).

[10] Y. Nishi, K. Tanaka, A. Ohwada, *Jpn. J. Appl. Phys.* **11**, 85 (1972).

[11] P. J. Caplan, E. H. Poindexter, B. E. Deal, and R. R. Razouk, *J. Appl. Phys.* **50**, 5847 (1979).

[12] E. H. Poindexter, P. J. Caplan, J. J. Finnegan, N. M. Johnson, D. K. Biegelsen, and M. D. Moyer in *The Physics of MOS Insulators* edited by G. Lucovsky, S. T. Pantelides, and F. L. Galeener, Pergamon, New York, 1980, p. 326.

[13] P. M. Lenahan and P. V. Dressendorfer, *Appl. Phys. Lett.* **44**, 96 (1984).

[14] P. M. Lenahan, K. L. Brower, P. V. Dressendorfer, W. C. Johnson, *IEEE Trans. Nucl. Sci.* **NS-28**, 4105 (1981).

[15] P. M. Lenahan and P. V. Dressendorfer, *J. Appl. Phys.* **54**, 1457 (1983).

[16] Y. Y. Kim and P. M. Lenahan, *J. Appl. Phys.* **64**, 3551 (1988).

[17] R. A. Weeks, *J. Appl. Phys.* **27**, 1376 (1956).

[18] R. H. Silsbee, *J. Appl. Phys.* **32**, 1459 (1961).

[19] F. J. Feigl, W. B. Fowler, and K. L. Yip, *Solid State Commun.* **14**, 225 (1974).

[20] C. L. Marquandt and G. H. Sigel, *IEEE Trans. Nucl. Sci.* **22**, 2234 (1975).

[21] P. M. Lenahan and P. V. Dressendorfer, *IEEE Trans. Nucl. Sci.* **NS-29**, 1459 (1982).

[22] P. M. Lenahan and P. V. Dressendorfer, *IEEE Trans. Nucl. Sci.* **NS-30**, 4602 (1983).

[23] H. S. Witham and P. M. Lenahan, *Appl. Phys. Lett.* **51**, 1007 (1987).

[24] H. S. Witham and P. M. Lenahan, *IEEE Trans. Nucl. Sci.* **NS-39**, 1147 (1987).

[25] T. Takahashi, B. B. Triplett, K. Yokogawa, and T. Sugano, *Appl. Phys. Lett.* **51**, 1334 (1987).

[26] H. Miki, M. Noguchi, K. Yokogawa, B. Kim, K. Osada, and T. Sugano, *IEEE Trans. Electron Devices* **35**, 2245 (1988).

[27] D. J. Lepine, *Phys. Rev. B6*, 436 (1972).

[28] I. Solomon, *Solid-State Comm.* **20**, 215 (1976).

[29] I. Solomon, D. Biegelsen, and J. C. Knights, *Solid State Comm.* **22**, 505 (1977).

[30] P. M. Lenahan and W. K. Schubert, *Phys. Rev. B30*, 1544 (1984).

[31] M. C. Chen and D. V. Lang, *Phys. Rev. Lett.* **51**, 427 (1983).

[32] B. Henderson, *Appl. Phys. Lett.* **44**, 228 (1984).

[33] R. L. Vranch, B. Henderson, and M. Petter, *Appl. Phys. Lett.* **52**, 1161 (1988).

[34] R. M. White and J. F. Gouyet, *Phys. Rev. B16*, 3596 (1977).

[35] V. S. Livov, O. V. Tretyak, and J. A. Kolomiets, *Sov. Phys. Semicond.* **11**, 661 (1977).

[36] D. Kaplan, I. Solomon, and N. F. Mott, *J. Phys. Lett. (Paris)* **39**, L51 (1978).

[37] A. S. Grove and D. J. Fitzgerald, *Solid-State Electron.* **9**, 783 (1966).

[38] D. J. Fitzgerald and A. S. Grove, *Surface Sci.* **9**, 347 (1968).

[39] E. H. Snow, A. S. Grove, and D. J. Fitzgerald, *Proc. IEEE* **55**, 1168 (1967).

[40] D. J. Fitzgerald and A. S. Grove, *Proc. IEEE Lett.* **54**, 849 (1966).

[41] R. F. Pierret, *Solid-State Electron.* **17**, 1257 (1974).

[42] W. Shockley and W. T. Read, *Phys. Rev.* **87**, 835 (1952).

[43] R. Castagne and A. Vapaille, *Surface Sci.* **28**, 157 (1971).

[44] L. M. Terman, *Solid-State Electron.* **5**, 285 (1962).

[45] E. H. Nicollian and J. R. Brews, *MOS Physics and Technology*, Wiley, New York, 1982, Chap. 6.

[46] E. H. Poindexter, P. J. Caplan, B. E. Deal, and R. R. Razouk, *J. Appl. Phys.* **52**, 879 (1981).

[47] A. Abragam and B. Bleaney, *Electron Paramagnetic Resonance of Transition Ions*, Oxford University Press, Oxford, England, 1970, Chap. 9.

[48] T. R. Oldham, A. J. Lelis, and F. B. McLean, *IEEE Trans. Nucl. Sci.* **NS-33**, 1203 (1986).

[49] F. J. Grunthaner, B. F. Lewis, N. Zamani, and J. Maserjian, *IEEE Trans. Nucl. Sci.* **NS-27**, 1640 (1980).

[50] F. J. Grunthaner, P. J. Grunthaner, and J. Maserjian, *IEEE Trans. Nucl. Sci.* **NS-29**, 1462 (1982).



APPENDIX B  
SPIN DEPENDENT RECOMBINATION AT THE SILICON/  
SILICON DIOXIDE INTERFACE

# Spin Dependent Recombination at the Silicon/Silicon Dioxide Interface

P.M. LENAHAN and M.A. JUPINA

*Pennsylvania State University, University Park, PA 16802 (U.S.A.)*

## ABSTRACT

We demonstrate that spin dependent recombination (SDR) has the sensitivity to explore interface and near interface defects in metal/oxide/silicon field effect transistors (MOSFETs) in integrated circuits. We also show that the SDR response of  $P_b$  centers is at least qualitatively consistent with the standard Shockley-Read-Hall recombination model. We also show that SDR measurements in the MOS system may provide a critical evaluation of several models which have been proposed to explain the SDR effect.

## INTRODUCTION

Semiconductor interfaces, particularly the interfaces of silicon, play an extremely important role in modern microelectronic technology. According to Pantelides [1], one interface in particular – the Si/SiO<sub>2</sub> boundary, is “the heart and soul” of modern microelectronics. This is so because the dominant device of modern microelectronics is the metal/oxide/silicon field effect transistor (MOSFET). Although the interfaces of modern microelectronics technology are remarkably perfect, low densities of imperfections (electrically active point defects) limit the performance of these devices. The amorphous SiO<sub>2</sub> films and their interface with the crystalline silicon substrates are susceptible to several poorly understood instabilities which are quite technologically important [2]. These instabilities generally result from the presence of either conduction electrons (more importantly) holes in the SiO<sub>2</sub>. Among the most important instabilities are those caused by exposure to the ionizing radiation of outer space, X-ray, and e-beam lithography, hot carrier injection in small geometry devices and high electric field injection in thin oxide devices.

Studies involving standard electron spin resonance [3,4] (ESR) detection techniques have already indicated that two point defects,  $P_b$  centers and E' centers, play important roles in the instabilities. However, these standard ESR studies have been restricted to quite large  $\sim 1 \text{ cm}^2$  MOS capacitor structures

and have been hampered by an extremely low rate of data acquisition (many hours to several days per data point). Since it has been shown that at least some of these instabilities are strongly affected by rather subtle changes in processing chemistry [5-7] it is important that the point defects be observed in transistors in integrated circuits. Since even the best commercial ESR spectrometers are sensitive to  $\gtrsim 10^{11}$  spins (for several Gauss wide lines which saturate at low levels of microwave power) ordinary ESR measurements on a fairly good MOSFET are impossible. Furthermore, one would like to be able to study these point defects as a function of Si/SiO<sub>2</sub> surface potential, and as a function of electron and hole concentration in order to understand the electronic properties of the point defects and their role in device operation.

We show that the technique of spin dependent recombination (SDR) has the sensitivity to detect the presence of paramagnetic point defects at a rather high quality ( $\sim 10^{11}$  cm<sup>-2</sup> defect density) Si/SiO<sub>2</sub> density in a MOSFET in an integrated circuit. We also show that the response of one of these centers depends upon charge carrier concentration, surface electrostatic potential, and the frequency at which the SDR response is modulated.

In addition to providing useful information to the solid state technologist, SDR measurements on the MOS system may lead to a much better understanding of the physics of SDR. Several models with quite different underlying assumptions have been proposed to explain SDR. Which, if any, of these models is consistent with reality is not yet entirely clear.

Due to its great technological importance, the electronic properties of the Si/SiO<sub>2</sub> system have been characterized in great detail. Reliable techniques have been developed to measure interface state densities, densities of trapped carriers in the oxides, etc. Most significantly, recombination at the Si/SiO<sub>2</sub> interface has been analyzed with considerable success using the model of Shockley and Read [8] and Hall [9] (SRH model).

Shockley, Read and Hall proposed that deep levels in the band gap will dominate recombination in indirect band gap semiconductors. In the SRH model, a deep level captures a charge carrier of one sign and then, before emitting that carrier, captures a second charge carrier of opposite sign. The capture of charge carriers of both signs results in the recombination of an electron and a hole.

#### SPIN DEPENDENT RECOMBINATION

Spin dependent recombination was discovered by Lepine [10] who showed that when paramagnetic deep level traps capture charge carriers, the capture process can be spin dependent. The technique of SDR has been applied to unoxidized silicon surfaces [10], *pn* junction diodes [11], amorphous hydrogenated silicon thin films, silicon grain boundaries [13] and the MOS system [14-16]. Vranch et al. [16] recently demonstrated SDR in a gate controlled

diode; their diode was quite large ( $0.25 \text{ cm}^2$ ) and possessed an extremely high surface state density.

In his pioneering study, Lepine [10] proposed a very simple model for the spin dependent effect. The application of a magnetic field will polarize both trap and electron spin systems with  $P_e \simeq P_t \simeq 2 \beta H/kT$ , where  $\beta$  is the Bohr magneton and  $H$  is the applied field. If the applied field is 3500 G (typical for X-band ESR) this polarization is of order one part in one thousand ( $10^{-3}$ )

An electron interacting with a paramagnetic deep level may be captured only if the trap and conduction electrons spins are antiparallel. A trapping event involving parallel spins would not conserve spin angular momentum. So an expression for a spin dependent capture cross-section would be

$$\sigma_{SD} = \sigma_0 (1 - P_e P_t) \quad (1)$$

where  $\sigma_0$  is the capture cross-section prior to application of the magnetic field. The effect of the applied magnetic field would be to decrease the recombination rate proportionally to  $\sigma_{SD}$ . Since  $P_e \simeq P_t \simeq 2 \beta H/kT$  we would expect

$$\sigma_{SD} \simeq \sigma_0 \left( 1 - \frac{4\beta^2 H^2}{k^2 T^2} \right) \quad (2)$$

at room temperature this would lead to a reduction of the capture cross-section of about  $\sim 10^{-6}$  for  $H \simeq 3500$  G.

Suppose that we apply a strong microwave field at the frequency which satisfied the ESR condition of the deep trap ( $\nu = g_t \beta H / \hbar$ ). If we saturate the trap spin system, we reduce the net polarization at the trap to zero, thereby restoring the zero magnetic field capture cross-section  $\sigma_0$ .

In a semiconductor sample in which conductance is dominated by recombination we can measure this spin dependent change in capture cross-section by measuring field amplitude  $H$ , microwave field of frequency  $\nu$  so that  $\hbar\nu = g\beta H$ . If the microwave field is intense enough to "saturate" the spin resonance signal the polarization is destroyed and we would expect to observe the effect of a  $\Delta\sigma/\sigma_0 \simeq 4\beta^2 H^2/k^2 T^2$  induced change in recombination rate.

The Lepine model is appealing but, unfortunately, it does not fit the data. Lepine, who observed a spin dependent change in recombination at a silicon surface, observes an effect about one order of magnitude larger than a simple polarization model predicts. He proposed that the difference between his model and results involved a spin dependent change in the surface potential – leading to an amplification of the spin dependent effect. L'vov et al. [17] extended Lepine's pioneering work on unoxidized silicon surfaces. They pointed out that the (very small) changes in surface potential which SDR might conceivably cause could not result in a large change in the size of the effect since recombination at a surface is only rather weakly dependent upon potential. They also

varied surface potential over a wide range and showed that SDR amplitude could reach as high a level as  $\Delta\sigma/\sigma = 10^{-3}$ .

To explain their results, L'vov et al. proposed a "cluster model". They proposed that the recombination centers are not randomly distributed but have a tendency to form in clusters. They supposed that in each cluster, the unpaired electrons are coupled by a ferromagnetic exchange interaction. A cluster of  $Z$  traps thus has magnetic moment  $M = Zg\beta$ . Therefore, the polarization in these traps would be about  $Zg\beta/kT$ . If  $Z$  is large, the polarization is large – greatly increasing the magnitude of the spin dependent effect.

White and Gouyet [18], discussing SDR in plastically damaged silicon, propose that the charge carrier spin traps itself through a local atomic rearrangement. They assume that photocreated electrons and holes drop into shallow states near the conduction and valence bands. Once this happens the carriers may either be reemitted to the valence or conduction bands or drop into a deep localized state with the emission of phonons. In their model the role of the microwave resonance is to "heat up the local environment thereby enhancing phonon emission, i.e. increasing the sticking probability."

The most frequently invoked SDR model is probably that of Kaplan et al. [19] (KSM model). They propose, as Lepine originally did, that the recombination transitions must conserve spin angular momentum. The "new ingredient" in the KSM model is the concept of a pair. They assume that "before recombination takes place the electron and hole go through an intermediate state in which they are in a situation of proximity." They argue that "from this pair state the electron-hole system can either recombine or dissociate but not recombine with other electrons and holes".

They cite as examples of such a recombination process exciton and donor/acceptor recombination and propose that if both the electron and the hole are trapped before recombining, the concept of a pair is approximately applicable. They claim that the recombination of a trapped electron with the nearest neighbor trapped hole will have higher probability than with holes further away. The KSM model thus has little to do with the SRH model in which an electron is trapped at a deep level and subsequently a hole is trapped at the same site.

KSM suppose that the recombination probability of an electron hole pair in a triplet state, spins parallel ( $\uparrow\uparrow$ ), is negligible and that the recombination rate in the semiconductor system  $W$  is given by the singlet ( $\uparrow\downarrow$ ) rate  $W_s$ . They further suppose that the possible pair sites are weakly populated so that the creation rate is independent of the steady state concentration of pairs. The pairs are created by capture from carriers with an isotropic spin distribution. KSM define a ratio  $\lambda = W_D/W_s$  where  $W_D$  is the rate of dissociation of electron hole pairs. If  $\lambda \ll 1$ , singlet pairs will rapidly combine leaving an abundance of triplet pairs for which recombination is forbidden. They now consider

the addition of a microwave resonant field which saturates the ESR of either the electron or hole spin - this restores the former ratio of 1/4 of singlet to triplet pairs.

If the ratio of singlet to triplet pairs is continually maintained at 1/4 and the ratio of dissociation rate to singlet recombination  $\lambda$  is relatively small, we would expect the recombination rate ( $R$ ) to equal the rate ( $C$ ) at which the localized electron hole pairs are initially created. Without the saturating microwave irradiation, the rate would be significantly lower. According to KSM, the rate without saturating microwave radiation would be, in general,

$$R = C \left[ 1 - 2\lambda \ln \left( \frac{1+2\lambda}{2\lambda} \right) \right] \quad (3)$$

The rate at saturating microwave power is, in general,

$$R_{\text{sat}} = \frac{C}{1+4\lambda} \quad (4)$$

The difference in rates peaks around  $\lambda=0.3$  and can be as large as 0.1. If  $10^{-3} \leq \lambda \leq 10^2$ , the difference in rate is greater than one part in one thousand.

#### *Earlier standard ESR studies of the MOS system*

We have applied SDR detection techniques in the observation of two point defects involved in MOS instabilities, the  $P_b$  and  $E'$  centers. Earlier studies have shown that these two centers are the dominant "radiation damage" centers in in MOS devices.

The  $P_b$  center was discovered by Nishi [20]. Nishi and coworkers studied unirradiated MOS structures. Nishi et al. [20,21] identified the  $P_b$  center as a trivalent silicon at or very near the  $\text{Si}/\text{SiO}_2$  interface. They demonstrated [21] that high temperature processing steps which yield high  $\text{Si}/\text{SiO}_2$  interface state density also yield high  $P_b$  density, and that high temperature processing steps which yield low interface state density, also yield low  $P_b$  density. Nishi et al. [21] established that the Hall mobility of inversion layer electrons at the  $\text{Si}/\text{SiO}_2$  interface decreases with increasing  $P_b$  concentration. They showed that this correlation between processing induced  $P_b$  and electron mobility could be explained in terms of coulombic scattering from negatively charged  $P_b$  interface state centers at the  $\text{Si}/\text{SiO}_2$  boundary. They also showed that the MOS-FET's transconductance increases with decreasing  $P_b$  concentration and, furthermore, specifically noted that the dependence of  $P_b$  density on the partial pressure of water during oxidation is quite similar to that of the  $\text{Si}/\text{SiO}_2$  interface state density. These observations convincingly established the strong cor-

relation between interface states created by high temperature processing and  $P_b$  centers.

Caplan et al. [22] also studying unirradiated devices, later provided an ingenious proof that  $P_b$  is a silicon bonded to three other silicons at the Si/SiO<sub>2</sub> interface. Poindexter et al. [23] additionally established that  $P_b$  spin-lattice relaxation time is strongly dependent upon gate bias, but they were unable to establish whether or not the  $P_b$  center charge state and spin state are bias dependent – that is whether or not the  $P_b$  levels are themselves interface states.

Lenahan and Dressendorfer [3,4,23] established that the  $P_b$  center is an amphoteric interface state defect with levels in the band gap matching the electronic density of interface states. Their ESR work indicates that when the Fermi level is at mid-gap there is approximately zero net charge in the  $P_b$  center interface state defects. Lenahan and coworkers furthermore demonstrated that  $P_b$  centers and radiation induced interface states [25,26] are generated in approximately equal numbers and that they exhibit the same annealing characteristics [26]. Their work, however, was restricted to (111) substrate silicon devices. Kim and Lenahan have found quite similar results for  $P_b$  centers on (100) substrates [27].

Over 30 years ago, Weeks [28] discovered the E' center in irradiated crystalline SiO<sub>2</sub>. He proposed that E' is an electron trap with an unpaired electron residing on a silicon atom [28]. Silsbee [29] and Feigl et al. [30] refined Week's initial assessment of E' in crystalline quartz. Feigl et al. [30] argued that the E' center is essentially a hole trapped in an oxygen vacancy. An asymmetric relaxation of the silicons on either side of the vacancy occurs upon hole capture; the relaxation results in the unpaired spin residing almost entirely at one of the silicons.

Marquardt and Sigel [31] were apparently the first to observe E' centers in a MOS structure. They observed a weak narrow resonance with the appropriate *g* value in heavily irradiated (220 Mrad), rather thick (up to 11 000 Å) oxides on silicon. Although they did not report the results of any electrical measurements on their devices, they suggested (correctly) that E' centers could be the trapped hole centers in the oxide.

Lenahan and coworkers showed that the E' center is primarily responsible for the buildup of positive charge in irradiated oxides. They found that the densities of E' centers and holes trapped in the oxide are approximately equal [4,27,32,33], that the E' centers and trapped holes have identical annealing characteristics [4] and that the E' centers and trapped holes are identically distributed in the oxide [4]. Combining vacuum ultraviolet ( $\hbar c/\lambda \approx 10.2$  eV) and ultraviolet ( $\hbar c/\lambda \approx 5$  eV) illumination sequences with ESR and CV measurements, Witham and Lenahan [34,35] showed that the hole trapping process involving E' centers is entirely consistent with the simple oxygen vacancy model of Feigl et al. [30].

Quite recent electron spin resonance studies of Takahashi et al. [36] and

Miki et al. [37] also show a correspondence between E' centers and trapped holes in MOS oxides.

The Si/SiO<sub>2</sub> interface of MOS devices is fairly well understood from an electronic standpoint. In order to study the Si/SiO<sub>2</sub> boundary with SDR, it is useful to consider the analysis of Si/SiO<sub>2</sub> recombination first developed over 20 years ago by Fitzgerald and coworkers [38,40]. They studied the Si/SiO<sub>2</sub> system using a gate controlled diode and the recombination SRH model. Their analysis provides a framework for understanding SDR in the Si/SiO<sub>2</sub> system.

### *The Shockley-Read-Hall model and the Si/SiO<sub>2</sub> interface*

The SRH model is frequently used to explain recombination via deep levels in semiconductors.

The processes involved are; (A) electron capture, (B) electron emission, (C) hole capture, and (D) hole emission. The four processes are illustrated in Fig. 1. We could envision hole capture (C) as the transition of an electron from the trap to the valence band. We could also envision hole emission (D) as a transition of an electron from the valence band.

If the concentration of traps is given by  $N_t$ , in equilibrium the concentration of unoccupied traps would be given by  $N_t(1-f)$ , where  $f$  is the Fermi-Dirac distribution function evaluated at the trap energy level ( $E_t$ ):  $f=1+\exp[(E_t-E_F)/kT]$ . The rate at which the traps capture electrons (in equilibrium) is

$$r_a = n v_{th} \sigma_n N_t (1-f) \quad (5)$$

where  $n$  is the density of conduction electrons,  $v_{th}$  is the thermal velocity of conduction electrons,  $v_{th} = (3kT/m_e)^{1/2}$ , and  $\sigma_n$  is the capture cross-section. In order for the electron to become captured it must come close to the trap; we

### Shockley, Read, Hall Model

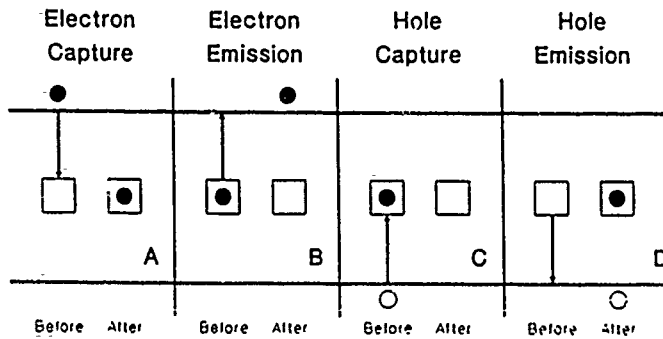


Fig. 1. An illustration of the processes involved in the Shockley-Read-Hall recombination model.

suppose that if the electron comes within a distance  $r = (\sigma/\pi)^{1/2}$  it will be captured.

The rate of electron emission will be proportional to the number of occupied traps. If we define a constant  $e_n$ , the emission probability per unit time of an electron jumping from the trap to the conduction band, the rate of electron emission will be

$$r_B = e_n N_t f \quad (6)$$

In analogy with Eqn (5) the rate of hole capture will be

$$r_C = v_{th} \sigma_p p N_t f \quad (7)$$

where  $p$  is the density of holes.

The rate of hole emission is, by analogy with Eqn (2),

$$r_D = e_p N_t (1-f) \quad (8)$$

where  $e_p$  is the hole emission probability.

These four expressions provide the basis for the SRH theory and the basis for understanding recombination through deep levels in semiconductors. In order to complete the analysis however, we need to obtain expressions for electron and hole emission probabilities  $e_n$  and  $e_p$ . It is easy to do this if we consider an equilibrium situation. In equilibrium, common-sense tells us that the rates at which electrons and holes are trapped must equal the rates at which electrons and holes are emitted ( $r_A = r_B$  and  $r_C = r_D$ ). Setting  $r_A$  and  $r_B$  equal using Eqns (5) and (6) we find

$$e_n = v_{th} \sigma_n n (1-f) / f \quad (9)$$

In equilibrium, the number of electrons in the conduction band is

$$n = n_i \exp(E_F - E_i) / kT \quad (10)$$

where  $E_i$  is the intrinsic Fermi level and  $n_i$  is the intrinsic carriers concentration. Combining Eqns (9) and (10) yields an expression for emission rate.

$$e_n = v_{th} \sigma_n n_i \exp(E_i - E_F) / kT \quad (11)$$

Since the hole concentration  $p$  is given by

$$p = n_i \exp(E_i - E_F) / kT \quad (12)$$

the equality of hole emission and capture rates requires that

$$e_p = v_{th} \sigma_p n_i \exp(E_i - E_t) / kT \quad (13)$$

Suppose we uniformly generate electron hole pairs at a rate  $G$  per unit volume. In steady state, the rate at which electrons enter the conduction band must equal the rate electrons leave the conduction band

$$\frac{dn}{dt} = G - (r_A - r_B) = 0 \quad (14)$$

Also the rate at which holes enter the valence band must equal the rate at which holes leave the valence band

$$\frac{dp}{dt} = G - (r_C - r_D) = 0 \quad (15)$$

If we set Eqns (10) and (11) equal,

$$r_A - r_B = r_C - r_D \quad (16)$$

By combining our four rate expressions in the nonequilibrium occupation probability  $f'$ :

$$f' = \frac{\sigma_n n + \sigma_p n_i \exp(E_i - E_t)/kT}{\sigma_n [n + n_i \exp(E_t - E_i)/kT] + \sigma_p [p + n_i \exp(E_i - E_t)/kT]} \quad (17)$$

Using this expression to obtain the rates of the individual processes yields the rate  $U$  of recombination through the trap centers.

$U$  = rate of electron capture ( $r_A$ ) - rate of electron emission ( $r_B$ )

= rate of hole capture ( $r_C$ ) - rate of hole emission ( $r_D$ )

$$= \frac{\sigma_p \sigma_n v_{th} N_t [pn - n_i^2]}{\sigma_n [n + n_i \exp(E_t - E_i)/kT] + \sigma_p [p + n_i \exp(E_i - E_t)/kT]} \quad (18)$$

It is difficult to visualize the behavior of  $U$  from an expression as complex as Eqn (18). It can be simplified considerably if we set  $\sigma_p = \sigma_n$ . With this approximation,

$$U = \sigma v_{th} N_t \frac{(np - n_i^2)}{n + p + 2n_i \cosh[(E_t - E_i)/kT]} \quad (19)$$

Fitzgerald and Grove have applied Eqn (19) to the interfaces of semiconductors. They find that the recombination rate per unit area  $U_s$  will be given by

$$U_s = \sigma_s v_{th} \left\{ \int_{E_v}^{E_c} \frac{D_{it}(E) dE}{p_s + n_s + 2n_i \cosh[(E - E_i)/kT]} \right\} [p_s N_s - n_i^2] \quad (20)$$

where  $p_s$  and  $n_s$  are the electron and hole concentrations at the interface,  $D_{it}(E)$  is the density of states of the interface traps,  $\sigma_s$  is the trap capture cross-section and  $E_c$  and  $E_v$  are the energies of the conduction and valence band edges.

Considering the silicon/silicon dioxide interface, we can simplify the expression further. The  $D_{it}(E)$  distribution is slowly varying around the middle of the band gap. Since  $\cosh[(E - E_i)/kT]$  blows up for  $[E - E_i] \gg kT$ , only levels near mid-gap contribute substantially to the integrand; we may therefore take  $D_{it}(E)$  as a constant – the interface state density evaluated at mid-gap  $D_{it}$ . If we consider the case  $p_s + n_s \gg n_i$ , the expression can be simplified still further. With  $p_s + n_s \gg n_i$ , the integrand is constant  $[D_{it}/(p_s + n_s)]$  for energies around mid-gap. The denominator blows up when

$$p_s + n_s < 2 n_i \cosh[(E - E_i)/kT] \quad (21)$$

To a good approximation then, we can take the integrand as  $[D_{it}/(p_s + n_s)]$  around the middle of the gap, and zero when Eqn (21) is satisfied. These considerations yield

$$U_s \cong \sigma_s v_{th} D_{it} \frac{[p_s n_s - n_i^2]}{[p_s + n_s]} \int_{E_i - \Delta}^{E_i + \Delta} dE \quad (22)$$

where

$$\Delta = kT \operatorname{arc} \cosh[(p_s + n_s)/2n_i] \quad (23)$$

Our final expression for recombination rate is thus

$$U_s \cong 2\sigma_s v_{th} D_{it} kT \frac{[p_s n_s - n_i^2]}{[p_s + n_s]} \operatorname{arc} \cosh\left(\frac{p_s + n_s}{2n_i}\right) \quad (24)$$

#### *Application of the Shockley-Read-Hall model to the Si/SiO<sub>2</sub> interface*

Surface recombination at the Si/SiO<sub>2</sub> interface can conveniently be explored in a MOSFET configured as a gate controlled diode. A device configured in this way and a band diagram are illustrated in Fig. 2. The source and drain are connected together, a second connection to the substrate completes the  $p^+/n$  junction, a third contact to the gate allows in control of the surface potential  $\phi_s$ .

With no voltage applied to the source or drain, the concentration of electrons and holes at the surface can be varied by applying a voltage to the gate; the gate voltage controls the surface potential. Straightforward analysis shows that

$$n_s \cong N_D \exp(q\phi_s/kT) \quad (25a)$$

$$p_s \cong \frac{n_i^2}{N_D} \exp(-q\phi_s/kT) \quad (25b)$$

where  $N_D$  is the donor density.

If we apply a forward bias across the  $p^+/n$  junctions we will inject holes into

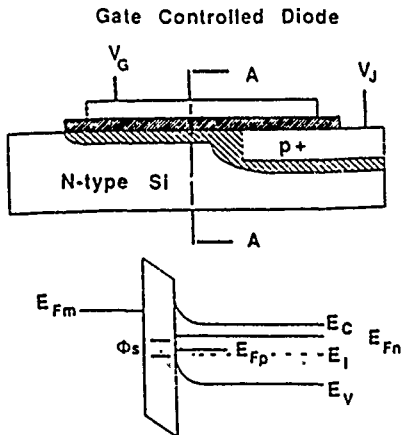


Fig. 2. At the top of the figure, we show a gated diode forward biased with gate area depleted of carriers. Below we show an energy band diagram for the cross-section AA of the gated-diode.

the region between the source and drain. This will result in an extremely large increase in hole density but, to first order, little change in electron density. If the forward bias voltage is  $V_j$ , the hole density will increase by a factor of  $\exp(q|V_j|/kT)$ . Under forward bias conditions then,

$$p_s \cong \frac{n_i^2}{N_D} \exp(-q\phi_s/kT) \exp(q|V_j|/kT) \quad (26a)$$

$$n_s \cong N_D \exp(q\phi_s/kT) \cong n_i \exp(q\phi_b/kT) \exp(q\phi_s/kT) \quad (26b)$$

where  $\phi_b$  is the difference in energy between the bulk Fermi energy and the Fermi energy of the intrinsic semiconductor.

Having determined  $p_s$  and  $n_s$  (approximately) all of the parameters of Eqn (24) are determined. The surface recombination rate is given by

$$U_s \cong \left\{ 2\sigma_s v_{th} D_{it} kT \left[ \frac{n_i^2 \exp(q|V_j|/kT) - n_i^2}{(n_i/N_D) \exp[q(|V_j| - \phi_s)/kT] + N_D \exp(q\phi_s/kT)} \right] \right\}. \quad (27)$$

$$\arccosh \left[ \frac{(n_i/N_D) \exp[q(|V_j| - \phi_s)/kT] + N_D \exp(q\phi_s/kT)}{2n_i} \right] \quad (27)$$

Although Eqn (27) may be evaluated by computer, casual inspection of the equation yields little insight. However Eqns (22) and (23) indicate that the

recombination rate will peak when  $n_s + p_s$  is minimized. We find the conditions required to minimize  $p_s$  and  $n_s$  by setting the derivative with respect to  $\phi_s$  of their sum equal to zero:

$$\phi_b = \frac{|V_j|}{2} - \phi_s \quad (28)$$

which yields

$$U_{sp} \approx 2\sigma_s v_{th} D_{it} kT n_i \left( \frac{q|V_j|}{kT} \right) \exp[(q|V_j|)/2kT] \quad (29)$$

if  $|V_j| \geq (2kT)/q$ .

If the gate area is  $A_G$  this corresponds to a recombination current of

$$I_{rec,p} \cong A_G q [2\sigma_s v_{th} D_{it} n_i q |V_j|] \exp[(q|V_j|)/2kT] \quad (30)$$

From Eqn (23), the centers involved in this recombination current are in a band  $\sim q|V_j|$  wide centered around the middle of the gap.

Although the analysis leading to Eqn (30) involved quite a few approximations, Grove and coworkers [38-40] have shown that it leads to reasonable results; they also showed that if the electron and hole capture cross-sections are not extremely different, the substitution of  $(\sigma_p \sigma_n)^{1/2}$  for  $\sigma$ , is appropriate.

This analysis of recombination at the Si/SiO<sub>2</sub> interface of MOSFET provides an approach to SDR investigations of integrated circuit problems. If we set  $|V_j|/2 - \phi_s = \phi_b$  the surface recombination current will be maximized; in general if  $V_j$  is not too large ( $|V_j| < 0.4$  V), this recombination current will dominate the device current. By varying  $V_j$  we can vary the range of the band gap energy of the recombination centers involved in the process. By varying  $V_j$  we also vary  $n_s$  and  $p_s$  over wide range. From Eqn (26) we can calculate  $n_s$  and  $p_s$ .

#### THE EXPERIMENTAL DEVICE

In our experiments, a MOSFET is used as a gate controlled diode [38-40] to study radiation-induced paramagnetic trapping centers. The  $p-n$  junction of the gated-diode is slightly forward biased ( $V_j \leq 0.3$  V), so that changes in the recombination current associated with deep trap levels can be monitored while their spin resonance condition is satisfied. For low forward biases, with

the surface under the gate in accumulation, only those centers that are within the depletion region of the  $p-n$  junction contribute to the recombination current and SDR. If the surface under the gate is inverted, centers within the depletion region of the field-induced junction between the inversion layer and the underlying substrate also contribute to the total recombination current and SDR (which are, therefore, larger than in accumulation). In depletion, interface states will provide another contribution to the total recombination current, resulting in a peak in the forward current versus gate voltage characteristic. It is the SDR spectra in depletion which we are primarily concerned with in this study.

The MOSFET's used in this study were p-channel with (100) substrate orientation. Both moderately radiation tolerant (hard) and radiation intolerant (soft oxides) were grown in dry  $O_2$  at  $1000^\circ C$  to 37 mm. The soft oxide was annealed in situ in  $N_2$  for 25 min at  $1000^\circ C$ , while the hard was annealed in situ in  $N_2$  for 25 min at  $900^\circ C$ . The  $n$ -well doping was  $1.5 \cdot 10^{16} \text{ cm}^{-3}$  with a well depth of 6  $\mu\text{m}$ . The gate area of the devices was  $10^{-4} \text{ cm}^2$  and the  $p+$  source and drain dopings were  $3 \cdot 10^{19} \text{ cm}^{-3}$ .

### *Experimental technique*

The SDR spectrometer employed in this study is schematically illustrated in Fig. 3. The gated-diode was mounted on a rectangular quartz rod and centered inside an X-band  $TE_{102}$  microwave cavity with a resonant frequency of  $\sim 9.5 \text{ GHz}$ . The (100)  $\text{Si}/\text{SiO}_2$  interface of the device was perpendicular to the applied field. Care was taken to minimize the microwave electric field at the

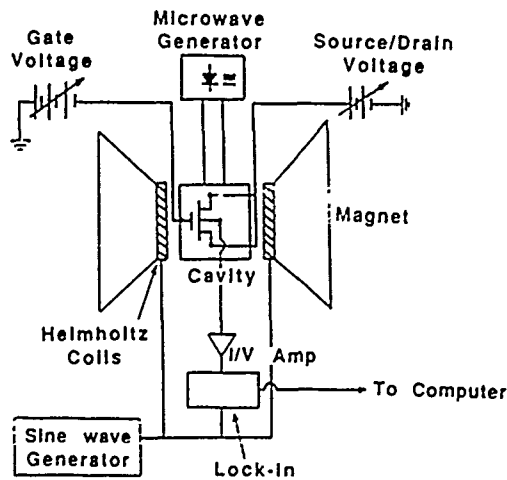


Fig.3. Block diagram of the SDR spectrometer.

device, since the diode acts as a microwave detector generating pick-up current. The loaded cavity had a  $Q$  of about 5000. The microwave source was a low noise 100 mW X-band solid state oscillator. The cavity was placed in an electromagnet ( $\sim 3500$  G) and Helmholtz coils were used for magnetic field modulation (audio frequencies and  $4$  G<sub>pp</sub> amplitude). The microwave cavity, microwave generator, magnet, and controller were taken from a Micro-Now Model 8300 ESR spectrometer.

The gated-diode was biased at a fixed gate and junction voltage while spin dependent variations in the recombination current at resonance were monitored using a current-to-voltage pre-amplifier and lock-in amplifier (Ithaco Dynatrac Model 393). With continuous wave microwave excitation, the magnetic field was slowly ramped ( $\sim 50$  G in 2 min) while the SDR signal was cycled in and out of resonance and monitored by the lock-in amplifier. The resulting spectra are approximately the first derivative of an "absorption-like" curve. For  $g$ -value determination of the paramagnetic recombination centers, a commercial NMR (nuclear magnetic resonance) gaussmeter (Micro-Now Model 515) was used in conjunction with a frequency meter.

#### DISCUSSION AND RESULTS

Both the relatively hard and relatively soft devices were irradiated with  $^{60}\text{Co}$   $\gamma$ -rays to a total dose of 5 Mrads. A gate bias of +5 V was applied during irradiation. The effects of the radiation on the electrical characteristics of the devices are displayed in Fig. 4 in the form of recombination current versus gate voltage for a given forward bias. Pre- and post-irradiation curves are shown for both the hard and soft devices. The radiation generated interface states in both hard and soft devices have increased the surface recombination current by a factor of about twenty in both cases. The increase in trapped positive

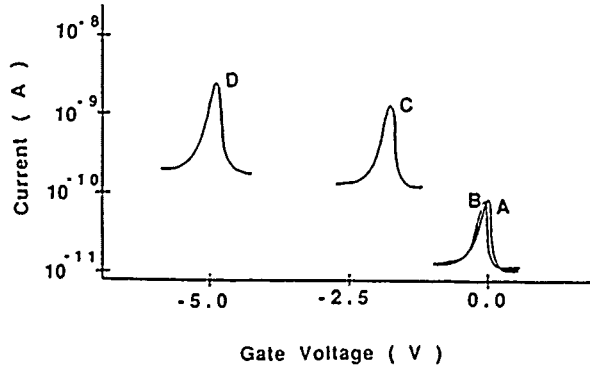


Fig. 4. Pre-irradiation and post-irradiation  $I$ - $V$  curves for both hard (A and C) and soft (B and D) oxides. The post irradiation curves are C and D.

charge in the oxide has shifted the  $I$ - $V$  (current versus voltage) curves more negatively along the voltage axis. The MOSFETs' electrical characteristics, both before and after irradiation, are summarized in Table 1. Mid-gap interface state densities ( $D_{it}$ ) before irradiation were determined by the high-low C-V (capacitance versus voltage) technique [41] on test capacitors fabricated with the same processing steps as the MOSFETs. Mid-gap  $D_{it}$  after irradiation was determined by the Terman technique [42] on the actual MOSFETs used in this study. The post-irradiation HF (high frequency) C-V curves of the MOSFETs (source and drain shorted to substrate) are shown in Fig. 5. The "stretchout" of these curves was due entirely to interface states, and no lateral charge nonuniformities were present as determined by a standard test [43].

In irradiated hard and soft gated diodes, we observe SDR spectra in accumulation depletion, and inversion at low forward bias. (Attempts to observe SDR in either devices before irradiation failed. The limit of our detection was a variation  $\Delta I$  in the recombination current at resonance of approximately  $10^{-14}$  A.) Spectra, qualitatively representative of both types of oxides, are displayed in Fig. 6. In Fig. 6A, the surface under the gate is in accumulation, so only those paramagnetic recombination centers in the depletion region of the  $p$ - $n$  junction contribute to the SDR signal. A similar signal with a  $g$ -value of

TABLE 1

Summary of electrical characteristics for pre- and post-irradiated devices of hard and soft oxides

	Pre-irradiation		Post-irradiation	
	Hard	Soft	Hard	Soft
Mid-gap $D_{it}$ ( $10^{11}$ cm $^{-2}$ eV) from C-V	0.3	0.2	2.0	3.5
$\Delta V_{mg}$ (volts)	-	-	-1.6	-4.8

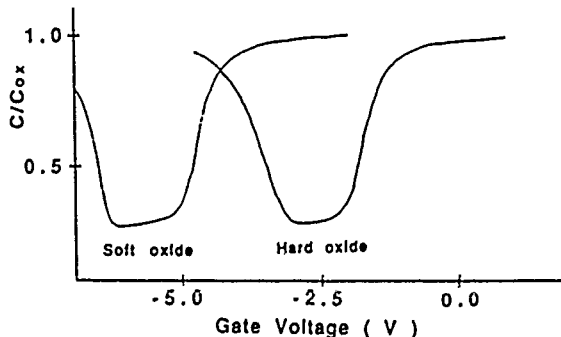


Fig. 5. Post-irradiation HF C-V curves for both hard and soft oxides.

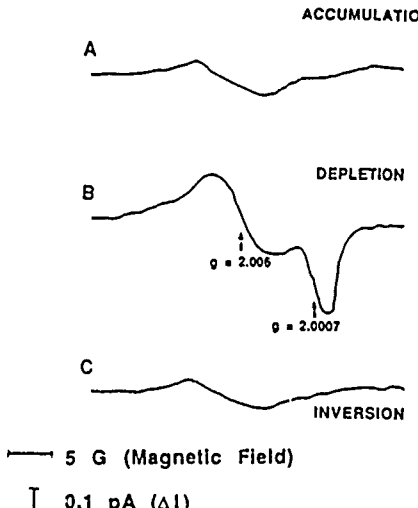


Fig. 6. SDR spectra for the irradiated hard device in: (A) accumulation; (B) depletion; (C) inversion.

2.0055 and a 10 G<sub>pp</sub> width has been observed by Solomon [28] in a depletion region of an ordinary *p-n* diode. In Fig. 6B, the surface under the gate is in depletion, so the paramagnetic recombination centers at the Si/SiO<sub>2</sub> interface generate most of the SDR signal. On (100) surfaces with process-induced interface states, Poindexter et al. [44] observed two P<sub>b</sub> centers, termed P<sub>b0</sub> and P<sub>b1</sub>. The P<sub>b0</sub> defect is a silicon bonded to three other silicons at the Si/SiO<sub>2</sub> interface; the structure of P<sub>b1</sub> is not yet clearly established. In Fig. 6B, both P<sub>b0</sub> ( $g=2.006 \pm 0.0003$ ) and E' ( $g=2.0007 \pm 0.0003$ ) centers are visible as in previous ESR studies done by Kim and Lenahan [27] on radiation-induced defects in (100) MOS structures. Just as they reported, we find that the radiation-induced interface state buildup consists mostly of P<sub>b0</sub> centers. In Fig. 6C, the surface under the gate is in inversion, so the paramagnetic recombination centers within the depletion region of the field-induced junction between the inversion layer and the underlying substrate contribute to the SDR signal. This SDR signal ( $g=2.0055$  and 10 G<sub>pp</sub> width) is very much like the resonance signal found in the depletion region of the *p-n* junction for accumulation (but larger).

#### Semiquantitative analysis of P<sub>b0</sub> Results

Recombination current ( $I$ ) and the peak-to-peak magnitude of the P<sub>b0</sub> center's SDR signal ( $\Delta I$ ) versus gate bias are plotted in Figs 7 and 8 where the maximum  $\Delta I/I = \sim 5 \cdot 10^{-4}$  in both plots. Shockley-Read statistics [38-40] for nonequilibrium predict that the recombination current should peak when

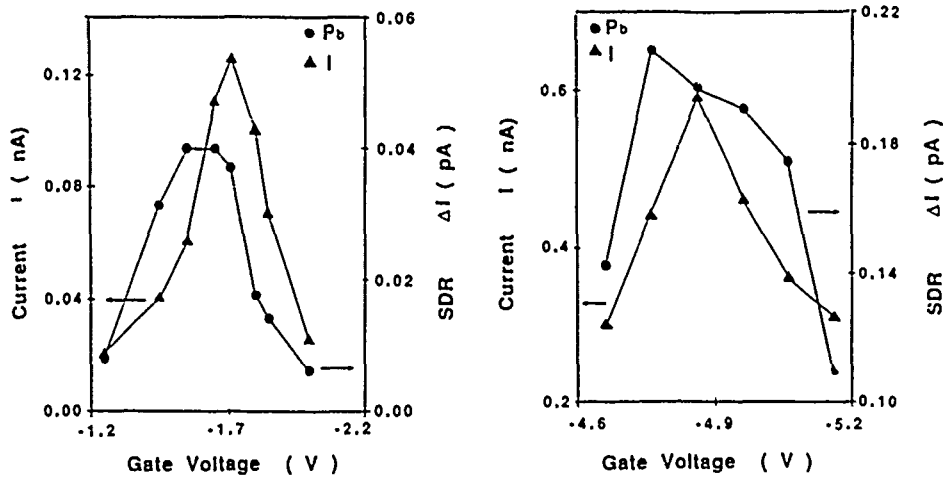


Fig. 7. (left) Recombination current ( $I$ ) and  $P_{b0}$  center SDR signal ( $\Delta I$ ) versus gate voltage for the hard device.

Fig. 8. (right) Recombination current ( $I$ ) and  $P_{b0}$  center SDR signal ( $\Delta I$ ) versus gate voltage for the soft device.

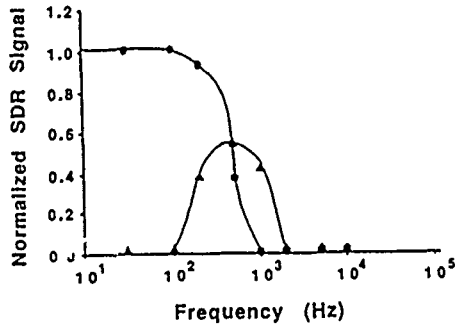


Fig. 9.  $P_{b0}$  center's in-phase and out-of-phase SDR signals versus magnetic field modulation frequency.

$\phi_s = \phi_{Fn} - q|V_j|/2$ . Qualitatively, the  $P_{b0}$  signals in both the hard and the soft oxides also peak in the gate bias regime where surface recombination dominates, as one would expect for interface defects with levels near mid-gap.

In Fig. 9 the magnetic field modulation frequency dependence of the  $P_{b0}$  center is displayed (where the  $\Delta I$ 's are normalized to their maximum values). Similar results were found in both the hard and soft oxides. (The junction was forward biased at 0.2 V; the frequency dependence varied little with gate bias for depletion.) By using a small sinusoidal magnetic field at various frequencies, the system is driven in and out of resonance about a steady state value.

The result being the determination of an electronic relaxation time associated with the rate limiting process at that paramagnetic center. With a dual-phase lock-in amplifier, both the in-phase and out-of-phase SDR signal can be monitored for various modulation frequencies. The frequency response of a system in SDR normalized to steady state is [10,13]

$$\Delta I = \omega \tau \sin(\omega \tau) / (\omega^2 \tau^2 + 1) + \cos(\omega \tau) / (\omega^2 \tau^2 + 1) \quad (31)$$

where  $\omega$  is the angular modulation frequency,  $\tau$  is the electronic relaxation time,  $1/(\omega^2 \tau^2 + 1)$  is the in-phase component, and  $\omega \tau / (\omega^2 \tau^2 + 1)$  is the out-of-phase component. From Eqn (4), the electronic relaxation times associated with the  $P_b$  center is 0.3 ms. This  $\tau$  should be the average time required for a neutral paramagnetic  $P_{b0}$  center to capture either an electron or a hole. This time is given by the inverse of the product of the number of electrons or holes times the thermal velocity ( $v_{th}$ ) times the capture cross-section of a trap. The number of electrons and holes under the gate at the maximum surface recombination rate is obtained by substituting Eqn (28) into Eqn (26); we find that

$$\tau = ([n_i \exp(qV_j/2kT)] v_{th} \sigma)^{-1} \quad (32)$$

For a forward bias of  $V_j = +0.2$  V, taking  $v_{th} \approx 10^7$  cm $^{-1}$ s, and  $\sigma = 4 \cdot 10^{-16}$  cm $^{-2}$ , we arrive at  $\tau = 0.3$  ms, the value obtained in Fig. 9 for the  $P_{b0}$  center's modulation frequency dependence.

#### *Qualitative discussion of E' results*

The E' signal observed by standard ESR in MOS structures was shown to be a hole trapped in an oxygen vacancy very near the Si/SiO<sub>2</sub> interface [4,24,25,33]. Whether the E' centers observed in SDR are associated with the deep hole trap cannot be ascertained with absolute certainty at this time. What is certain, though, is that the E' center must reside close enough to the Si/SiO<sub>2</sub> interface to play some role in an SDR event. In Fig. 10, the  $P_{b0}$  and E' resonances are displayed for the hard and soft devices. Although the  $P_{b0}$  and E' amplitudes are roughly equal in the hard oxide, the E' signals are considerably smaller in the soft oxide. Simple SDR theory indicates that only E' centers which act as recombination levels near mid-gap could be detected; however, it is well established [45] that paramagnetic centers which are relatively close to one another may exchange energy with one another via a spin-spin interaction. The strength of the spin-spin interaction is proportional to the inverse cube of the distance between the centers [45]. It is conceivable that E' centers near the Si/SiO<sub>2</sub> interface could be detected via an indirect spin-spin interaction.

Previous studies have investigated differences in radiation hard (tolerant) and soft (intolerant) oxides [46-48]. One recent study, involving annihilation of holes via tunneling [46], shows that quite substantial differences exist in

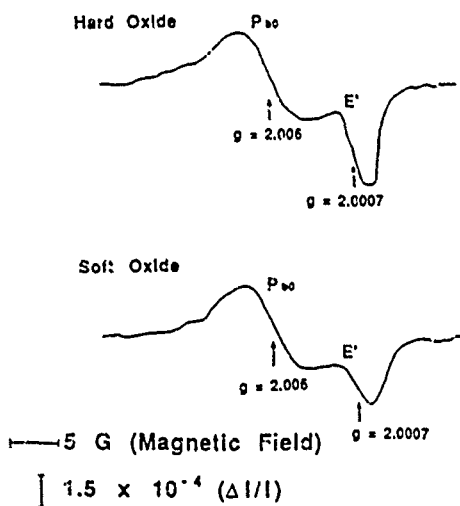


Fig. 10.  $P_{b0}$  and  $E'$  spectra for both hard and soft oxides.

the distribution of trapped holes in hard and soft oxides. The trapped holes are trapped very close to the  $Si/SiO_2$  interface in hard oxides; the trapped hole distribution extends well into the oxide in softer devices. Another study involving XPS (X-ray photoemission spectroscopy) revealed differences in the amount of strain at the  $Si/SiO_2$  interface in hard and soft oxides [47,48]. The results indicated that in hard oxides the strained transition region was much narrower than in the soft oxides.

Our results regarding  $E'$  must be regarded as preliminary at this time. The SDR technique is clearly sensitive to  $E'$ 's presence in MOSFETs; SDR shows they are not present prior to irradiation, but are present after irradiation. SDR shows that they are "close" to the  $Si/SiO_2$  interface. The SDR results suggest that the  $E'$  centers are closer to the  $Si/SiO_2$  boundary in hard oxides than in soft oxides.

*Which (if any) of the SDR models are consistent with our results?*

Our SDR results for  $E'$  centers are clearly difficult (at this time) to reconcile in detail with any of the SDR models since earlier ESR work establishes  $E'$  as a hole trapped in an oxygen vacancy in the oxide. Since the distribution of trapped holes is closer to the interface in hard oxides and since the  $E'$  SDR signal is larger in hard oxides we provisionally suppose that  $E'$  plays an indirect role in the SDR process which probably involves a spin-spin interaction with unpaired electrons at the  $Si/SiO_2$  boundary.

Our results for  $P_b$  centers seem to be qualitatively consistent with a standard Shockley-Read-Hall picture of recombination events at the  $Si/SiO_2$  bound-

ary. Since the  $P_b$  centers are the dominant surface states and since the density of surface states is low in our devices ( $\approx 10^{11} \text{ cm}^{-2} \text{ eV}$ ) it is difficult to see how any SDR model involving a cooperative interaction between several trapping sites could be involved. Since the  $P_b$  centers are neutral when paramagnetic we are clearly not observing ESR at a trapped electron or hole site as envisioned by Kaplan, Solomon and Mott.

Our limited results regarding the rate limiting step in  $P_{b0}$  SDR indicate that the process involves the capture of a charge carrier at a neutral  $P_{b0}$  site; this is qualitatively consistent with the Lepine model; however, the size of the effect  $\Delta I/I \approx 5 \cdot 10^{-4}$  is far too large for the Lepine model.

We reluctantly conclude that our results do not seem to provide convincing evidence for the validity of any of the current SDR models. Our results regarding  $P_b$  centers do indicate that the rate limiting step is the spin dependent capture of a charge carrier at a single neutral paramagnetic point defect.

#### CONCLUSIONS

In this study we used SDR to observe the radiation induced buildup of  $P_{b0}$  and  $E'$  centers in relatively hard and soft oxide devices. The SDR technique allowed rapid detection of low ( $\approx 10^{11} P_{b0} \text{ cm}^{-2}$ ) densities of radiation induced defects in individual MOSFETs in integrated circuits, where conventional ESR detection is impossible. Confirming earlier studies,  $P_{b0}$  centers were found to play a dominant role in surface recombination, as one would expect for interface defects with levels near mid-gap. The average capture time of the mid-gap interface states was found to agree quite well with the SDR's modulation frequency dependence for the  $P_{b0}$  center. Finally, differences in the magnitude of the  $E'$  spectra in both the hard and soft oxides is tentatively attributed to  $E'$  centers residing, on average, closer to the interface in a hard oxide.

#### ACKNOWLEDGEMENTS

This work has been supported by the Defense Nuclear Agency under contract number DNA0001-86-C-0055 and grant number N00014-89-J-2022 and by Sandia National Laboratories under contract 03-3999. We gratefully acknowledge Greg Dunn of Massachusetts Institute of Technology, Lincoln Laboratory, Carl Schlier of IBM Federal Systems Laboratory, and Fred Sexton of Sandia National Laboratory for providing us with MOS devices used in our study.

#### REFERENCES

- 1 S.T. Pantelides, in S.T. Pantelides (Ed.), *The Physics of  $\text{SiO}_2$  and Its Interfaces*, Pergamon, New York, 1978 p.v.
- 2 These instabilities are discussed at great length in two recent books: P.V. Dressendorfer and T.P. Ma, *Ionizing Radiation Effects in MOS Devices and Circuits*, Wiley Interscience, New York, 1989, and E.H. Nicollian and J.R. Brews, *MOS Physics and Technology*, Wiley Interscience, New York, 1982.
- 3 P.M. Lenahan and P.V. Dressendorfer, *Appl. Phys. Lett.*, 41 (1982) 542.
- 4 P.M. Lenahan and P.V. Dressendorfer, *J. Appl. Phys.*, 55 (1984) 3495.

- 5 E.P. EerNisse and G.F. Derbenwick, *IEEE Trans. Nucl. Sci.*, 23 (1976) 1534.
- 6 N. Shiono, M. Shionaya and K. Sano, *Jpn. J. Appl. Phys.*, 22 (1983) 1430.
- 7 G.F. Derbenwick and B.L. Gregory, *IEEE Trans. Nucl. Sci.*, 22 (1975) 2151.
- 8 W. Shockley and W.T. Read, *Phys. Rev.*, 87 (1952) 835.
- 9 R.N. Hall, *Phys. Rev.*, 87 (1952) 387.
- 10 D.J. Lepine, *Phys. Rev. B*, 6 (1972) 436.
- 11 I. Solomon, *Solid-State Commun.*, 20 (1976) 215.
- 12 I. Solomon, D. Biegleson and J.C. Knights, *Solid State Commun.*, 22 (1977) 505.
- 13 P.M. Lenahan and W.K. Shubert, *Phys. Rev. B*, 30 (1984) 1544.
- 14 M.C. Chen and D.V. Lang, *Phys. Rev. Lett.*, 51 (1983) 427.
- 15 B. Henderson, *Appl. Phys. Lett.*, 44 (1984) 228.
- 16 R.L. Vranch, B. Henderson and M. Petter, *Appl. Phys. Lett.*, 52 (1988) 1161.
- 17 V.S. L'vov, O.V. Tretyak, and J.A. Kolomiets, *Sov. Phys. Semicond.*, 11 (1977) 661.
- 18 R.M. White and J.F. Gouyet, *Phys. Rev. B*, 16 (1977) 3596.
- 19 D. Kaplan, I. Solomon and N.F. Mott, *J. Phys. Lett. (Paris)*, 39 (1978) L51.
- 20 Y. Nishi, *Jpn. J. Appl. Phys.*, 10 (1971) 52.
- 21 Y. Nishi, K. Tanaka and A. Ohwada, *Jpn. J. Appl. Phys.*, 11 (1972) 85.
- 22 P.J. Caplan, E.H. Poindexter, B.E. Deal and R.R. Razouk, *J. Appl. Phys.*, 50 (1979) 5847.
- 23 E.H. Poindexter, P.J. Caplan, J.J. Finnegan, N.M. Johnson, D.K. Biegelsen and M.D. Moyer, in G. Lucovsky, S.T. Pantelides and F.L. Galeener (Eds), *The Physics of MOS Insulators*, Pergamon, New York, 1980, p. 326.
- 24 P.M. Lenahan and P.V. Dressendorfer, *Appl. Phys. Lett.*, 44 (1984) 96.
- 25 P.M. Lenahan, K.L. Brower, P.V. Dressendorfer and W.C. Johnson, *IEEE Trans. Nucl. Sci.*, 28 (1981) 4105.
- 26 P.M. Lenahan and P.V. Dressendorfer, *J. Appl. Phys.*, 54 (1983) 1457.
- 27 Y.Y. Kim and P.M. Lenahan, *J. Appl. Phys.*, 64 (1988) 3551.
- 28 R.A. Weeks, *J. Appl. Phys.*, 27 (1956) 1376.
- 29 R.H. Silsbee, *J. Appl. Phys.*, 32 (1961) 1459.
- 30 F.J. Feigl, W.B. Fowler and K.L. Yip, *Solid State Commun.*, 14 (1974) 225.
- 31 C.L. Marquardt and G.H. Sigel, *IEEE Trans. Nucl. Sci.*, 22 (1975) 2234.
- 32 P.M. Lenahan and P.V. Dressendorfer, *IEEE Trans. Nucl. Sci.*, 29 (1982) 1459.
- 33 P.M. Lenahan and P.V. Dressendorfer, *IEEE Trans. Nucl. Sci.*, 30 (1983) 4602.
- 34 H.S. Witham and P.M. Lenahan, *Appl. Phys. Lett.*, 51 (1987) 1007.
- 35 H.S. Witham and P.M. Lenahan, *IEEE Trans. Nucl. Sci.*, 39 (1987) 1147.
- 36 T. Takahashi, B.B. Triplett, K. Yokogawa and T. Sugano, *Appl. Phys. Lett.*, 51 (1987) 1334.
- 37 H. Miki, M. Noguchi, K. Yokogawa, B. Kim, K. Osada and T. Sugano, *IEEE Trans. Electron Devices*, 35 (1988) 2245.
- 38 A.S. Grove and D.J. Fitzgerald, *Solid-State Electron.*, 9 (1966) 783.
- 39 D.J. Fitzgerald and A.S. Grove, *Surf. Sci.*, 9 (1968) 347.
- 40 E.H. Snow, A.S. Grove and D.J. Fitzgerald, *Proc. IEEE*, 55 (1967) 1168.
- 41 R. Castagne and A. Vapaille, *Surf. Sci.*, 28 (1971) 157.
- 42 L.M. Terman, *Solid-State Electron.*, 5 (1962) 285.
- 43 E.H. Nicollian and J.R. Brews, *MOS Physics and Technology*, Wiley, New York, 1982, Chap. 6.
- 44 E.H. Poindexter, P.J. Caplan, B.E. Deal and R.R. Razouk, *J. Appl. Phys.*, 52 (1981) 879.
- 45 A. Abragam and B. Bleaney, *Electron Paramagnetic Resonance of Transition Ions*, Oxford University Press, Oxford, 1970, Chap. 9.
- 46 T.R. Oldham, A.J. Leis and F.B. McLean, *IEEE Trans., Nucl. Sci.*, 33 (1986) 1203.
- 47 F.J. Grunthaner, B.F. Lewis, N. Zamani and J. Maserjian, *IEEE Trans. Nucl. Sci.*, 27 (1980) 1640.
- 48 F.J. Grunthaner, P.J. Grunthaner and J. Maserjian, *IEEE Trans. Nucl. Sci.*, 29 (1982) 1462.

## APPENDIX C

### RELATED STUDIES

#### A. Radiation Damage in (100) Silicon Substrate Devices

Earlier ESR studies explored (111) substrate structures because of the simplicity of the ESR spectron and the relative ease of ESR detection. However, the (100) silicon substrate is utilized in virtually all MOS technology. In order to resolve questions regarding the relevance of the (111) ESR studies to technologically relevant structures we have extensively explored irradiated (100) substrate structures with ESR. The results were recently (October 1988) published in the Journal of Applied Physics.

# Electron-spin-resonance study of radiation-induced paramagnetic defects in oxides grown on (100) silicon substrates

Yong Yun Kim

Department of Electrical Engineering, The Pennsylvania State University, University Park, Pennsylvania 16802

P. M. Lenahan

Department of Engineering Science and Mechanics, The Pennsylvania State University, University Park, Pennsylvania 16802

We have used electron-spin resonance to investigate radiation-induced point defects in Si/SiO<sub>2</sub> structures with (100) silicon substrates. We find that the radiation-induced point defects are quite similar to defects generated in Si/SiO<sub>2</sub> structures grown on (111) silicon substrates. In both cases, an oxygen-deficient silicon center, the  $E'$  defect, appears to be responsible for trapped positive charge. In both cases, trivalent silicon ( $P_b$  centers) defects are primarily responsible for radiation-induced interface states. In earlier electron-spin-resonance studies of unirradiated (100) substrate capacitors two types of  $P_b$  centers were observed; in oxides prepared in three different ways only one of these centers, the  $P_{b0}$  defect, is generated in large numbers by ionizing radiation.

## I. INTRODUCTION

When silicon metal-oxide-semiconductors (MOS) field effect transistors are exposed to ionizing radiation, the irradiation results in the trapping of holes in the SiO<sub>2</sub> and the creation of localized states, called interface states, at Si-SiO<sub>2</sub> boundary.<sup>1-7</sup> The trapping of holes and the buildup of interface states seriously degrade the performance of silicon MOS integrated circuits; individual transistors experience a loss of transconductance and channel conductance as well as shifts in threshold voltage. Ionizing radiation may be encountered during integrated circuit fabrication processes such as electron-beam evaporation of the metal interconnection layer and vacuum ultraviolet (VUV) lithography.<sup>8</sup> Radiation effects are also quite important in several technologically significant applications, most importantly MOS integrated circuitry in satellites.

During the past dozen years numerous models have been proposed to account for the structure of the point defects responsible for the hole traps in the oxide<sup>9-11</sup> and the interface states.<sup>12-25</sup>

Recent electron-spin-resonance (ESR) work utilizing (111) silicon substrates has resulted in considerable progress in identifying the point defects which dominate the radiation damage process.<sup>20-26</sup> These experiments have utilized (111) silicon substrates since they generally yield the largest ESR signals. Although the electron-spin-resonance work has led to considerable progress in understanding the radiation damage process, virtually all MOS integrated circuitry utilizes the (100) silicon substrate. In this paper we extend the earlier ESR studies to the (100) silicon substrates which are utilized in MOS technology.

Earlier ESR studies on (111) silicon substrate/oxide capacitors showed that a trivalent silicon defect at the Si/SiO<sub>2</sub> interface, the  $P_b$  center, is largely responsible for the

radiation-induced interface states.<sup>20-25</sup> The  $P_b$  center was first observed by Nishi<sup>16</sup> in unirradiated capacitors; Nishi and his co-workers<sup>16,17</sup> established that  $P_b$ 's presence was strongly correlated with interface state variations induced by a number of high-temperature processing steps. Nishi, Tanaka, and Ohwada<sup>17</sup> furthermore identified  $P_b$  as a trivalent silicon at or near the Si/SiO<sub>2</sub> interface. Caplan *et al.*<sup>27,28</sup> later provided an ingenious proof that  $P_b$  is a silicon bonded to three other silicons at the Si/SiO<sub>2</sub> interface. Poindexter *et al.*<sup>29</sup> additionally established that  $P_b$  spin lattice relaxation time is strongly dependent upon gate bias, but they were unable to establish whether or not the  $P_b$  center charge state and spin state are bias dependent, that is whether or not the  $P_b$  levels are themselves interface states.

Lenahan and Dressendorfer<sup>22-25</sup> established that the  $P_b$  center is an amphoteric interface state defect and that its levels in the band gap closely match that of the electronic density of interface states for (111) silicon substrates. Their ESR work on (111) silicon substrates indicates that when the Fermi level is at midgap there is approximately zero net charge in the  $P_b$  center interface state defects.<sup>22-25</sup> Later, Poindexter *et al.*<sup>30</sup> also showed an excellent correspondence between the interface state and  $P_b$  level distribution induced by high-temperature processing. If the interface states are mostly  $P_b$  center levels, most of the interface states have zero net charge when the Fermi level is at midgap; thus, the density of holes trapped in the oxides can be expressed by  $C_{ox} \Delta V_{mg} / e$ , where  $C_{ox}$  is the oxide capacitance,  $\Delta V_{mg}$  is the shift in the capacitance-voltage (CV) curve for the Fermi level at midgap, and  $e$  is the electronic charge.

Lenahan and Dressendorfer's work<sup>21,24-26</sup> on irradiated (111) substrate capacitors also showed that a second center, called the  $E'$  center, is primarily responsible for the buildup of positive charge in irradiated oxides. They found that the densities of  $E'$  centers and holes trapped in the oxide are

approximately equal,<sup>21,24-26</sup> that the  $E'$  centers and trapped holes have identical annealing characteristics, and that the  $E'$  centers and trapped holes are identically distributed in the oxide.<sup>25</sup> They also observed a third resonance which they ascribed to nonbridging oxygen and/or peroxy centers; its role in the radiation damage process is not clear.<sup>21</sup>

Although very little effort has been expended in the study of radiation-induced centers in (100) substrate capacitors, considerable progress has been made in the study of centers induced by high-temperature processing. Poindexter, Caplan, Deal, and Razouk,<sup>27,28</sup> studying unirradiated MOS structures, identified two different  $P_b$  centers on (100) Si:  $P_{b0}$ , which has the structure  $\cdot\text{Si} \equiv \text{Si}_3$ , and  $P_{b1}$ , which is of uncertain identity, but is chemically and paramagnetically different in nature from  $P_{b0}$ . In a later extensive study, Stesmans *et al.*<sup>31</sup> also observed these two centers in oxides prepared in a variety of ways. Poindexter *et al.*<sup>27,28</sup> observed a correlation between the density of both processing-induced  $P_{b0}$  and  $P_{b1}$  centers and the midgap interface state density of unirradiated samples in oxides grown on the (100) surface. Gerardi, Poindexter, and Caplan<sup>32</sup> have established that both the (100)  $P_{b0}$  and  $P_{b1}$  centers are amphoteric interface state defects with levels broadly distributed throughout the gap.

In this paper, we present results of a study in which we investigate the radiation-induced trivalent silicon centers in MOS structures using a combination of ESR and  $C-V$  measurements to identify the point defects involved in radiation-induced MOS device degradation. In (100) substrate MOS capacitors prepared quite differently at two laboratories (IBM Federal Systems and Sandia National Laboratories) we observe that  $P_{b0}$  is primarily responsible for radiation-induced interface states. We also investigated traps in the oxide by measuring the density of radiation-induced paramagnetic  $E'$  centers generated by hole trapping and quantitatively evaluating the density of trapped charge from  $C-V$  measurements, utilizing the shift in the  $C-V$  curve corresponding to the Fermi level at midgap. Our results collectively demonstrate that the radiation damage process on (100) substrates devices is very similar to the process in (111) substrate devices.

## II. EXPERIMENTAL PROCEDURES

The samples utilized in the measurements were in the form of  $4 \times 30$ -mm bars cut with (011) long sides from 100-mm silicon wafers ( $p$ -type,  $\rho \sim 100 \Omega \text{ cm}$ ) with (100) surface orientation. Three different sets of oxides were prepared to examine the general radiation response of oxides grown on (100) Si substrates. The first set of oxides was grown in a sequence of dry/wet/dry oxygen ambients at 1000 °C to a thickness of 1000 Å. A second set of oxides was grown in a sequence of dry/wet/dry oxygen ambients at a temperature of 1000 °C to a thickness of approximately 1240 Å and annealed in  $\text{N}_2$  at 1140 °C for 720 min. After oxide growth, approximately 200 Å of Al was evaporated on the surfaces. A third set of oxides was grown in steam at 900 °C to a thickness of 1000 Å. After oxide growth approximately 0.6  $\mu\text{m}$  of polysilicon was deposited on the oxide surfaces.

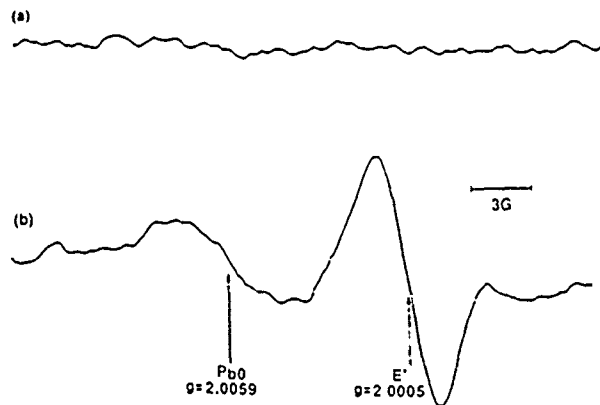


FIG. 1 Pre- and post-irradiation wide-scan ESR spectra of (100) Si/SiO<sub>2</sub> structures illustrating both  $P_{b0}$  and  $E'$  resonances. The  $E'$  resonance is somewhat saturated and overmodulated. The magnetic field is perpendicular to the plane of the (100) Si/SiO<sub>2</sub> interface.

The ESR measurements were made using an IBM Instruments ER-200 spectrometer with a TE<sub>104</sub> "double" cavity. The spin concentrations were calculated by comparison of unsaturated absorption spectra with the spectrum of a calibrated weak-pitch standard. The substrate edges were etched to eliminate any resonance signals from damage at the edges of the samples. High-frequency  $C-V$  (1 MHz) measurements were made using a mercury probe. We estimate that the absolute spin concentration measurements of  $P_b$  and  $E'$  are accurate to somewhat better than a factor of 2; the relative spin concentrations are much more accurately determined ( $\pm 10\%$ ). We estimate electrical measurements ( $C-V$ ) reported in this work to be accurate to about  $\pm 10\%$ .

## III. EXPERIMENTAL RESULTS

In Fig. 1 we show ESR spectra of (100) silicon substrate MOS capacitors (A) before and (B) after exposure to approximately 6 Mrad (Si) of  $^{60}\text{Co} \gamma$  irradiation. The oxides were grown in dry/wet/dry oxygen ambients at 1000 °C to a thickness of 1240 Å and were subjected to a nitrogen anneal at 1140 °C for 720 min. During the irradiation the 1240-Å oxides were under a positive gate bias of 24 V. The aluminum gate was removed prior to ESR measurement. The spectrometer settings of Fig. 1 are not optimized for either  $P_b$  or  $E'$  but represent a compromise so that both are clearly visible. In Fig. 2 we illustrate capacitance-versus-voltage curves from these capacitors (A) before and (B) after the irradiation. These traces qualitatively indicate our essential observations. We find substantial generation of  $P_{b0}$  and  $E'$  centers in (100) substrates subjected to ionizing radiation. The generation of  $P_{b0}$  and  $E'$  centers accompanies the generation of positive charge in the oxide and interface states at the Si/SiO<sub>2</sub> interface.

In this paper, we present an extensive study which indicates that the  $P_{b0}$  centers are primarily responsible for the interface state generation and that the  $E'$  centers are primarily responsible for the hole trapping.

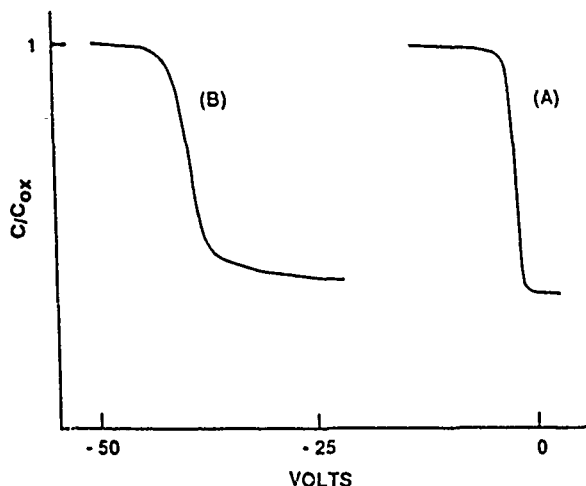


FIG. 2. High-frequency  $C$ - $V$  curves (A) before and (B) after exposure to approximately 6 Mrad (Si) of  $^{60}\text{Co}$   $\gamma$  irradiation.

### A. Radiation-induced interface state defects

Several samples of all three varieties of MOS capacitors were subjected to approximately 6 Mrad (Si) of  $^{60}\text{Co}$   $\gamma$  irradiation with positive gate potential corresponding to an average oxide field of 1 MV/cm. After irradiation, the gates were removed and the samples were subjected to sub- $\text{SiO}_2$  band-gap ( $hc/\lambda < 5.5$  eV) illumination from a xenon-mercury lamp. This illumination results in the internal photoemission of electrons from the silicon into the oxide. The photoemitted electrons recombine with the trapped holes, thereby annihilating the  $E'$  resonance which would otherwise interfere somewhat with our ESR measurements of  $P_b$  centers.<sup>33,34</sup>

Three ESR spectra, one for each variety of oxide, are illustrated in Fig. 3. In each case the trace was taken with magnetic field perpendicular to the (100) surface. In all oxides we observe a single strong resonance at  $g = 2.0059$ . (Prior to the subband gap illumination we would also observe a very strong  $E'$  resonance at  $g = 2.0005$ .) The  $g$  factor is defined by the expression  $g = h\nu/\beta H$  where  $h$  is Planck's constant,  $\nu$  is the microwave frequency,  $\beta$  is the Bohr magneton, and  $H$  is the magnetic field at which resonance occurs. The anisotropy of the  $g$  factor is generally summarized in the form of a second-rank tensor. According to Poindexter *et al.*<sup>35</sup> the  $P_{b0}$  center is a silicon bonded to three other silicons at the (100) surface. This is chemically identical to the  $P_b$  center found on (111) substrates. We would expect that these  $P_{b0}$  silicon dangling-bond centers would have approximately the same  $g$  tensor as the (111) centers, and would expect that the symmetry axis would also correspond to the direction in which the "dangling bond" points into the oxide. One would thus expect a  $g$  tensor with axial symmetry about the [111] axis, and  $g$  tensor elements  $g_{\parallel} = 2.0015$  and  $g_{\perp} = 2.008$ . With the magnetic field perpendicular to the (100) surface, this  $g$  tensor yields  $g = 2.0059$ , precisely the value we observe. According to Poindexter *et al.*<sup>35</sup> the  $g$  val-

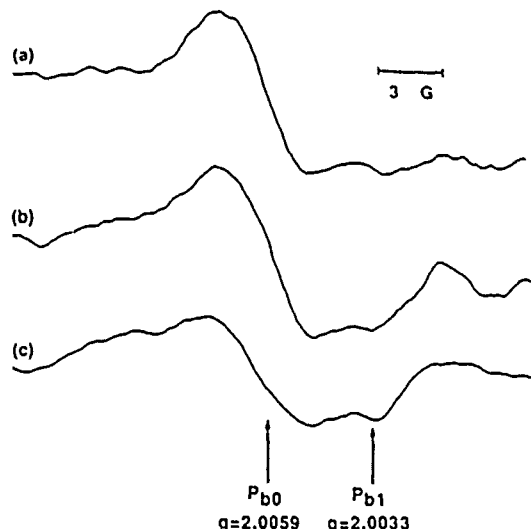


FIG. 3. ESR spectra of three different thermally grown oxides on (100) silicon substrates subjected to (a) 5.7 Mrad under a +20-V gate bias, (b) 6.6 Mrad under a +10-V gate bias, and (c) 10 Mrad under a +24-V gate bias of  $^{60}\text{Co}$   $\gamma$  irradiation. Oxide (a) was grown in a sequence of dry/wet/dry oxygen ambients at 1000 °C to a thickness of 1000 Å; oxide (b) was grown in a sequence of dry/wet/dry oxygen ambients at 1000 °C to a thickness of 1240 Å and annealed in  $\text{N}_2$  at 1140 °C for 720 min; oxide (c) was grown in steam at 900 °C to a thickness of 1000 Å. The magnetic field is perpendicular to the (100) surface.

ue anticipated for  $P_{b1}$  at this orientation would be  $g = 2.0033$ . We observe a very weak resonance at  $g = 2.0033$ , presumably this is due to a very much smaller concentration of  $P_{b1}$  centers. Thus the results of Fig. 3 strongly suggest that the  $P_{b0}$  center is the dominant radiation-induced point defect at the (100) interface, at least for the three oxides evaluated in this experiment.

In order to more convincingly establish whether or not this resonance is the  $P_{b0}$  center, we have measured the  $g$  values as a function of sample orientation. The results are illustrated in Fig. 4. Irradiated oxides were rotated about the [011] axis with the magnetic field rotated from perpendicular to parallel to the (100) crystal face. Since several orientations of  $P_{b0}$  are possible on a single surface, the resonance splits into several lines as the sample is rotated. The solid lines of the figure represent a plot of  $g$  values utilizing  $g_{\parallel} = 2.0015$  and  $g_{\perp} = 2.008$ , where the  $g_{\parallel}$  value corresponds to the [111] axes. (In order to clearly define the  $g$  values we utilized a second derivative technique<sup>35,36</sup> in this mapping study.) Our results clearly demonstrate the presence of the  $P_{b0}$  center in these irradiated Si/ $\text{SiO}_2$  structures.

As mentioned earlier, Lenahan and Dressendorfer<sup>22-24</sup> demonstrated that the  $P_b$  center [on (111) silicon substrates] is an amphoteric interface state with levels widely distributed throughout the gap. Gerardi, Poindexter, and Caplan<sup>12</sup> later found nearly identical behavior for the  $P_{b0}$  center generated by high-temperature processing. We have determined the behavior of radiation-induced  $P_{b0}$  centers as a function of oxide bias in a manner quite similar to that of Lenahan and Dressendorfer<sup>22-24</sup> and Gerardi and co-workers.<sup>12</sup>

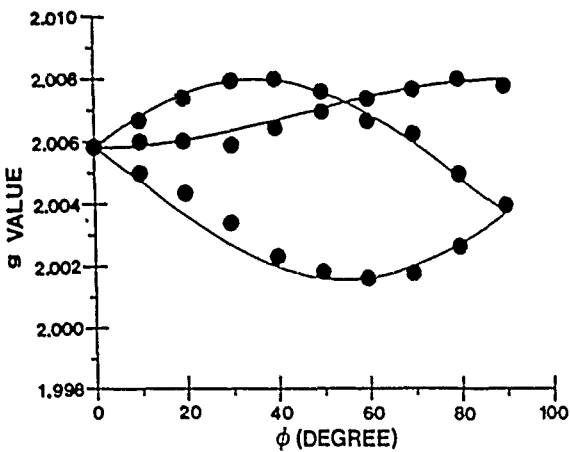


FIG. 4. ESR g-value anisotropy map for  $P_{b0}$  centers on (100) silicon substrates at different values of angle for rotation of the magnetic field in the (011) plane. The solid lines are given by the relation  $g^2 = g_b^2 \cos^2 \theta + g_t^2 \sin^2 \theta$  with  $g_b = 2.0015, g_t = 2.008$ , where  $\theta$  is the angle between the magnetic field and the [111] directions. The abscissa ( $\phi$ ) in the figure is the angle between the magnetic field and the [100] direction.

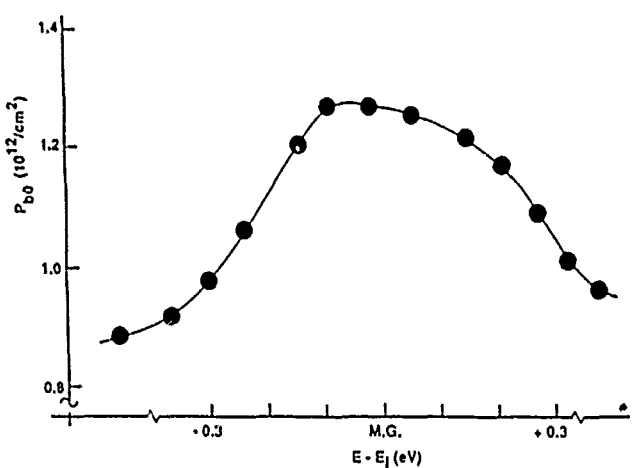


FIG. 6. Population of paramagnetic  $P_{b0}$  centers vs Fermi level. Results were obtained from the data of Fig. 5.

To determine  $P_{b0}$  population as a function of Fermi level at the interface, a potential was applied to irradiated bare oxide Si/SiO<sub>2</sub> structures utilizing a corona-discharge apparatus.<sup>37</sup> This potential was measured with a commercial Kelvin probe electrostatic voltmeter (Monroe 170). The charged bare oxide structures were placed in the TE<sub>104</sub> "double" cavity of an IBM Instruments ER-200 spectrometer. The spin concentrations were calculated by comparison of unsaturated absorption spectra with the spectrum of a calibrated weak-pitch standard. We obtained the position of the Fermi level at the interface from a high-frequency C-V measurement. Results of both measurements are illustrated in Fig. 5. Apparently, most of the change in  $P_{b0}$  signal occurs

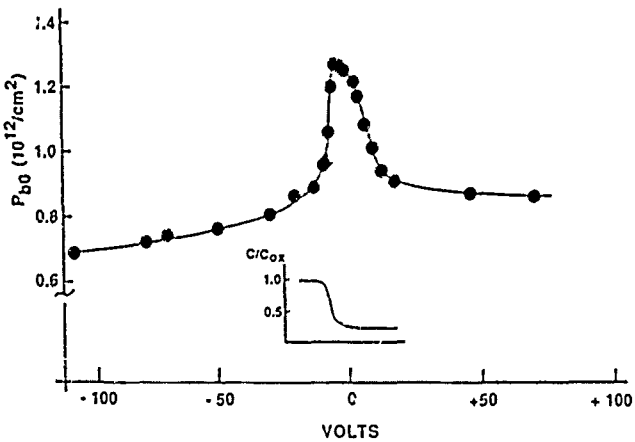


FIG. 5. Density of radiation-induced  $P_{b0}$  centers as a function of bias. The relative spin concentrations are accurate to about  $\pm 10\%$ ; however, absolute spin concentration may be in error by up to a factor of 2. The inset shows high-frequency capacitance  $C$  versus voltage measurements on  $\gamma$ -irradiated (6.6 Mrad) oxide after ultraviolet illumination ( $h\nu/\lambda \approx 5.5$  eV).

in the range of bias in which the Fermi level sweeps through most of the forbidden gap at the interface. The distribution of paramagnetic  $P_{b0}$  versus the position of the Fermi level at the interface is shown in Fig. 6. The distribution of paramagnetic  $P_{b0}$  centers is broadly peaked around midgap. As the Fermi level moves from near the valence-band edge towards midgap, the positively charged  $P_{b0}$  centers accept an electron and become paramagnetic and neutral. As the Fermi level moves from the vicinity of midgap towards the conduction-band edge, the  $P_{b0}$  center picks up another electron, becoming negatively charged and again diamagnetic. In the lower part of the gap  $P_{b0}$  is a donorlike center; in the upper part of the band gap  $P_{b0}$  is an acceptorlike center. The  $P_{b0}$  center is paramagnetic only when it has an unpaired spin (one electron), the paramagnetic  $P_{b0}$  center is converted to a diamagnetic state by either donating or accepting an electron. Our biasing results with regard to the radiation-induced  $P_{b0}$  are thus similar to the results of Lenahan and Dressendorfer<sup>22-25</sup> on the (111) substrate  $P_b$  and are also quite similar to the more recent observation of Gerardi and co-workers<sup>32</sup> on  $P_{b0}$  centers generated by high-temperature processing. The results indicate that radiation-induced  $P_{b0}$  defects are amphoteric interface states with levels widely distributed throughout the band gap.

In Fig. 7, we plot the average density of interface states in the middle half of the band gap versus the density of paramagnetic  $P_{b0}$  centers generated by different radiation dose of  $^{60}\text{Co}$   $\gamma$  irradiation under positive bias (+24 V). We calculate the interface state density from high-frequency (1 MHz) C-V measurements using the Terman technique.<sup>38</sup> The value for  $D_{\text{av}}$  represents the average over the middle half of the band gap, which is thus somewhat arbitrary; it is likely proportional to, but only approximately equal to, the total number of radiation-induced interface states. The  $P_{b0}$  centers and interface states in the middle half of the band gap are generated in approximately equal numbers. Since the  $P_{b0}$  centers are amphoteric interface state defects with levels broadly distributed throughout the band gap, we conclude

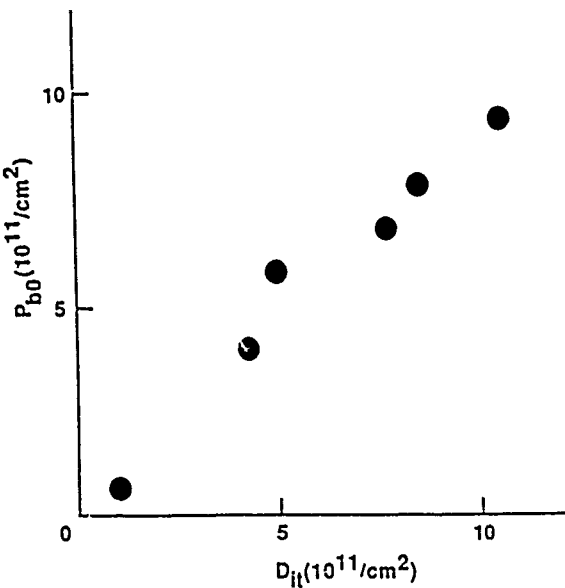


FIG. 7. Density of radiation-induced  $P_{b0}$  centers vs mid-half-band-gap interface state density in MOS devices subjected to  $^{60}\text{Co} \gamma$  irradiation.

the  $P_{b0}$  is the dominant interface state generated by the irradiation.

We subjected irradiated (100) Si/SiO<sub>2</sub> structures to a sequence of 1-h anneals in air. The radiation-induced  $P_{b0}$  and  $D_{it}$  plotted versus isochronal annealing temperature is illustrated in Fig. 8. This figure shows that radiation-induced  $P_{b0}$  density has essentially the same annealing characteristics as radiation-induced interface state density, again strongly indicating that the  $P_{b0}$  centers are primarily responsible for the radiation-induced interface states.

Summarizing our interface center results, we find that  $P_{b0}$  centers are generated in numbers approximately equal

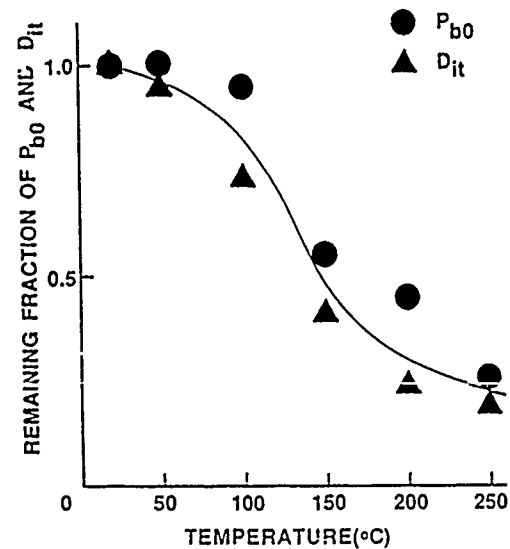


FIG. 8. Plot of remaining fractions of  $P_{b0}$  and  $D_{it}$  as a function of 1 h isochronal annealing temperature.

to that of the radiation-induced interface states, and that these  $P_{b0}$  centers have the same annealing behavior as the radiation-induced interface states. Since the  $P_{b0}$  centers are amphoteric interface state defects we conclude that they are primarily responsible for radiation-induced interface states. Although we have studied only three different sets of processing steps, the fact that we observe an overwhelming preponderance of the  $P_{b0}$  centers in all three suggests that the  $P_{b0}$  center is primarily responsible for the radiation-induced interface states.

### B. Hole traps in the oxide and $E'$ centers

Earlier ESR studies (111) silicon substrate MOS structure have established that  $E'$  centers are primarily responsible for the positive charge buildup.<sup>21,24-26</sup> Although one might naively anticipate that the deep hole trapping centers would be unaffected by the silicon surface orientation, it has been suggested that this is not the case.<sup>39</sup>

We have investigated  $E'$  centers in Al gate MOS devices subjected to approximately 6 Mrad (Si) of  $^{60}\text{Co} \gamma$  irradiation under + 24-V gate bias. The oxides were grown in dry/wet/dry oxygen ambients at 1000 °C to a thickness of 1240 Å and were then annealed in nitrogen at 1140 °C for 720 min. The high-temperature nitrogen anneal renders the oxide relatively radiation intolerant. We have explored  $E'$  centers in these oxides with a combination of ESR, C-V, optical irradiation, and annealing experiments in order to identify the role of  $E'$  in hole trapping.

In Fig. 9(a) a narrow ESR scan illustrates an  $E'$  resonance in a (100) substrate MOS capacitor irradiated to approximately 6 Mrad under positive bias (+ 1 MV/cm). In Fig. 9(b) a preirradiation trace is shown. The resonance line shape, width, and  $g$  value are all virtually identical to those of  $E'$  centers observed earlier on (111) substrate structures.<sup>24-26</sup> Furthermore, the line shape is quite similar to the "powder pattern" one would anticipate if these centers were randomly oriented defects with structure identical to that of  $E'$  centers in irradiated crystalline quartz.<sup>40</sup>

In Fig. 10 we compare the concentration of radiation-induced  $E'$  centers to the concentration of holes trapped in

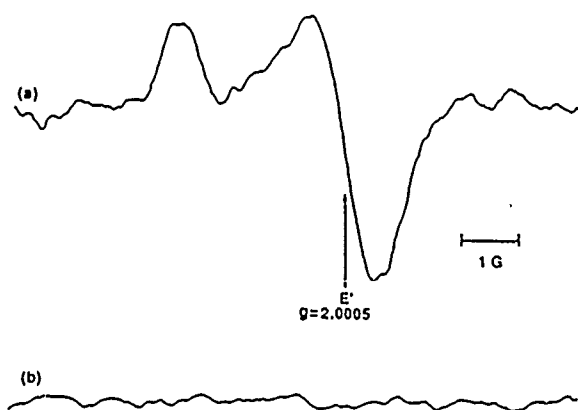


FIG. 9. ESR spectra. (a) Post-irradiation exposed to 6.6 Mrad and (b) preirradiation. The sample gates were biased to + 10 V during the irradiation.

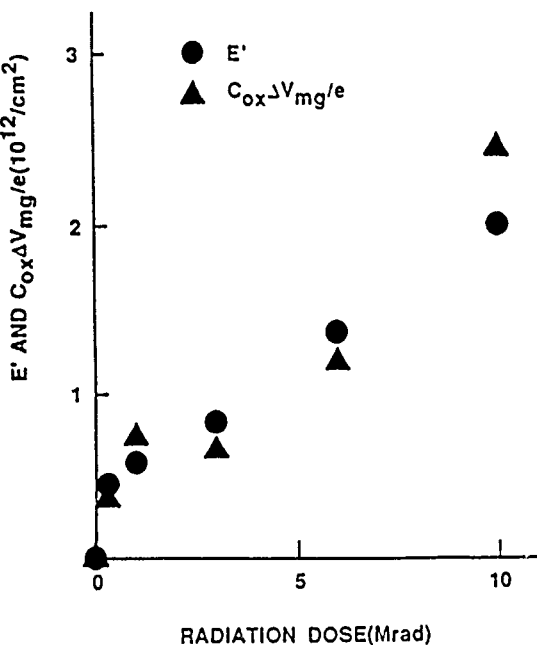


FIG. 10. Density of  $E'$  and  $C_{ox} \Delta V_{mg}/e$  vs irradiation dose for MOS structures with oxides grown on (100) silicon substrates.

the oxide. In order to compute trapped hole concentration we measured the  $C-V$  curve shift corresponding to the Fermi level at midgap  $\Delta V_{mg}$  and multiplied it by the ratio of oxide capacitance ( $C_{ox}$ ) to electronic charge ( $C_{ox} \Delta V_{mg}/e$ ). Since the  $P_{b0}$  interface state centers are electrically neutral when the Fermi level is at midgap, the midgap  $C-V$  shift should accurately represent space charge in the oxide.<sup>24,25</sup> Our results clearly indicate that the number of  $E'$  centers and the number of trapped holes are approximately equal.

In Fig. 11 we investigate the annihilation of  $E'$  centers and trapped positive charges by illuminating irradiated Si/ $\text{SiO}_2$  structures with ultraviolet light ( $h\nu/\lambda < 5.5$  eV). The gates were etched off the 1240-Å oxides which had earlier

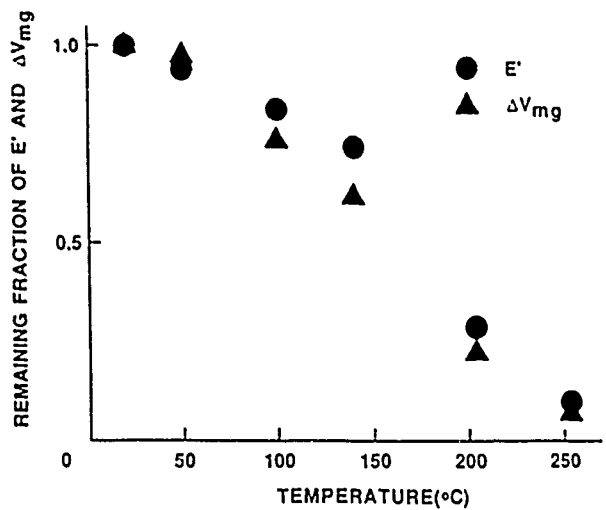


FIG. 12. Plot of remaining fractions of  $E'$  and  $\Delta V_{mg}$  as a function of isochronal annealing (1 h in air) temperature.

been irradiated to approximately 6 Mrad with a +24-V gate bias. The UV irradiation results in the internal photoemission of electrons into the oxide.<sup>33,34</sup> The photoemitted electrons annihilate the trapped positive charges. As the figure clearly shows, the annihilation of positive charge is accompanied by the elimination of  $E'$  centers.

In Fig. 12 we present the results of a sequence of isochronal anneals on both the positive charge in the oxide (percentage of  $\Delta V_{mg}$ ) and  $E'$  concentration. As the figure shows, the annealing characteristics of  $E'$  and positive charge are, within experimental error, identical.

Summarizing our hole trap results, we find that  $E'$  centers are generated in numbers approximately equal to the number of holes trapped in the oxides, the trapped holes and  $E'$  centers have identical annealing characteristics and are identically annihilated by the photoemission of electrons into the oxide. Our results for the  $E'$  centers are thus completely consistent with earlier results of studies involving (111) substrate MOS capacitors. Apparently, the  $E'$  center is the dominant deep hole trap in thermal oxides on both (100) and (111) silicon substrates.

#### IV. DISCUSSION

One of the great mysteries of the radiation damage phenomena is the mechanism by which positive charge in the oxide creates interface states. Winokur *et al.*<sup>4,5,11-13</sup> have extensively characterized the effects of oxide field and temperature upon both the rate and final density of radiation-induced interface states. Winokur *et al.*<sup>5</sup> have proposed that the damage process involves some sort of interaction of the hole in the oxide which creates a species (perhaps hydrogen) which then drifts to the Si/ $\text{SiO}_2$  interface creating a silicon dangling bond ( $P_b$  center). Lyon and co-workers<sup>44-46</sup> have attempted to link the trapped hole to the process which leads to the eventual creation of the interface states. Grunthaner *et al.*<sup>47-49</sup> have proposed a complex stress-related bond-breaking process at the site of hole capture which eventually leads

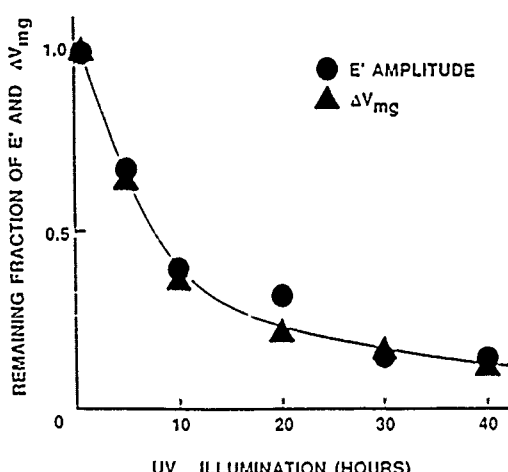


FIG. 11. Plot of remaining fractions of  $E'$  and  $\Delta V_{mg}$  as a function of UV illumination.

to a creation of the interface states. Zekeriya and Ma<sup>50</sup> have provided experimental evidence which suggests that stress may indeed play a role in the process.

Our study may provide some insight into the interface state creation process. Poindexter *et al.*<sup>28</sup> were able to observe two kinds of interface defects ( $P_{b0}$  and  $P_{b1}$ ) in their studies of high-temperature processing variations. Our results, although they involve only three kinds of oxides, suggest that a single center,  $P_{b0}$ , is largely responsible for the radiation-induced interface state defects. The mechanism which creates dangling bonds at the interface is far more capable of creating  $P_{b0}$  centers than  $P_{b1}$  centers. Our observation regarding the preponderance of  $P_{b0}$  centers and almost complete absence of  $P_{b1}$  may be useful in evaluating detailed models of interface state formation.

## V. CONCLUSIONS

We find that the  $P_{b0}$  center appears to be primarily responsible for radiation-induced interface states in Si/SiO<sub>2</sub> structures on (100) silicon substrates. We also find that the  $E'$  spectrum on (100) silicon substrates is virtually identical to the quartz  $E'$  powder pattern and the spectrum observed in oxides grown on (111) silicon substrates. We find that  $E'$  centers are largely responsible for trapped positive charges in (100) silicon substrate oxides. Our results for (100) substrate oxides demonstrate that the earlier results obtained on (111) substrate devices<sup>20-25</sup> are generally valid, essentially the same defects are responsible for the radiation damage process in both cases.

## ACKNOWLEDGMENTS

We wish to thank Carl Schlier of IBM Federal Systems, and Paul Dressendorfer of Sandia National Laboratories, for providing us with MOS devices. This work was supported by IBM Federal Systems under Contract No. WF-158675 and by Sandia National Laboratories under Contract No. 02-8399.

- <sup>1</sup>H. L. Hughes and R. R. Giroux, *Electronics* 37, 58 (1964).
- <sup>2</sup>J. R. Szedon and J. E. Sandor, *Appl. Phys. Lett.* 6, 181 (1965).
- <sup>3</sup>R. J. Powell and G. F. Derbenwick, *IEEE Trans. Nucl. Sci.* NS-18, 99 (1971).
- <sup>4</sup>P. S. Winokur and M. M. Sokoloski, *Appl. Phys. Lett.* 28, 627 (1976).
- <sup>5</sup>P. S. Winokur, H. E. Boesch, Jr., J. M. McGarrity, and F. B. McLean, *J. Appl. Phys.* 50, 3492 (1979).
- <sup>6</sup>G. Hu and W. C. Johnson, *Appl. Phys. Lett.* 36, 590 (1980).
- <sup>7</sup>F. B. McLean, *IEEE Trans. Nucl. Sci.* NS-27, 1651 (1980).

- <sup>8</sup>S. M. Sze, *ICSI Technology* (McGraw-Hill, New York, 1983), p. 267, and references therein.
- <sup>9</sup>A. G. Revesz, *IEEE Trans. Nucl. Sci.* NS-18, 113 (1971).
- <sup>10</sup>W. C. Johnson, *IEEE Trans. Nucl. Sci.* NS-22, 2144 (1975).
- <sup>11</sup>C. T. Sah, *IEEE Trans. Nucl. Sci.* NS-23, 1563 (1976).
- <sup>12</sup>M. Pepper, *Thin Solid Films* 14, S7 (1972).
- <sup>13</sup>B. E. Deal, *J. Electrochem. Soc.* 121, 198C (1974).
- <sup>14</sup>C. T. Sah, *IEEE Trans. Nucl. Sci.* NS-23, 1563 (1976).
- <sup>15</sup>C. Svensson, in *The Physics of SiO<sub>2</sub> and Its Interface*, edited by S. T. Pantelides (Pergamon, New York, 1978), p. 328.
- <sup>16</sup>Y. Nishi, *Jpn. J. Appl. Phys.* 5, 333 (1965).
- <sup>17</sup>Y. Nishi, T. Tanaka, and Ohwada, *Jpn. J. Appl. Phys.* 11, 85 (1972).
- <sup>18</sup>R. B. Laughlin, J. O. Joannopoulos, and D. J. Chadi, *Phys. Rev. B* 21, 5733 (1980).
- <sup>19</sup>J. Singh and A. Madhukar, *Appl. Phys. Lett.* 38, 884 (1981).
- <sup>20</sup>P. M. Lenahan, K. L. Brower, P. V. Dressendorfer, and W. C. Johnson, *IEEE Trans. Nucl. Sci.* NS-28, 4105 (1981).
- <sup>21</sup>P. M. Lenahan and P. V. Dressendorfer, *IEEE Trans. Nucl. Sci.* NS-29, 1459 (1982).
- <sup>22</sup>P. M. Lenahan and P. V. Dressendorfer, *Appl. Phys. Lett.* 41, 542 (1982).
- <sup>23</sup>P. M. Lenahan and P. V. Dressendorfer, *J. Appl. Phys.* 54, 1457 (1983).
- <sup>24</sup>P. M. Lenahan and P. V. Dressendorfer, *Appl. Phys. Lett.* 44, 96 (1984).
- <sup>25</sup>P. M. Lenahan and P. V. Dressendorfer, *J. Appl. Phys.* 55, 3495 (1984).
- <sup>26</sup>P. M. Lenahan and P. V. Dressendorfer, *IEEE Trans. Nucl. Sci.* NS-30, 4602 (1983).
- <sup>27</sup>P. J. Caplan, E. H. Poindexter, B. E. Deal, and R. R. Razouk, *J. Appl. Phys.* 50, 5847 (1979).
- <sup>28</sup>E. H. Poindexter, P. J. Caplan, B. E. Deal, and R. R. Razouk, *J. Appl. Phys.* 52, 879 (1981).
- <sup>29</sup>E. H. Poindexter, P. J. Caplan, J. J. Finnegan, N. M. Johnson, D. K. Biegelson, and M. D. Moyer, in *The Physics of MOS Insulators*, edited by G. Lucovsky, S. T. Pantelides, and F. L. Galeener (Pergamon, New York, 1980), p. 326.
- <sup>30</sup>E. H. Poindexter, G. J. Gerardi, M.-E. Rueckel, and P. J. Caplan, *J. Appl. Phys.* 56, 2844 (1984).
- <sup>31</sup>A. Stesmans, J. Braet, J. Witters, and R. F. Dekeersmaecker, *Surf. Sci.* 141, 255 (1984).
- <sup>32</sup>G. J. Gerardi, E. H. Poindexter, and P. J. Caplan, *Appl. Phys. Lett.* 49, 348 (1986).
- <sup>33</sup>H. S. Witham and P. M. Lenahan, *Appl. Phys. Lett.* 51, 1007 (1987).
- <sup>34</sup>H. S. Witham and P. M. Lenahan, *IEEE Trans. Nucl. Sci.* NS-34, 1147 (1987).
- <sup>35</sup>D. E. Wood, in *Electron Spin Resonance of Metal Complexes*, edited by T. F. Yen (Plenum, New York, 1969), p. 135.
- <sup>36</sup>T. Halpern and W. D. Phillips, *Rev. Sci. Instrum.* 41, 1038 (1970).
- <sup>37</sup>Z. A. Weinberg, D. L. Matthies, W. C. Johnson, and M. A. Lampert, *Rev. Sci. Instrum.* 46, 201 (1975).
- <sup>38</sup>L. M. Terman, *Solid State Electron.* 5, 285 (1962).
- <sup>39</sup>W. E. Carlos, *Appl. Phys. Lett.* 49, 1767 (1986).
- <sup>40</sup>R. A. Weeks, *J. Appl. Phys.* 27, 1376 (1956).
- <sup>41</sup>P. S. Winokur, E. B. Errett, D. M. Fleetwood, P. V. Dressendorfer, and D. C. Turpin, *IEEE Trans. Nucl. Sci.* NS-32, 3954 (1985).
- <sup>42</sup>P. S. Winokur, J. M. McGarrity, and H. E. Boesch, Jr., *IEEE Trans. Nucl. Sci.* NS-23, 1580 (1976).
- <sup>43</sup>P. S. Winokur, H. E. Boesch, Jr., J. M. McGarrity, and F. B. McLean, *IEEE Trans. Nucl. Sci.* NS-24, 2113 (1977).
- <sup>44</sup>S. A. Lyon, *AIP Conf. Proc.* 122, 8 (1984).
- <sup>45</sup>S. Pang, S. A. Lyon, and W. C. Johnson, *Appl. Phys. Lett.* 40, 709 (1982).
- <sup>46</sup>S. T. Chang, J. K. Wu, and S. A. Lyon, *Appl. Phys. Lett.* 48, 662 (1986).
- <sup>47</sup>F. J. Grunthaner, P. J. Grunthaner, and J. Maserjian, *IEEE Trans. Nucl. Sci.* NS-29, 1462 (1982).
- <sup>48</sup>F. J. Grunthaner, B. F. Lewis, N. Zaman, J. Maserjian, and A. Madhukar, *IEEE Trans. Nucl. Sci.* NS-27, 1640 (1980).
- <sup>49</sup>F. J. Grunthaner and P. J. Grunthaner, *Mater. Sci. Rep.* 1, 09 (1980).
- <sup>50</sup>V. Zekeriya and T. P. Ma, *IEEE Trans. Nucl. Sci.* NS-31, 1261 (1984).

### B. Fundamental Nature of the Deep Hole Trap

We use ultraviolet irradiations, alternately flooding MOS oxides with holes and electrons, to explore the fundamental nature of the (E') deep hole trap. The results were published in the December 1987 issue of IEEE Transactions on Nuclear Science.

# THE NATURE OF THE DEEP HOLE TRAP IN MOS OXIDES

Howard S. Witham and Patrick M. Lenahan  
The Pennsylvania State University  
University Park, PA 16802

## ABSTRACT

We have investigated hole and electron trapping events at E' deep hole traps in metal-oxide-semiconductor oxides. Using a sequence of ultraviolet irradiations, electron spin resonance measurements, and capacitance versus voltage measurements, we have obtained results which are completely consistent with a simple oxygen vacancy model for the hole trap. However, our results are inconsistent with the bond strain gradient model proposed by Grunthaner et al.

## INTRODUCTION

In 1964 Hughes and Giroux [1] found that ionizing radiation can be severely damaging to metal-oxide-silicon (MOS) field effect transistors (MOSFETS). Over the past twenty years it has been well established that the radiation damage process results in the creation of interface states at the Si-SiO<sub>2</sub> interface [2-11]. The creation of interface states and the buildup of positive charge due to ionizing radiation causes a reduction of transconductance and channel conductance and also causes threshold voltage shifts. The technological significance of the problem has stimulated intense study. Many models have been formulated to describe the chemical structure of the point defects responsible for the hole traps in the oxide [12-14] and the interface states [13-26]. It has been established that the radiation induced interface states are primarily caused by the presence of a center at the Si-SiO<sub>2</sub> interface called the P<sub>b</sub> defect. Nishi et al. [27] first saw the P<sub>b</sub> electron spin resonance (ESR) signal in unirradiated oxides and proposed that the P<sub>b</sub> defect was a trivalent silicon center at or near the Si-SiO<sub>2</sub> interface. Later Caplan et al. [28] followed with experimental evidence that proved that the P<sub>b</sub> defect was a trivalent silicon bonded to three other silicon atoms with an unsatisfied bond. Recently, Lenahan and Dressendorfer [24] have found the P<sub>b</sub> center to be an amphoteric interface state defect and also have shown that the density of radiation induced interface state defects equaled the number of P<sub>b</sub> defects [25,26].

Although the structure of the P<sub>b</sub> defect is fairly well established, there are still questions regarding the defect responsible for trapping holes. Lenahan and Dressendorfer have also found that an oxygen deficient silicon defect in the oxide, termed the E' center [27,30-32] is the deep hole trap. Among the various models proposed to account for the radiation induced hole trap, two have emerged as the most popular. One point of view is that the entire radiation damage process is initiated by a bond breaking event at the site of hole capture. Grunthaner and co-workers have proposed two variations of what they term the bond strain gradient (BSG) model [33-36]. In both variations the radiation damage process is initiated by the capture of a hole at the site of a strained

silicon-oxygen bond. In both cases the subsequent capture of an electron at the hole trap site leads to a complex rearrangement process culminating in the creation of a P<sub>b</sub> center interface state defect at the Si-SiO<sub>2</sub> boundary. Another prominent point of view proposed by Deal [17], Johnson [13], and Woods and Williams [37], suggests that the hole trap is simply an oxygen vacancy. In an oxygen vacancy model, an oxygen deficient Si-Si site would capture a hole leaving behind an unpaired electron residing primarily in an sp hybridized orbital on one of the silicon atoms. The unpaired electron on the silicon atom would be paramagnetic and ESR detectable.

## RESULTS AND DISCUSSION

In our experiments we subjected MOS devices to a series of ultraviolet (UV) irradiations to distinguish between the two most commonly held views of the hole trap. The samples utilized in measurements reported in this paper were all in the form of 4 x 30 mm bars of lightly doped ( $\rho=100$  ohm-cm) thermally oxidized (111) silicon substrates with semitransparent metal gates. We used 3500 Å thick oxides on n-type substrates and 1000 Å thick oxides on p-type substrates. Both oxides were grown in a sequence of dry oxygen-steam-dry oxygen ambients at a temperature of 1000° C. The 3500 Å thick oxides had sputtered palladium gates of 150 Å. The 1000 Å thick oxides had evaporated aluminum gates of 200 Å. We found that both oxides gave qualitatively very similar results. Thus, we present only the results obtained from the 3500 Å samples.

With the 3500 Å thick oxides we first subjected the devices to a forty-five minute irradiation in a vacuum ultraviolet (VUV) system with a positive gate bias. In this irradiation VUV light ( $hc/\lambda > 10$  eV) from a 50 watt McPherson model 632 deuterium source with a LiF window penetrates through the semitransparent gate and is absorbed in the top 100 Å of the oxide, creating electron-hole pairs. The deuterium source provides a very sharp emission line at 10.2 eV. With an absorption depth of 100 Å into the oxide for  $hc/\lambda > 10$  eV, virtually no light reaches the Si-SiO<sub>2</sub> interface. As shown in Figure 1, by applying a bias of 35 volts to the gate, we drive holes to the deep oxide traps (E' centers) near the Si-SiO<sub>2</sub> interface [5,8] while the electrons are swept out the gate. After VUV irradiation the semitransparent gates were removed to facilitate ESR measurements. All ESR measurements were made using an IBM Instruments ER 200 X-band electron spin resonance spectrometer. After the initial VUV irradiation under bias, the devices were subjected to a second UV irradiation of sub SiO<sub>2</sub> band gap illumination from a 4 watt xenon-mercury lamp ( $hc/\lambda < 5.5$  eV). In this illumination there are essentially no photons incident on the samples (i.e.  $hc/\lambda > 8.8$  eV, the bandgap of SiO<sub>2</sub>) which will be absorbed by the SiO<sub>2</sub>. Thus the second

irradiation causes photons to pass through the  $\text{SiO}_2$  and into the Si resulting in the internal photoemission of electrons from the Si into the  $\text{SiO}_2$  where they are then trapped at the positively charged  $E'$  sites. Figure 2 illustrates the internal photoemission of electrons from the silicon into the oxide.

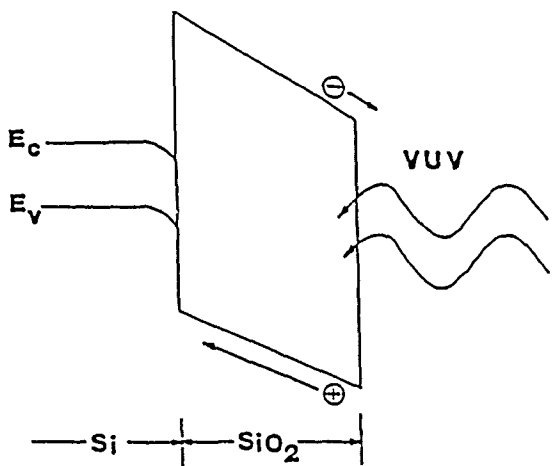


Figure 1 This figure shows a band diagram in which electron-hole pairs are created by the VUV photons. With a strong positive bias applied the holes drift toward the interface and are trapped at  $E'$  center hole traps.

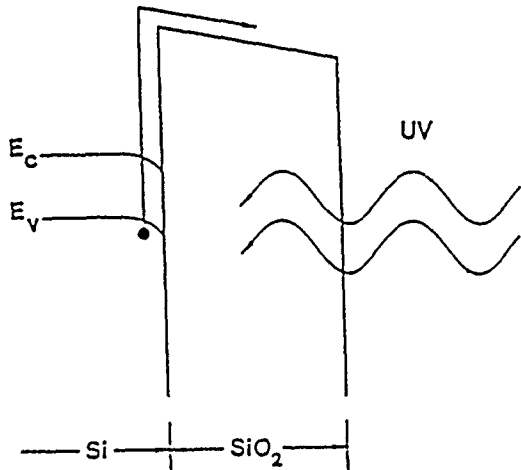


Figure 2 This is a band diagram showing the second UV illumination ( $hc/\lambda < 5.5$  eV) and internal photoemission of electrons. This figure illustrates that electrons are injected into the silicon dioxide.

The electrical and ESR results of both irradiations are shown in Figures 3 and 4. In Figure 3a, the preirradiation capacitance versus voltage (CV) curve indicates almost no surface states or positive charge in the oxide. Figure 3b shows a CV curve after the initial irradiation and hole injection. It can be seen from the negative midgap voltage shift that positive charge has been trapped in the oxide. The stretch out of this curve indicates that

interface states have been generated. In Figure 3c the midgap voltage has shifted back to nearly the preirradiation value after the second UV illumination and internal photoemission of electrons. In Figure 4a we illustrate the post VUV (first irradiation and hole injection) ESR trace of the  $E'$  center. Figure 4b illustrates the ESR trace of the  $E'$  center after the second UV illumination and electron injection. Figure 4 indicates a dramatic decrease in the  $E'$  resonant amplitude which is consistent with the decrease in positive charge observed in the CV measurement of Figure 3, further indicating a common origin of the  $E'$  ESR center and the positive charge.

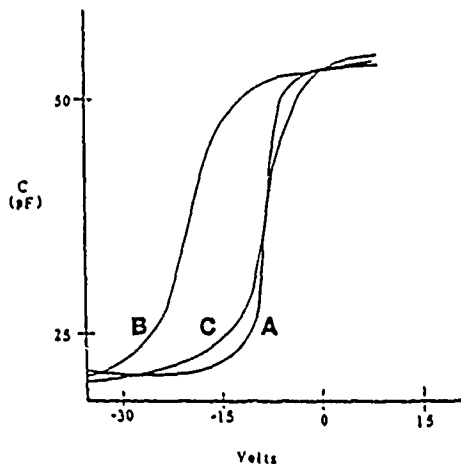


Figure 3 CV curves taken (A) before VUV illumination (B) after VUV illumination and (C) after VUV illumination and subsequent ( $hc/\lambda < 5.5$  eV) UV illumination.

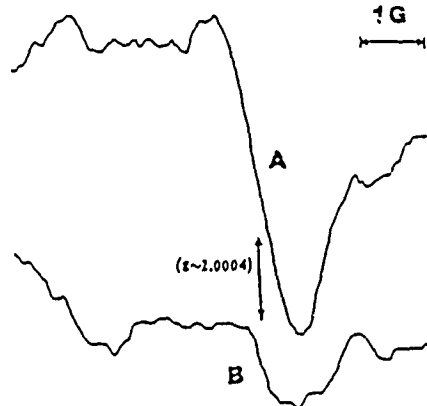


Figure 4 ESR traces of the  $E'$  center taken (A) after VUV illumination and (B) after subsequent ( $hc/\lambda < 5.5$  eV) UV illumination.

Figure 5 illustrates several "wide" scan ESR traces with the magnetic field parallel to the  $\text{Si}-\text{SiO}_2$  interface. These "wide" scan traces illustrate the effect of the ultraviolet illuminations on both the  $P_b$  and  $E'$  centers. Figure 5a is a preirradiation ESR trace showing no  $P_b$  or  $E'$  centers in the samples. In 5b the

ESR curve shows that both  $P_b$  (interface state defect) and  $E'$  (hole trap defect) resonances are generated after irradiation under a positive bias. Again the generation of interface states ( $P_b$  centers) and positive charge in the oxide ( $E'$  centers) is consistent with the stretch out and negative midgap voltage shift in the CV curve of Figure 3b. Figure 5c is a "wide" scan ESR trace after UV illumination and electron injection. The  $E'$  resonance amplitude has been substantially reduced while the  $P_b$  resonance has remained relatively unchanged. This is also consistent with the stretch out and midgap voltage shift of the CV curve in Figure 4c which indicates the presence of surface states and little positive charge in the oxide.

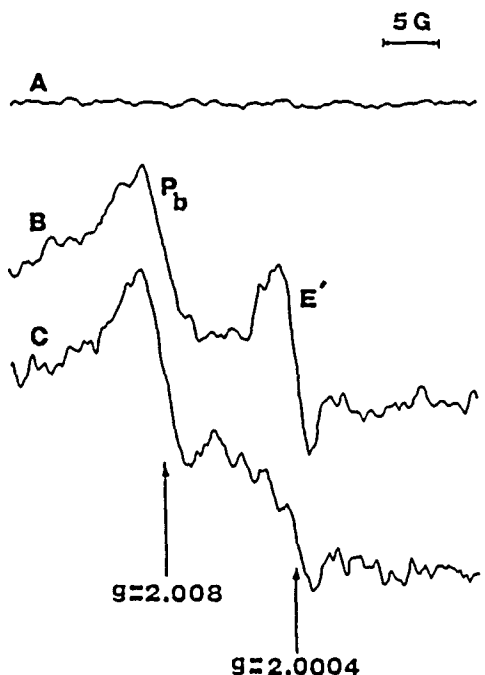


Figure 5 Wide scan ESR traces of  $P_b$  and  $E'$  centers (A) before VUV illumination, (B) after VUV illumination, and (C) after subsequent ( $h\nu/\lambda < 5.5$  eV) UV illumination.

Both variations of the BSG model [33,36] propose that the capture of holes would result in irreversible Si-O bond breaking events. Our results are inconsistent with both of the BSG variations, but are totally consistent with a simple oxygen vacancy model for the  $E'$  hole trap. In the more recent BSG model [36] the trapping of holes ruptures strained Si-O bonds in the near interfacial region. This results in the generation of two species: (1) a neutral non-bridging oxygen defect and (2) a positively charged trivalent silicon (the positive charge resides on the silicon side of the broken bond). The positively charged silicon is not ESR active. This is inconsistent with the  $E'$  ESR trace (Figure 4a) we see after the first VUV illumination and hole trapping. It is quite well established that the  $E'$  ESR center is an unpaired electron on a Si atom [38-40]. In Figure 4a we see an ESR trace which indicates the presence of unpaired electrons on silicon atoms after hole trapping. The fact that an  $E'$  ESR trace appears

after the trapping of holes directly contradicts the most recent BSG model. Furthermore, the fact that subsequent electron capture at the hole trap site annihilates the  $E'$  resonance is also inconsistent with the more recent BSG model. In the more recent BSG model, the electron capture event would create a paramagnetic trivalent silicon center (ESR active  $E'$  center).

Both the earlier Grunthaner BSG model and the oxygen vacancy model predict  $E'$  center (unpaired electrons on Si atoms) generation at the site of hole capture after irradiation with a positive gate. The models differ radically in predicting what would happen when an electron is captured at the positively charged  $E'$  site. In the oxygen vacancy model, one would expect electron capture to render the  $E'$  site diamagnetic and ESR inactive. In the earlier BSG model, if an electron is captured at the broken bond site, it is captured on the oxygen side of the broken bond which then drifts to the Si-SiO<sub>2</sub> interface and creates the trivalent  $P_b$  defect. If the Grunthaner model were correct, the ESR  $E'$  center would not disappear after electron injection. In Figures 6-8, we illustrate the predictions of both BSG models and the oxygen vacancy model with regard to the hole capture, electron capture sequence.

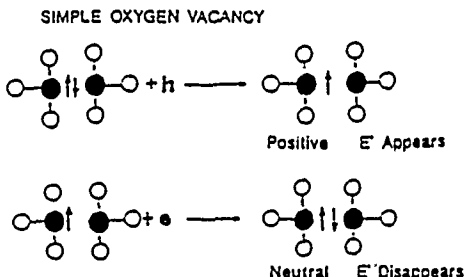


Figure 6 Schematic illustration of the hole trapping event followed by subsequent electron capture in the simple oxygen vacancy model.

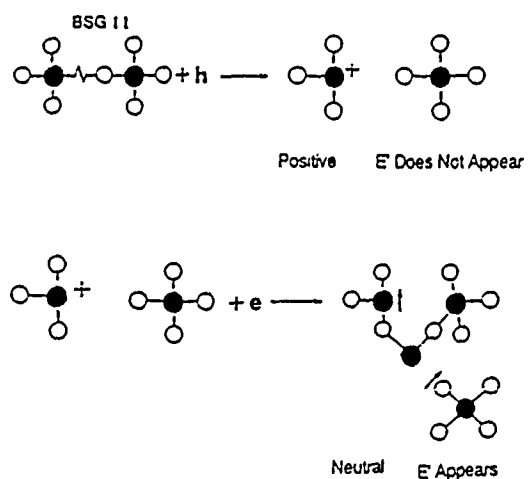


Figure 7 Schematic illustration of the hole trapping event followed by subsequent electron capture in the more recent bond strain gradient model.

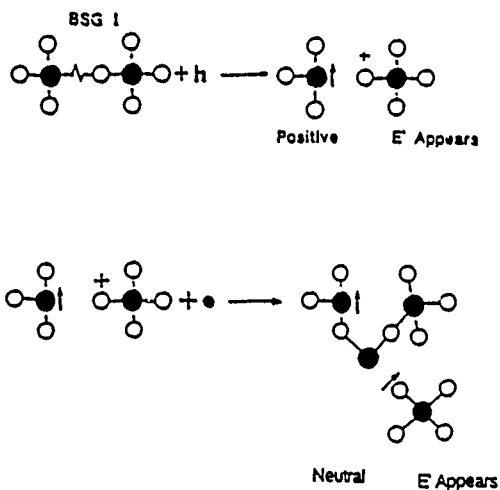


Figure 8 Schematic illustration of the hole trapping event followed by subsequent electron capture in the original bond strain gradient model.

The results of our ultraviolet illumination experiments are completely consistent with the oxygen vacancy model for the hole trap. If the E' centers are simple oxygen vacancies, the capture of a hole renders them paramagnetic and ESR active. The ESR trace of Figure 4a shows that E' centers are generated after VUV illumination with positive gate bias. The negative midgap voltage shift of Figure 3b indicates positive charge is generated in the oxide by the VUV illumination. The results of the second illumination with sub SiO<sub>2</sub> bandgap ( $h\nu/\lambda < 5$  eV) photons (after hole trapping) are also consistent with the oxygen vacancy model. In the oxygen vacancy model, after electron injection one would expect that the positively charged E' centers would trap the electrons, leaving the E' centers paramagnetic (ESR inactive) and electrically neutral. In the sub SiO<sub>2</sub> bandgap UV irradiation, we find the E' ESR signal decreases dramatically as shown in Figure 4b. Figure 3c shows that the midgap voltage has shifted back to nearly the preirradiation value after the second UV illumination. This indicates that most of the trapped positive charge has been eliminated. Clearly, our data strongly supports an oxygen vacancy model. In addition to our results, the work of Griscom [38] and Feigl *et al.* [40] involving E' centers in bulk SiO<sub>2</sub> strongly suggests that the E' s they observed are simply holes trapped in oxygen vacancies.

An extremely significant difference between the two chemical models (BSG and oxygen vacancy) is that of reversibility. One would expect the hole trapping event in the BSG model to be a completely irreversible process. In the earlier BSG view, the capture of an electron would not render the positively charged paramagnetic hole trap diamagnetic. In the more recent BSG model the initial capture of a hole at the trap site would not generate an unpaired spin on a silicon atom. In this more recent model, the subsequent capture of an electron at the positively charged center would generate an unpaired spin on a silicon. Our results are fundamentally inconsistent with both sets of predictions. Our results demonstrate that the deep hole trap is fundamentally a reversible defect. This is

inconsistent with both bond strain gradient models. If the hole trap is a simple oxygen vacancy, one would clearly anticipate an electron capture event to render the positively charged paramagnetic center diamagnetic and ESR inactive. This is consistent with our experiments, and strongly suggests that the deep hole trap in MOS SiO<sub>2</sub> is a Si-Si defect deficient of an oxygen atom. Our results do not disprove the idea of strain-gradient driven defect migration, but do show that the BSG model of Grunthaner *et al.* is not the mechanism for the generation of radiation induced Pb interface states and E' hole trap centers.

#### ACKNOWLEDGMENTS

We wish to thank Carl Schlier of IBM Federal Systems and Paul Dressendorfer of Sandia National Laboratories for the provision of samples. This work is supported by IBM Federal Systems under contract XW-131570 and WF-158675 and Sandia National Laboratories under contract 95-0018.

#### REFERENCES

- [1] H.L. Hughes and R.R. Giroux, *Electronics* 37, 58 (1964).
- [2] K.H. Zaininger, *IEEE Trans. Nucl. Sci.* NS-13, 237 (1966).
- [3] J.R. Szedon and J.E. Sandor, *Appl. Phys. Lett.* 6, 181 (1965).
- [4] E. Kool, *Phillips Res. Rep.*, 20, 306 (1965).
- [5] R.J. Powell and G.F. Derbenwick, *IEEE Trans. Nucl. Sci.* NS-18, 99 (1971).
- [6] A.M. Goodman, *Phys. Rev.* 152, 780 (1966).
- [7] E.H. Snow, A.S. Grove and D.J. Fitzgerald, *Proc. IEEE* 55, 1168 (1967).
- [8] P.S. Winokur and M.M. Sokoloski, *Appl. Phys. Lett.* 28, 627 (1976).
- [9] P.S. Winokur, H.E. Boesch, Jr., J.M. McGarrity, and F.B. McLean, *Appl. Phys.* 50, 3492 (1979).
- [10] G.H. Hu and W.C. Johnson, *Appl. Phys. Lett.* 36, 590 (1980).
- [11] F.B. McLean, *IEEE Trans. Nucl. Sci.* NS-27, 1651 (1980).
- [12] A.G. Revesz, *IEEE Trans. Nucl. Sci.* NS-18, 113 (1971).
- [13] W.C. Johnson, *IEEE Trans. Nucl. Sci.* NS-22, 2144 (1975).
- [14] C.T. Sah, *IEEE Trans. Nucl. Sci.* NS-23, 1563 (1976).
- [15] C.M. Svensson, In the *Physics of SiO<sub>2</sub> and Its Interfaces*, Edited by S.T. Pantelides (Pergamon, New York, 1978), p. 238.
- [16] C.T. Sah, *IEEE Trans. Nucl. Sci.* NS-23 1563 (1976).
- [17] B.E. Deal, *J. Electrochem. Soc.* 121, 198c (1974).
- [18] K.J. Nagi and C.T. White, *J. Appl. Phys.* 52, 320 (1981).
- [19] T. Sakurai, and T. Sugano, *J. Appl. Phys.* 52, 2889 (1981).
- [20] A.G. Revesz, *IEEE Trans. Nucl. Sci.* NS-24, 2102 (1977).
- [21] M. Pepper, *Thin Solid Films* 14, 57 (1972).
- [22] R.B. Laughlin, J.O. Joannopoulos, and D.J. Chadi, *Phys. Rev. B* 21, 523 (1980).
- [23] J. Singh and A. Madhukar, *Appl. Phys. Lett.* 38, 884 (1981).
- [24] P.M. Lenahan and P.V. Dressendorfer, *Appl. Phys. Lett.* 41, 542 (1982).
- [25] P.M. Lenahan and P.V. Dressendorfer, *IEEE Trans. Nucl. Sci.* NS-28, 4105 (1981).
- [26] P.M. Lenahan and P.V. Dressendorfer, *J. Appl. Phys.* 54, 1457 (1983).

- [27] P.M. Lenahan and P.V. Dressendorfer, *J. Appl. Phys.* 55, 3495 (1984).
- [28] Y. Nishi, K. Tanaka, and A. Ohwada, *J. Appl. Phys.* 11, 85 (1972).
- [29] P.J. Caplan, E.H. Poindexter, B.E. Deal, and R.R. Razouk, *J. Appl. Phys.* 50, 5847 (1979).
- [30] P.M. Lenahan and P.V. Dressendorfer, *IEEE Trans. Nucl. Sci.* NS-29, 1459 (1982).
- [31] P.M. Lenahan and P.V. Dressendorfer, *Appl. Phys. Lett.* 44, 96 (1984).
- [32] R.A. Weeks, *J. Appl. Phys.* 27, 1376 (1956).
- [33] F.J. Grunthaner, P.J. Grunthaner, and J. Maserjian, *IEEE Trans. Nucl. Sci.* NS-29, 1462 (1982).
- [34] F.J. Grunthaner, B.F. Lewis, N. Zamani, and J. Maserjian, *IEEE Trans. Nucl. Sci.* NS-27, 1640 (1980).
- [35] F.J. Grunthaner, P.J. Grunthaner, R.P. Vasquez, B.F. Lewis, and J. Maserjian, *Phys. Rev. Lett.* 43, 1683 (1979).
- [36] F.J. Grunthaner and P.J. Grunthaner, *Mat. Sci. Rep.* 1, 69 (1986).
- [37] M.H. Woods and R. Williams, *J. Appl. Phys.* 47, 1082 (1976).
- [38] D.L. Griscom, *Phys. Rev.* 22, 4192 (1980).
- [39] F.J. Feigl, W.B. Fowler, and K.L. Yip, *Solid State Commun.* 14, 225 (1974).
- [40] R.H. Silsbee, *J. Appl. Phys.* 32, 1459 (1961).

### C. Comparison of Radiation and High Field Stressing Damage in MOS Devices

We have compared gamma irradiated and high field stressed MOS oxides via ESR. We find that the Si/SiO<sub>2</sub> interface is affected in about the same way by irradiation and high field stressing ; in both cases we observe substantial generation of P<sub>b</sub> centers. We find qualitative differences defect generation in the oxides. After irradiation we observe a nearly one to one correspondence between positive charge and E' centers. This is not the case in high field stressed oxides. We published our findings in the December 1987 issue of IEEE Transactions on Nuclear Science.

A COMPARISON OF POSITIVE CHARGE  
GENERATION IN HIGH FIELD STRESSING AND  
IONIZING RADIATION ON MOS STRUCTURES

W.L. Warren and P.M. Lenahan  
The Pennsylvania State University  
Department of Engineering Science and Mechanics  
University Park, PA 16802

ABSTRACT

We compare the effects of ionizing radiation and high field stressing on Metal-Oxide-Silicon oxides. Using electron spin resonance, we compare the point defects responsible for the positive charge generated by ionizing radiation and high field stressing. We find the two processes to be different in that the positive charge generated by ionizing radiation is almost entirely due to E' centers in the oxide; however, less than half the positive charge generated by high field stressing can be accounted for by E' centers.

INTRODUCTION

The effects of ionizing radiation and high field stressing on Metal-Oxide-Silicon (MOS) structures are of considerable interest. In both cases the electronic properties of the oxide and the silicon/silicon dioxide ( $\text{Si}/\text{SiO}_2$ ) interface are damaged by the generation of positive charge and interface states.<sup>1-6</sup> Several investigators<sup>5,6</sup> have compared the effects of these two processes. Boesch and McGarrity<sup>6</sup> have shown that high field electron injection measurements can be used to predict the radiation hardness of MOS devices. They suggested that high field stressing measurements could allow inexpensive monitoring of the radiation hardness of MOS structures.

Extensive electron spin resonance (ESR) studies have identified two major defects generated in radiation damaged MOS devices. One center, termed P<sub>b</sub>,<sup>7-12</sup> is a "trivalent silicon" bonded to three other silicons at the  $\text{Si}/\text{SiO}_2$  interface; it is responsible for radiation induced interface states.<sup>10-12</sup> Another center, termed E',<sup>13,14</sup> a "trivalent silicon" hole trap, is responsible for most of the positive charge generated in irradiated oxides.<sup>10,11</sup>

To date, only electrical measurements have been used to compare high field stressing and ionizing radiation. In this study we use ESR to compare the positive charge generated by irradiating and high field stressing (HFS) MOS oxides. We find that although the E' center accounts for most of the positive charge in irradiated oxides, it does not account for most of the positive charge generated by HFS.

EXPERIMENTAL DETAILS

The samples used for HFS were  $0.4 \times 2 \text{ cm}^2$   $\text{Si}/\text{SiO}_2$  bars cut from 4 inch diameter wafers with a (111) surface orientation. Seven oxide thicknesses were utilized in this study, three "thick" oxides ( $t > 1100\text{\AA}$ ) and four "thin" oxides ( $t < 500\text{\AA}$ ). Two thick oxides (1150 $\text{\AA}$ , 1750 $\text{\AA}$ ) were grown in steam and annealed in forming gas at Sandia National Laboratory's Center for Radiation Hardened Microelectronics. Five oxides (2700, 408, 265 $\text{\AA}$ , 230 $\text{\AA}$ , 123 $\text{\AA}$ ) were grown in dry oxygen at IBM Federal Systems Laboratory.

In our HFS experiments the oxide surface is charged by low energy ions from a corona discharge apparatus; these positive ions are generated by a sharp needle under a large (+8000V) voltage. These ions produce a high ( $\geq 7\text{MV}/\text{cm}$ ) uniform electric field over a large ( $\sim 1\text{cm}^2$ ) surface area without destructive breakdown.<sup>15</sup> We have injected between .01 and 2 coulomb/ $\text{cm}^2$  of charge into the oxides. (It is considerably harder to damage the thin oxides.)

High frequency (1MHz) capacitance vs. voltage (CV) measurements were made with a mercury probe. Ultraviolet (UV) light (photon energy 55.5eV) from a mercury xenon source photo-emitted electrons into the oxide to neutralize the positive charge generated by the Fowler-Nordheim tunneling of electrons from the Si into the  $\text{SiO}_2$ .

ESR measurements were made using an IBM Instruments ER-200 (X-Band) spectrometer with a TE<sub>104</sub> "double" cavity. By comparison with a calibrated weak pitch standard, absolute spin concentrations were calculated from unsaturated absorption spectra. The substrate edges were etched to eliminate any resonance signals from damage at the edges.

RESULTS

In Figure 1 we show the effect of HFS on E' centers in thick and thin oxides. All traces were centered on the E' zero crossing g value of 2.0006. Spectrometer settings, sample size, and, for the stressed samples, approximate areal density of HFS induced space charge are the same in all cases. (HFS space charge  $\sim 10^{13}$  positive charges/ $\text{cm}^2$ ). Although only two oxide thicknesses are utilized in the illustrated comparison, the results are typical of those obtained on all thick ( $1150\text{\AA} \leq t \leq 2700\text{\AA}$ ) and thin ( $125\text{\AA} \leq t \leq 408\text{\AA}$ ) oxides. In Figure 1A and B we show prestressing traces of (A) a thick (1750 $\text{\AA}$ ) and (B) thin (230 $\text{\AA}$ ) oxides. We are unable to observe an E' resonance in these and in

all other oxides prior to HFS. In Fig. 1C we show a strong E' resonance for the HFS 1750A oxide; in 1D we are unable to observe an E' resonance from the HFS 230A oxide. The E' line shape of trace 1C has the "standard" E' powder pattern one would expect from a randomly oriented array of quartz E' centers. It is believed that the quartz E' center is a hole trapped in an oxygen vacancy.<sup>13</sup> It should be noted that we sometimes observe a weak (as yet unidentified) resonance in HFS thin oxides; however, this weak resonance does not have either the zero crossing value or the "standard" E' line shape.

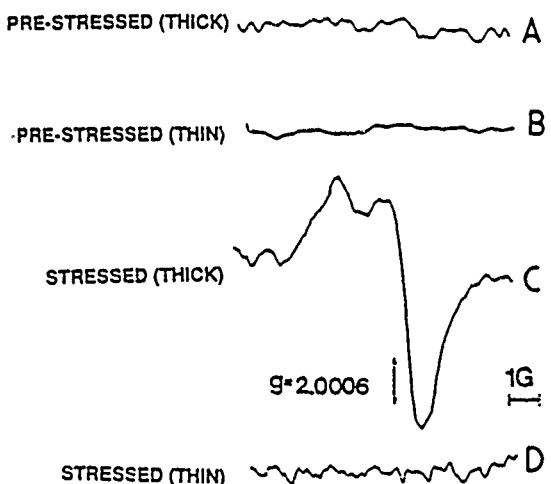


Figure 1: ESR Spectra. A and B - Spectra showing no paramagnetic centers for thick (A) and thin (B) oxides before stressing. C - Spectrum of an E' resonance after HFS a thick (1750A) oxide sample; D - Spectrum showing no E' resonance after HFS a thin (230A) oxide sample. (The magnetic field is parallel to the (111) plane of the Si/SiO<sub>2</sub> structure.)

Fig. 2 compares the E' resonance generated by HFS (trace 2A) a thick (1750A) oxide to that generated by gamma irradiating a thick oxide (trace 2B). Trace 2B was taken from the work of Lenahan and Dressendorfer<sup>12</sup>. The HFS and gamma radiation induced line shapes are virtually identical, suggesting that the HFS and gamma irradiation induced E' centers are identical in structure.

The fact that we consistently observe "standard" E' centers in stressed thick oxides but cannot detect them in stressed thin oxides (<500A) indicates that there are significant qualitative differences in the response of thin and thick oxides subjected to high electric fields. Our inability to detect a substantial E' resonance in high field stressed thin oxides may be due to the absence of impact ionization. It has been suggested by Brorson<sup>14</sup> et al. that in oxides less than 500A thick, few carriers have the energy required for impact ionization in SiO<sub>2</sub>. This absence of impact ionization could explain our failure to detect a substantial E' resonance in thin oxides.

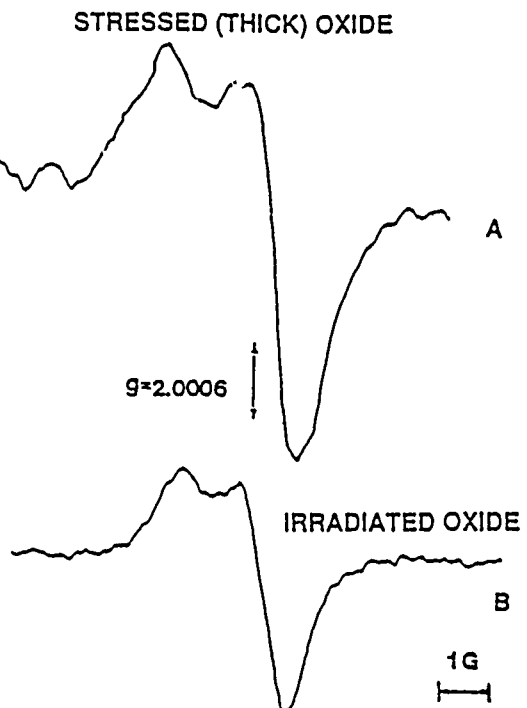


Figure 2: ESR Spectra. A - Spectrum showing an E' resonance after HFS thick (1750A) samples. B - Spectrum illustrating an E' resonance generated by ionizing radiation. (Spectrum B was analyzed by Lenahan and Dressendorfer in an earlier publication.)<sup>11</sup>

In Fig. 3 we illustrate the effect of electron photoinjection in the stressed thick oxides. (All traces were taken with identical spectrometer settings, identical cavity Q, and nonsaturating microwave power). Trace 3A shows a typical E' resonance generated by HFS thick oxides. Trace 3B was taken after photoinjecting electrons (without bias) into the same samples using a small (5 watt) mercury-xenon UV light source. This UV light source internally photoemitted electrons from the silicon valence band into the SiO<sub>2</sub> conduction band; illumination time was 48 hours. Note that most of the E' centers have been annihilated.

The CV results are illustrated in Fig. 4 for the same thick (1750 A) oxide samples shown in Fig. 3. Curve 4A was taken before HFS. Curve 4B was taken after HFS. The negative shift in the CV curve, indicates that positive charge has been generated. Curve 4C was taken after exposing the stressed sample to UV light. The positive shift in the CV curve indicates most of the positive charge in the oxide has been annihilated.

The number of positive charges/cm<sup>2</sup> and E' centers/cm<sup>2</sup> are not equal, within experimental error, in the thick or thin oxides subjected to high electric fields. In Fig. 5 we illustrate the discrepancy between the E' density and positive charge density in stressed oxides. (The positive charge in the oxide was calculated from

midgap shifts in the CV curves. Positive charge/cm<sup>2</sup> =  $\Delta V_{mg}C_{ox}/e$  where  $\Delta V_{mg}$  is the mid-gap voltage shift,  $C_{ox}$  is the oxide capacitance and  $e$  is the electronic charge. This assumes that all of the positive charge resides near the Si/SiO<sub>2</sub> interface).

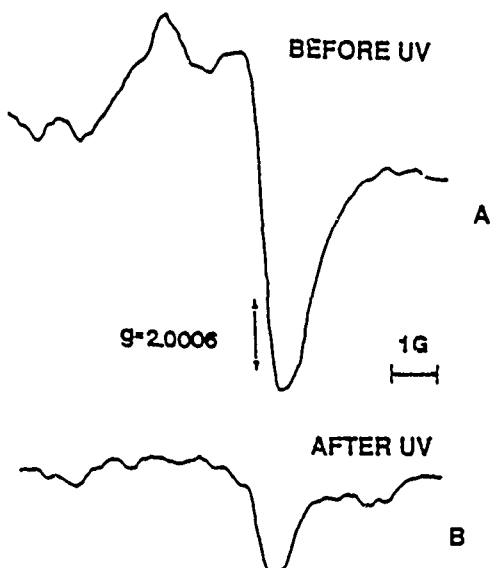


Figure 3: ESR Spectra. A - Spectrum showing an E' resonance after HFS thick oxides. B - Spectrum of stressed thick oxides after photoinjecting electrons showing a diminished E' resonance.

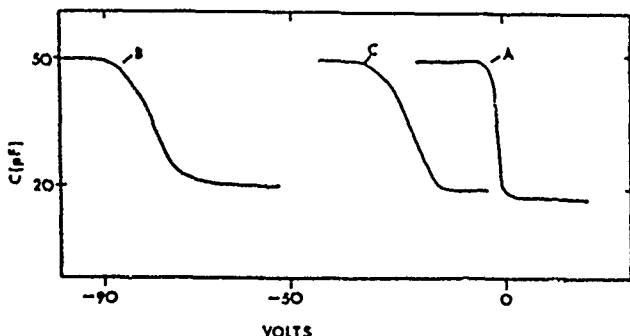


Figure 4: CV Curves. A - Curve of an unstressing thick oxide (1750 Å). B - Curve taken after HFS. C - Curve of stressed sample after photoinjecting electrons into the oxide.

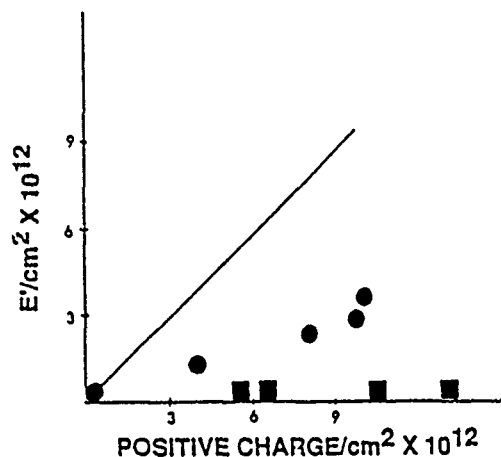


Figure 5: Comparison of the density of E' centers vs. the positive charge density generated in oxides by HFS. (Circles; thick oxides ( $\geq 1150$  Å); Squares; thin oxides ( $\leq 500$  Å)).

#### CONCLUSION

A comparison of Figs. 1-5 allows one to draw several conclusions. Although we observe substantial generation of positive charge in both thick and thin oxides; we observe substantial E' generation only in the thick ( $\geq 1150$  Å) oxides. Photoinjecting electrons into the thick oxides eliminates most of the E' centers as well as most of the positive charge. The simultaneous disappearance of the positive charge and E' center is consistent with the idea that the E' center is a hole trapped in an oxygen vacancy.<sup>14</sup> When a hole is captured at a neutral oxygen vacancy site it is positive and paramagnetic; returning the lost electron (via photoinjection) returns the center to something like its original (neutral) state. The appearance and disappearance of E' and positive charge is consistent with earlier work of Lenahan and Dressendorfer<sup>11</sup>, who found that E' centers are responsible for the positive charge buildup in irradiated MOS oxides.

The discrepancy between the E' density and the positive charge density suggests the presence of another positively charged defect center in HFS oxides. DiMaria<sup>17</sup> et al. have argued that the positive charge generated by high field stressing may be due to anomalous positive charge. Our work does not identify the source of the additional positive charge; it simply shows that there is another source of positive charge. Our results are thus consistent with, but do not prove DiMaria's<sup>17</sup> hypothesis. At this time the mechanism responsible for the rest of the positive charge is not known; we are currently looking for other oxide centers using ESR, hoping to identify their structure.

#### SUMMARY

Previous work has shown that the E' center is responsible for the oxide positive charge generated by ionizing radiation.<sup>11,12</sup> We now show that the E' center is only partly responsible for the positive charge generated from the Fowler-Nordheim tunneling of electrons

from the silicon into the silicon dioxide in thick ( $\geq 1150 \text{ \AA}$ ) oxides; in thin oxides ( $\leq 500 \text{ \AA}$ ) we are unable to observe any E' centers generated by high field electron injection. Thus there are significant qualitative and quantitative differences in the centers responsible for the positive charge generated by these two processes. Our observations suggest that there may be limitations to the use of high field measurements to predict the radiation hardness of MOS devices.

#### ACKNOWLEDGMENTS

We wish to thank Carl Schlier of IBM Federal Systems and Paul Dressendorfer of Sandia National Laboratories for the provision of samples. This work is supported by IBM Federal Systems under contracts XW-131570 and WF-158675 and Sandia National Laboratories under contract 95-0018.

#### REFERENCES

1. M. V. Fischetti, Z. A. Weinberg, and J. A. Calise, *J. Appl. Phys.* 57, 419 (1985).
2. C. Falcony and F. H. Salas, *J. Appl. Phys.*, 59, 3787 (1986).
3. P. Solomon and N. Klein, *Solid State Commun.*, 17, 1397 (1975).
4. Y. Nissan-Cohen, J. Shappir and D. Frohman-Bentchkowsky, *J. Appl. Phys.*, 57, 2830 (1985).
5. M. Knoll, D. Braunig, W. R. Fahrner, *Insulating Films on Semiconductors* edited by J. F. Verweij and D. R. Wolters (North Holland, New York, pg. 107, 1983).
6. H. E. Boesch and J. M. McGarrity, *IEEE Trans. NS-26*, 4814 (1979).
7. Y. Nishi, *Jpn. J. Appl. Phys.*, 10, 52 (1971).
8. P. J. Caplan, E. H. Poindexter, B. E. Deal and R. R. Razouk, *J. Appl. Phys.*, 50, 5847 (1979).
9. E. H. Poindexter, P. J. Caplan, B. E. Deal and R. R. Razouk, *J. Appl. Phys.*, 52, 879 (1981).
10. P. M. Lenahan and P. V. Dressendorfer, *J. Appl. Phys.*, 54, 1487 (1983).
11. P. M. Lenahan and P. V. Dressendorfer, *J. Appl. Phys.*, 55, 3495 (1984).
12. P. M. Lenahan and P. V. Dressendorfer, *Appl. Phys. Lett.* 41, 542 (1982).
13. D. L. Griscom, *The Physics of SiO<sub>2</sub> and Its Interfaces*, edited by S. T. Pantelides (Pergamon, New York, 1978) pg. 232
14. F. J. Feigl, W. B. Fowler and K. L. Yip, *Solid State Commun.*, 14, 225 (1974).
15. Z. A. Weinberg, W. C. Johnson and M. A. Lampert, *J. Appl. Phys.*, 47, 248 (1976).
16. S. D. Brorson, D. J. DiMaria, M. V. Fischetti, F. L. Pesavento, P. M. Solomon and D. W. Dong, *J. Appl. Phys.*, 58, 1302 (1985).
17. D. J. DiMaria, T. N. Theis, J. R. Kirtley, F. L. Pesavento, D.W. Dong, and S.D. Brorson, *J. Appl. Phys.*, 57, 1214 (1985).

#### D. Interaction of Molecular Hydrogen with Trapped Hole E' Centers in Irradiated and High Field Stressed Metal/Oxide/Silicon Oxides

A number of recent studies have focused upon the role of hydrogen on radiation damage in MOS devices. We have initiated a study (funded by Sandia National Laboratories) of hydrogen interactions with radiation induced point defects. Our initial results and discussed in a brief paper which we submitted to Applied Physics Letters in September 1989. Our results partially confirm and somewhat refine earlier results of Triplett, Sugano, and others who found that E' centers react readily with molecular hydrogen at relatively low temperature.

Interaction of Molecular Hydrogen with Trapped Hole E' Centers in  
Irradiated and High Field Stressed  
Metal/Oxide/Silicon Oxides

P. M. Lenahan, W. L. Warren, D. T. Krick\*

Department of Engineering Science and Mechanics  
The Pennsylvania State University  
University Park, PA 16802

P. V. Dressendorfer

Sandia National Laboratories  
Albuquerque, New Mexico 87185

Baylor B. Triplett

Intel Corporation  
Santa Clara, California 95051

We explore the effect of forming gas anneals at 110°C on E' centers in metal/oxide/semiconductor oxides subjected to gamma, electron, and vacuum ultraviolet irradiation, as well as high electric field stressing. We find that this brief low temperature anneal substantially reduces E' density in all cases, clearly demonstrating that hydrogen reacts readily with the E' sites. Although this work confirms a recent report of the reactivity of E' and hydrogen we fail to detect the reported reaction product known as the 74-G doublet.

\*Present Address: Intel Corporation  
5200 N.E. Elam Young Parkway  
Hillsboro, OR 97124-6497

## Introduction

The deleterious effects of ionizing radiation on metal/oxide/silicon (MOS) devices are among the most important problems in MOS device physics today. Two decades of intense investigation<sup>1-19</sup> have established that the radiation damage process involves the creation of interface states at the Si/SiO<sub>2</sub> boundary and the trapping of radiation induced holes in deep traps in the SiO<sub>2</sub>.

Numerous studies<sup>4,5,18,19</sup> have suggested a link between the presence of holes in the oxide and the interface state generation process. It has been widely suggested<sup>4,7,8,9,20</sup> that the motion of some form of hydrogen may be involved in the interface state formation process. It has also been suggested<sup>18,19,21,22,23</sup> that the hole trap site may be involved in the radiation induced interface state process. Schwank *etal*<sup>24</sup> have suggested that some of the hole trapping centers may be associated with hydrogen.

The technique of electron spin resonance (ESR) is uniquely well suited to the study of both radiation induced interface state defects and hole trapping centers. ESR is extremely sensitive to defects with unpaired electrons. It allows both the identification of defect structure and the measurement of defect density.

Electron spin resonance (ESR) studies have established<sup>11-14</sup> that the dominant radiation induced interface states are "trivalent silicon" centers at the Si/SiO<sub>2</sub> interface and that the dominant hole traps are oxygen deficient silicon defects, called E' centers. The E' center is an unpaired electron in a non-bonding sp<sup>3</sup> hybrid orbital on a silicon bonded to three oxygens Si=O<sub>3</sub>.<sup>15-17</sup>

Quite recently, Triplett *etal*.<sup>25</sup> and Takahashi *etal*.<sup>26</sup> reported the generation of a hydrogen associated E' hole trap center in MOS oxides subjected to heavy (2x10<sup>10</sup>Rads(Si)) soft x-ray irradiation, with oxides bare, and

unbiased in a vacuum. Ordinary E' centers, (holes trapped at oxygen vacancies) were then transformed in large numbers into hydrogenic E' centers called the 74-G doublet when an irradiated oxide was subjected to a brief (3 minute) anneal in forming gas (5%H<sub>2</sub>, 95%N<sub>2</sub>) at 110°C. Although these centers were observed in oxides subjected to rather extreme conditions, the observations are of considerable interest because they demonstrate a reaction involving hydrogen in the vicinity of the Si/SiO<sub>2</sub> interface, a feature of many radiation damage models<sup>4,7,8,9,20</sup>. The role of hydrogen in the transformation of E' to the doublet is indicated first by the fact that the reaction takes place quickly in the presence of forming gas at low temperature, with about 60% conversion to doublet, and secondly (and most convincingly) by the presence of a two line ESR spectrum (the "doublet") indicating a hyperfine interaction between an unpaired electron and an atom with a spin 1/2 nucleus. Several studies of the 74 Gauss doublet in bulk SiO<sub>2</sub> convincingly establish it as an E' defect with a hydrogen nearby.<sup>27,28</sup> Tsai and Griscom<sup>29</sup> have argued persuasively that the 74-G doublet is a trivalent Si bonded to two oxygens and one hydrogen.

In order to further characterize the interaction of hydrogen with point defects in MOS oxides, we have subjected MOS device oxides grown on (111) silicon substrates to widely varying levels of radiation and stressing damage, and subsequently performed low temperature anneals in forming gas in a procedure similar to that of Takahashi *etal.*<sup>25</sup> Measurements were made on samples both after damage and after annealing.

Prior to irradiation or stressing, we are unable to observe paramagnetic resonances in the oxides in the vicinity of  $g = 2.0$ . (The  $g$  value is defined  $g = h\nu / \beta H$ , where  $h$  is Planck's constant,  $\nu$  is microwave frequency,  $\beta$  is the Bohr magneton, and  $H$  is the applied magnetic field at which resonance

occurs.) After all irradiations and high field stressing two resonances are clearly visible; one with a zero crossing  $g=2.0004$  is the E center, a second center with  $g=2.0014$  and  $g=2.008$  is the  $P_b$  center. Earlier studies indicated that a very brief forming gas anneal should not greatly affect  $P_b$ ,<sup>30</sup> our results on irradiated samples are generally consistent with these earlier observations. However, in this paper we focus on the changes observed in the E' center formed under various conditions.

### Gamma Irradiation

We subjected MOS capacitors to 5.7 Mrad ( $SiO_2$ ) of gamma irradiation with +24 volts across the oxide during irradiation. The oxides were grown in dry oxygen to a thickness of 1000A on a p-type (111) silicon substrate ( $\rho=400\Omega cm$ ). The capacitor's aluminum gate was removed after irradiation. The post irradiation ESR trace is illustrated in Figure 1A, the post (3 minute) forming gas (5% $H_2$ /95% $N_2$ ) anneal (110°C) trace is illustrated in Figure 1B.

After the anneal, the E' resonance is reduced by about 60%, but the 74G doublet is not visible. (The 74G doublet should appear as two lines separated by 74 Gauss in the positions indicated on the figure). Our measurements show that the forming gas anneal does eliminate 60% of the E' center as Takahashi reported, but does not create the 74G doublet under these conditions. (Previous work indicates a brief 110°C anneal in air does very little to the E' amplitude.<sup>14</sup>)

### High Field Stressing

We subjected bare oxide  $Si/SiO_2$  structures to high electric field stressing by applying corona ions to the oxide surface utilizing a technique described in detail elsewhere.<sup>29,31</sup> The oxides were subjected to an electron

injection current density of approximately  $10^{-7}\text{A}/\text{cm}^2$  for eight hours. The oxides were grown in dry oxygen on (111) silicon substrates (p-type;  $\rho=100\Omega\text{-cm}$ ) to a thickness of 1700Å.

The post stressing ESR results are illustrated in figure 2A. The post forming gas anneal trace is shown in figure 2B. Once again, about 60% of the E' centers disappear but no 74G doublet is visible.

#### Vacuum Ultraviolet Irradiation

We subjected bare oxide Si/SiO<sub>2</sub> structures to brief (~ 5 minute) irradiation with 10.2eV photons from a 50 watt deuterium lamp (the vacuum ultraviolet photons electron/hole.) We estimate that the ultraviolet illumination sequence flooded the oxide with a hole flux roughly comparable to a 1 Mrad (SiO<sub>2</sub>) gamma radiation. The oxides were grown in steam on (111) silicon substrates (p-type;  $\rho = 100 \Omega \text{ cm}$ ) to a thickness of 1200Å. After oxidation they received a 30 minute anneal in dry nitrogen at 1100°C. After the high temperature anneal, they were annealed in forming gas at 400°C for 20 minutes. During the illumination, a positive bias (+1 MV/cm) was applied to the oxides with ions from a corona discharge apparatus. The UV photons are all absorbed in the top ~ 100Å of the oxide. With the positive corona bias, the holes are driven across the oxide to the deep hole traps, and the electrons recombine with the charged corona ions on the surface. The VUV irradiation generates E' centers when the VUV induced holes are captured at E' precursor sites near the Si/SiO<sub>2</sub> interface.<sup>33</sup>

The post irradiation trace is shown in figure 3A; the post annealing trace in figure 3B. Again, about 60% of the E' centers are annihilated, but no 74G doublet centers are observed.

### Electron Irradiation

We subjected a bare oxide Si/SiO<sub>2</sub> structure to very heavy (10<sup>10</sup>Rads(SiO<sub>2</sub>) electron irradiation (20keV) in vacuum in order to roughly approximate the irradiation conditions of Triplett *etal.*<sup>24</sup> and Takahashi *etal.*<sup>25</sup>. The 2500Å oxides were grown in dry oxygen with 3% HCl on p-type (111) silicon substrates ( $\rho=100\Omega\text{cm}$ ); these processing parameters are quite similar to those utilized by Triplett, Takahashi, and co-workers.<sup>25-26</sup>

The post irradiation trace is shown in Figure 4A; the post (3 min, 110°C) forming gas trace is shown in Figure 4B. Again, about a 60% decrease in E' is observed, exactly as reported by Takahashi *etal*, but no 74G doublet resonance is observed.

### Discussion

We find that a brief (~3 minute) anneal in forming gas (5%H<sub>2</sub>, 95% N<sub>2</sub>) at 110°C greatly decreases the amplitude of the E' center (trapped hole) ESR resonance in sets of oxides subjected to gamma radiation, electron irradiation, high electric field stressing and vacuum ultraviolet (hc/λ =10.2eV) irradiation. Our results clearly indicate an interaction between E' and hydrogen at these low temperatures. To this extent, our observations are consistent with and confirm the earlier results of Triplett *etal.*<sup>25</sup> and Takahashi *etal.*<sup>26</sup> In fact, we observed essentially the same 60% decrease in E' reported previously by Takahashi *etal.* in all of our samples. However we have not been able to observe the transformation of these centers to the 74-Gauss doublet reported by Triplett and Takahashi.

Since our annealing conditions closely match that of Takahashi *etal*, and one of our oxides was processed similarly to those used by Takahashi,

etal, the difference in outcome of our experiments (our failure to see the 74-G doublet) is almost certainly due to differences in the irradiation conditions.

The Takahashi etal oxides were irradiated bare and unbiased in a vacuum (pressure =  $2 \times 10^{-6}$  Torr) to extremely high dose levels ( $2 \times 10^{10}$  rads). Since the Takahashi oxides were placed close to the tungsten X-ray source they reached temperatures possibly as high as 300°C during irradiation.

In our current study we subjected a variety of oxides to a fairly wide range of irradiation and oxide biasing conditions; all of our irradiation and stressing took place at room temperature. Our oxide damage conditions involved zero bias across the (floating) oxides (electron irradiation), moderate ( $\approx 1$  MV/cm) bias across the oxide (gamma and VUV irradiation), and high ( $\approx 10$  MV/cm) bias across the oxide (high field stressing). Our oxide damage conditions involved moderate ( $5.7 \times 10^6$  rad gamma) and very high ( $10^{10}$  rad electron) levels of ionizing radiation, relatively low (10.2 eV vacuum ultraviolet) and quite high (1 MeV gamma) photon energies, oxides bare (electron, VUV, irradiation) and with gates (gamma irradiation). Our irradiations took place both in vacuum (vacuum ultraviolet irradiation and electron irradiation) and in air (gamma irradiation).

Our failure to observe the 74-G doublet in a samples subjected to a fairly wide range of irradiation conditions as well as high electric field stressing suggests that the 74-G doublet is not involved in general MOS radiation or high field stressing damage. However, our observations do not completely prove this; the 74-G doublet centers might be unstable under circumstances other than the Takahashi etal irradiation conditions. If that were to be the case, the centers would not be observable in our measurements but might play an intermediary role in radiation damage.

Our results do clearly indicate that E' centers generated in a number of ways react rapidly with hydrogen at relatively low temperatures. Our observations provide additional evidence suggesting that hydrogen may play an important role in the radiation damage process of MOS devices.

This work was supported by Sandia National Laboratories under Contract No. 03-3999. We wish to thank Michael Taylor of Sandia National Laboratories for technical assistance in this study.

## References

1. H. L. Hughes and R. R. Giroux, *Electronics* 37, 58 (1964).
2. E. H. Snow, A. S. Grove, and D. J. Fitzgerald, *Proc. IEEE* 55, 1168 (1967).
3. R. J. Powell and G. F. Derbenwick, *IEEE Trans. Nucl. & Sci.* NS-13, 237 (1966).
4. P. J. Winokur, H. E. Boesch, Jr., J. M. McGarrity, and F. B. McLean, *J. Appl. Phys.* 50 3492 (1979).
5. P. S. Winokur and M. M. Sokoloski, *Appl. Phys. Lett.* 28, 627 (1976).
6. A. G. Revesz, *IEEE Trans. Nucl. & Sci.* NS-18 113 (1971).
7. C. M. Svensson, in The Physics of SiO<sub>2</sub> and Its Interfaces, edited by S. T. Pantelides (Pergamon, New York 1978) p. 328.
8. A. G. Revesz, *IEEE Trans. Nucl. Sci.* NS-24 2102 (1977).
9. P. S. Winokur, F. B. McLean and H. E. Boesch, Jr., HDL Report, HDL-TR-2081 (1986).
10. P. M. Lenahan, P. V. Dressendorfer, K. L. Brower, W. C. Johnson *IEEE Trans. Nucl. Sci.* NS-28 4105 (1981).
11. P. M. Lenahan, P. V. Dressendorfer *Appl. Phys. Lett.* 41, 542 (1982).
12. P. M. Lenahan and P. V. Dressendorfer, *IEEE Trans. Nucl. Sci.* NS-30, 4602 (1983).
13. P. M. Lenahan and P. V. Dressendorfer, *Appl. Phys. Lett.* 44, 96 (1984).
14. P. M. Lenahan and P. V. Dressendorfer, *J. Appl. Phys.* 55, 3499 (1984).
15. F. J. Feigl, W. B. Fowler, and K. L. Yip, *Solid State Commun.* 14, 225 (1974).
16. R. H. Silsbee, *J. Appl. Phys.* 32, 1459 (1961).
17. D. L. Griscom, *Phys. Rev. B* 20, 1823 (1979).
18. G. J. Hu and W. C. Johnson, *Appl. Phys. Lett.* 35, 590 (1980).
19. S. T. Chang, J. K. Wu, and S. A. Lyon, *J. Appl. Phys.* 59, 662 (1986).

20. D. L. Griscom, *J. Appl. Phys.* 58, 2524 (1985).
21. S. J. Wang, J. M. Sung, S. A. Lyon, *Appl. Phys. Lett.* 52, 1431 (1988).
22. S. K. Lai, *J. Appl. Phys.* 54, 2540 (1983).
23. A. G. Sabinis, *IEEE Trans. Nucl. Sci.* NS-32 (6), 3905 (1985).
24. J. R. Schwank, D. M. Fleetwood, P. S. Winokur, P. V. Dressendorfer, D. C. Turpin, and D. T. Sanders, *IEEE Trans. Nucl. Sci.* NS-34, 1152 (1987).
25. B. B. Triplett, T. Takahashi, and T. Sugano, *Appl. Phys. Lett.* 50, 1163 (1987).
26. T. Takahashi, B. B. Triplett, K. Yokogawa, and T. Sugano, *Appl. Phys. Lett.* 51, 1344 (1987).
27. John Vitko, *J. Appl. Phys.* 49, 5530 (1978).
28. V. A. Radtsig, *Kinetica i Kataliz* 20 (2), 456 (1979).
29. T. E. Tsai and D. L. Griscom, *J. Non. Cryst. Solids* 91, 170 (1987).
30. Y. Nishi, T. Tanaka, and T. Ohwada, *Jpn. J. Appl. Phys.* 11, 85 (1972).
31. Z. A. Weinberg, W. C. Johnson, and M. A. Lampert, *J. Appl. Phys.* 47, 248 (1976).
32. R. Williams and M. H. Woods, *J. Appl. Phys.* 44, 1026 (1973).
33. H. S. Witham and P. M. Lenahan, *Appl. Phys. Lett.* 51, 1007 (1987).

## 74G Doublet

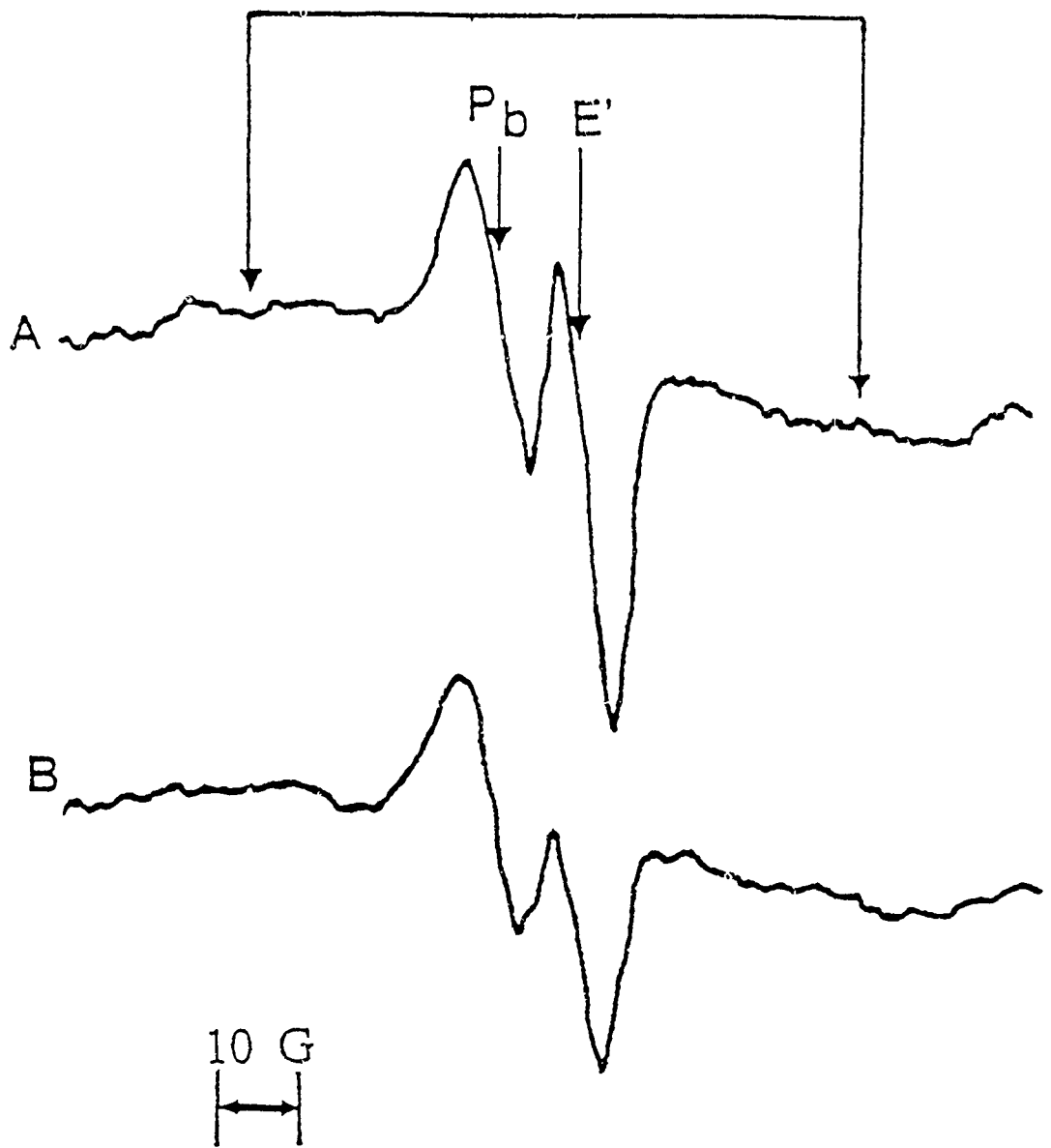


Figure 1. ESR resonances of a gamma irradiated (5.7MRAD)  $\text{SiO}_2/\text{Si}$  structure before (A) and after (B) 3 min  $110^\circ\text{C}$  anneal in forming gas (5%  $\text{H}_2$ /95%  $\text{N}_2$ ). Following the anneal,  $\text{E}'$  decreases significantly, but no 74G doublet resonance is detected. Spectrometer settings for both traces are identical, and are set to maximize the 74G doublet resonance amplitude.

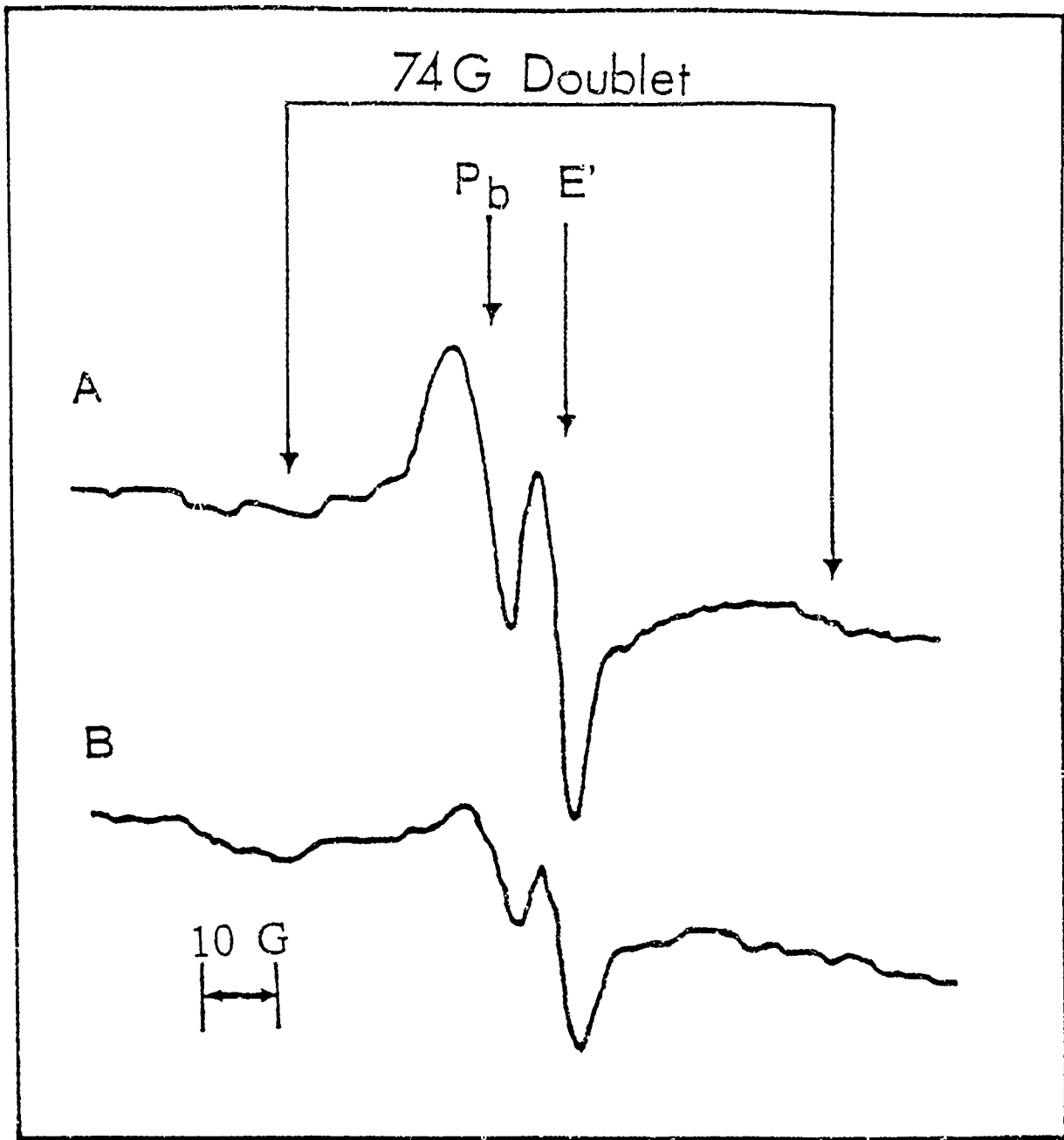


Figure 2. ESR resonances of high electric field stressing  $\text{SiO}_2/\text{Si}$  structure (A) before anneal, and (B), after a 3 min  $110^\circ\text{C}$  anneal in forming gas (5%  $\text{H}_2$ /95%  $\text{N}_2$ ). Following the anneal,  $\text{E}'$  decreases significantly, but no 74G doublet resonance is detected. Spectrometer settings for both traces are identical and are set to maximize the 74G doublet resonance.

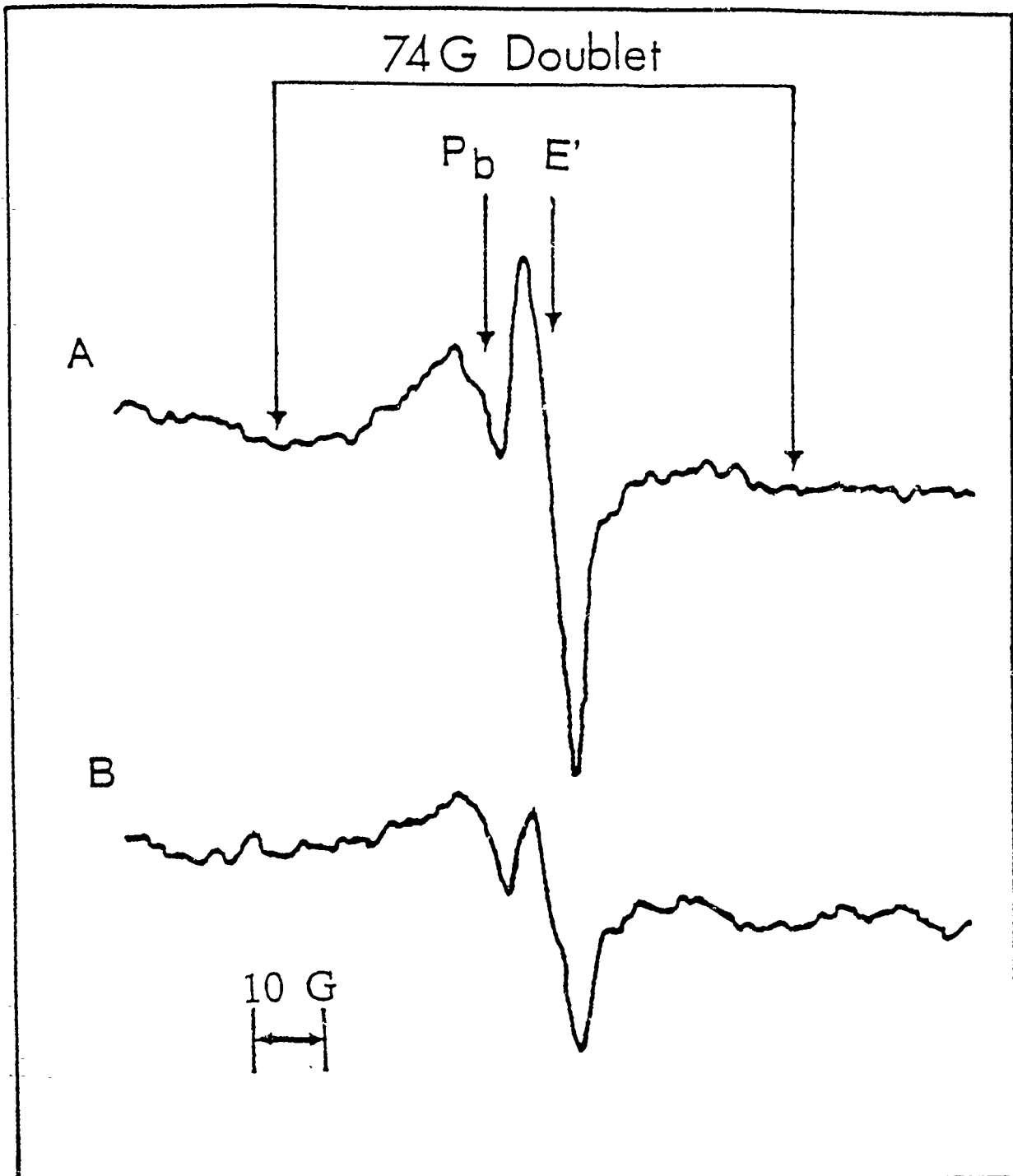


Figure 3. ESR resonances of vacuum ultraviolet irradiation (10.2eV)  $\text{SiO}_2/\text{Si}$  structure (A) before anneal, and (B), after a 3 min  $110^\circ\text{C}$  anneal in forming gas (5% $\text{H}_2$ /95% $\text{N}_2$ ). Following the anneal,  $\text{E}'$  decreases significantly, but no 74G doublet resonance is detected. Spectrometer settings for both traces are identical, and are set to maximize the 74G doublet resonance amplitude.

## 74 G Doublet

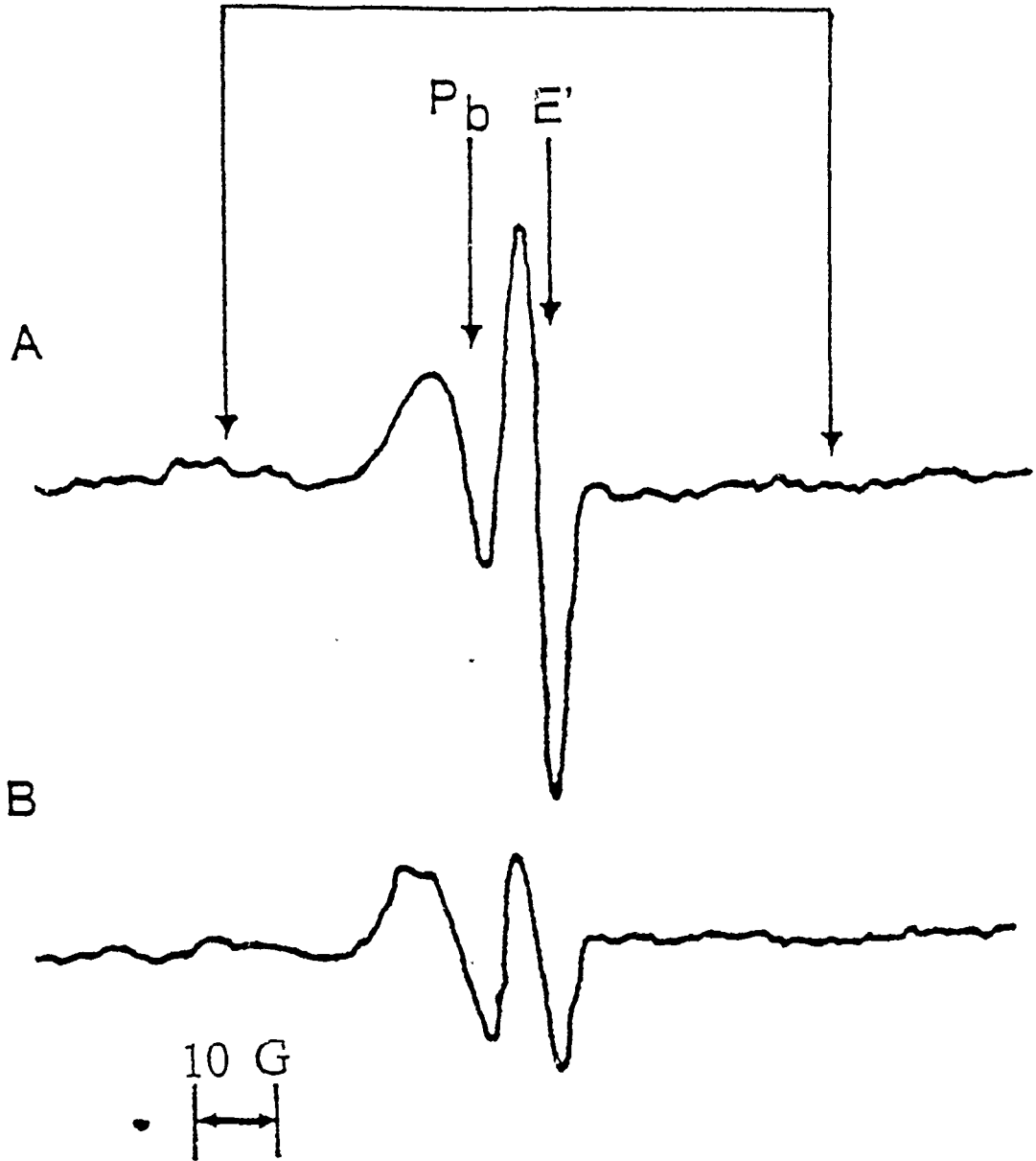


Figure 4. ESR resonances of an electron irradiated (20keV) ( $10^{10}$  rad)  $\text{SiO}_2/\text{Si}$  structure (A) before anneal, and (B), after a 3 min  $110^\circ\text{C}$  anneal in forming gas (5%H<sub>2</sub>/95%N<sub>2</sub>). Following the anneal, E' decreases significantly, but no 74G doublet resonance is detected. Spectrometer settings for both traces are identical, and are set to maximize the 74 G doublet resonance amplitude.

## DISTRIBUTION LIST

DNA-TR-89-242

### DEPARTMENT OF DEFENSE

ASSISTANT TO THE SECRETARY OF DEFENSE  
ATTN: EXECUTIVE ASSISTANT

DEFENSE ADVANCED RSCH PROJ AGENCY  
ATTN: ASST DIR  
ATTN: R REYNOLDS

DEFENSE ELECTRONIC SUPPLY CENTER  
ATTN: DESC-E

DEFENSE INTELLIGENCE AGENCY  
ATTN: DT-1B  
ATTN: RTS-2B

DEFENSE NUCLEAR AGENCY  
ATTN: RAEE (TREE)  
4 CYS ATTN: TITL

DEFENSE NUCLEAR AGENCY  
ATTN: TDNM  
2 CYS ATTN: TDTT W SUMMA

DEFENSE TECHNICAL INFORMATION CENTER  
2 CYS ATTN: DTIC/FDAB

DNA PACOM LIAISON OFFICE  
ATTN: DNALO

FIELD COMMAND DEFENSE NUCLEAR AGENCY  
ATTN: FCPF R ROBINSON

JOINT DATA SYSTEM SUPPORT CTR  
ATTN: C-330  
ATTN: JNSV

STRATEGIC AND THEATER NUCLEAR FORCES  
ATTN: DR E SEVIN

THE JOINT STAFF  
ATTN: JKC (ATTN: DNA REP)  
ATTN: JKCS  
ATTN: JPEM

### DEPARTMENT OF THE ARMY

HARRY DIAMOND LABORATORIES  
ATTN: SLCHD-NW-RP  
ATTN: SLCHD-NW-RP F MCLEAN  
ATTN: SLCHD-NW-TS

INFORMATION SYSTEMS COMMAND  
ATTN: STEWS-TE-AN J MEASON  
ATTN: STEWS-TE-N K CUMMINGS  
ATTN: STEWS-TE-N T ARELLANES

U S ARMY GARRISON  
ATTN: LIBRARY

U S ARMY MISSILE COMMAND  
ATTN: AMCPM-HA-SE-MS

U S ARMY MISSILE COMMAND/AMSMI-RD-CS-R  
ATTN: AMSMI-RD-CS-R (DOCS)

U S ARMY NUCLEAR & CHEMICAL AGENCY  
ATTN: MONA-NU

U S ARMY RESEARCH OFFICE  
ATTN: R GRIFFITH

U S ARMY STRATEGIC DEFENSE CMD  
ATTN: CSSD-H-YA (DUDNEY)

U S ARMY STRATEGIC DEFENSE COMMAND  
ATTN: CSSD-SL

### DEPARTMENT OF THE NAVY

NAVAL AIR SYSTEMS COMMAND  
ATTN: AIR 931A

NAVAL ELECTRONICS ENGRG ACTVY, PACIFIC  
ATTN: CODE 250

NAVAL POSTGRADUATE SCHOOL  
ATTN: CODE 1424 LIBRARY

NAVAL RESEARCH LABORATORY  
ATTN: CODE 4682 C DOZIER  
ATTN: CODE 4682 D BROWN  
ATTN: CODE 6813 N SAKS  
ATTN: CODE 6816 E D RICHMOND  
ATTN: CODE 6816 H HUGHES  
ATTN: CODE 6816 R HEVEY

NAVAL SURFACE WARFARE CENTER  
ATTN: CODE H21 F WARNOCK  
ATTN: CODE H23 R SMITH

NAVAL SURFACE WARFARE CENTER  
ATTN: CODE H-21

NAVAL TECHNICAL INTELLIGENCE CTR  
ATTN: LIBRARY

NAVAL WEAPONS EVALUATION FACILITY  
ATTN: CLASSIFIED LIBRARY

NAVAL WEAPONS SUPPORT CENTER  
ATTN: CODE 6054 D FLATTETER

### DEPARTMENT OF THE AIR FORCE

AERONAUTICAL SYSTEMS DIVISION  
ATTN: ASD/ENSS

AIR FORCE CTR FOR STUDIES & ANALYSIS  
ATTN: AFCSA/SAMI

AIR UNIVERSITY LIBRARY  
ATTN: AUL-LSE

**DNA-TR-89-242 (DL CONTINUED)**

OGDEN AIR LOGISTICS CENTER  
ATTN: OO-ALC/MMDEC  
ATTN: OO-ALC/MMGR

ROME AIR DEVELOPMENT CENTER, AFSC  
ATTN: RBR J BRAUER

ROME AIR DEVELOPMENT CENTER, AFSC  
ATTN: ESR

SPACE DIVISION/YA  
ATTN: YAS

SPACE DIVISION/YAR  
ATTN: YAR CAPT STAPANIAN

SPACE DIVISION/YD  
ATTN: YD

SPACE DIVISION/YE  
ATTN: YE

SPACE SYSTEMS DIVISION  
ATTN: SSD/MSGA, CAPT D ROBBINS

STRATEGIC AIR COMMAND/XRFS  
ATTN: XRFS

WEAPONS LABORATORY  
ATTN: NTCAS  
ATTN: NTCCR R MAIER  
ATTN: WL/SUL

WRIGHT RESEARCH & DEVELOPMENT CENTER  
ATTN: AFV:AL/ELE  
ATTN: WRDC/MTE

3416TH TECHNICAL TRAINING SQUADRON (ATC)  
ATTN: TTV

**DEPARTMENT OF ENERGY**

DEPARTMENT OF ENERGY  
ALBUQUERQUE OPERATIONS OFFICE  
ATTN: NESD

LAWRENCE LIVERMORE NATIONAL LAB  
ATTN: J YEE  
ATTN: H KRUGER  
ATTN: W ORVIS

LOS ALAMOS NATIONAL LABORATORY  
ATTN: E LEONARD

SANDIA NATIONAL LABORATORIES  
ATTN: DR T F WROBEL  
ATTN: P V DRESSENDORFER

**OTHER GOVERNMENT**

CENTRAL INTELLIGENCE AGENCY  
ATTN: OSWR/NED  
ATTN: OSWR/STD/MTB

DEPARTMENT OF TRANSPORTATION  
ATTN: ARD-350

NASA  
ATTN: CODE 313 V DANCHENKO

NATIONAL INSTITUTE OF STANDARDS & TECHNOLOGY  
ATTN: P ROITMAN

**DEPARTMENT OF DEFENSE CONTRACTORS**

AEROSPACE CORP  
ATTN: A AMRAM

ALLIED-SIGNAL, INC  
ATTN: DOCUMENT CONTROL

AMPEX CORP  
ATTN: B RICKARD

ANALYTIC SERVICES, INC (ANSER)  
ATTN: A HERNDON

BDM INTERNATIONAL INC  
ATTN: D WUNSCH

BOEING CO  
ATTN: A JOHNSTON

BOOZ-ALLEN & HAMILTON, INC  
ATTN: L ALBRIGHT

CALIFORNIA INSTITUTE OF TECHNOLOGY  
ATTN: C BARNES

CALSPAN CORP  
ATTN: R THOMPSON

CHARLES STARK DRAPER LAB, INC  
ATTN: N TIBBETTS

CINCINNATI ELECTRONICS CORP  
ATTN: L HAMMOND

CLEMSON UNIVERSITY  
ATTN: P J MCNULTY

COMPUTER SCIENCES CORP  
ATTN: A SCHIFF

DAVID SARNOFF RESEARCH CENTER, INC  
ATTN: R SMELTZER

E-SYSTEMS, INC  
ATTN: K REIS

EATON CORP  
ATTN: R BRYANT

ELECTRONIC INDUSTRIES ASSOCIATION  
ATTN: J KENN

FORD AEROSPACE CORPORATION  
ATTN: TECHNICAL INFORMATION SRVS

GENERAL ELECTRIC CO ATTN: DOCUMENTS LIBRARY ATTN: TECHNICAL LIBRARY	INSTITUTE FOR DEFENSE ANALYSES ATTN: TECH INFO SERVICES
GENERAL ELECTRIC CO ATTN: G BENDER	JAYCOR ATTN: M TREADAWAY
GENERAL ELECTRIC CO ATTN: G GATI	JAYCOR ATTN: R SULLIVAN
GENERAL ELECTRIC CO ATTN: DAREN NERAD	JAYCOR ATTN: R POLL
GENERAL ELECTRIC CO ATTN: J MILLER	JOHNS HOPKINS UNIVERSITY ATTN: R MAURER
GENERAL RESEARCH CORP ATTN: A HUNT	JOHNS HOPKINS UNIVERSITY ATTN: G MASSON
GEORGE WASHINGTON UNIVERSITY ATTN: A FRIEDMAN	KAMAN SCIENCES CORP ATTN: LIBRARY/B KINSLOW
GRUMMAN AEROSPACE CORP ATTN: J ROGERS	KAMAN SCIENCES CORP ATTN: DASIAK
GTE GOVERNMENT SYSTEMS CORP ATTN: GEORGE COWEN	KAMAN SCIENCES CORPORATION ATTN: DASIAK
H. M. WEIL CONSULTANTS, INC ATTN: H WEIL	KEARFOTT GUIDANCE AND NAVIGATION CORP ATTN: J D BRINKMAN
HARRIS CORP ATTN: J W SWONGER	LITTON SYSTEMS INC ATTN: F MOTTER ATTN: S MACKEY
HARRIS CORPORATION ATTN: W ABARE	LOCKHEED MISSILES & SPACE CO, INC ATTN: TECHNICAL INFORMATIION CNTR
HONEYWELL INC ATTN: R JULKOWSKI	LOCKHEED MISSILES & SPACE CO, INC ATTN: B KIMURA
HONEYWELL SYSTEMS & RESEARCH CENTER ATTN: R BELT	LOCKHEED SANDERS, INC ATTN: BRIAN G CARRIGG
HONEYWELL, INC ATTN: MS 725-5	LTV AEROSPACE & DEFENSE COMPANY 2 CYS ATTN: LIBRARY
HUGHES AIRCRAFT CO ATTN: SYSTEMS TECH DEPT	MARTIN MARIETTA CORP ATTN: TIC/MP-30
HUGHES AIRCRAFT COMPANY ATTN: E KUBO ATTN: L DARDA	MARTIN MARIETTA CORP ATTN: S BUCHNER
IBM CORP ATTN: DEPT L75	MARTIN MARIETTA DENVER AEROSPACE ATTN: RESEARCH LIBRARY
IBM CORP ATTN: J ZIEGLER	MARYLAND, UNIVERSITY OF ATTN: H C LIN
IBM CORP ATTN: N HADDAD	MCDONNELL DOUGLAS CORP ATTN: A P MUNIE ATTN: R L KLOSTER
IIT RESEARCH INSTITUTE ATTN: I MINDEL	MCDONNELL DOUGLAS CORPORATION ATTN: P ALBRECHT

MISSION RESEARCH CORP ATTN: R PEASE	SCIENCE APPLICATIONS INTL CORP ATTN: D MILLWARD ATTN: DAVID LONG
MISSION RESEARCH CORP ATTN: J LUBELL	SCIENCE APPLICATIONS INTL CORP ATTN: J RETZLER
MITRE CORPORATION ATTN: M FITZGERALD	SCIENCE APPLICATIONS INTL CORP ATTN: W CHADSEY
MOTOROLA, INC ATTN: A CHRISTENSEN	SCIENCE APPLICATIONS INTL CORP ATTN: P ZIELIE
MOTOROLA, INC ATTN: L CLARK	SUNDSTRAND CORP ATTN: C WHITE
NATIONAL SEMICONDUCTOR CORP ATTN: F C JONES	SYSTRON-DONNER CORP ATTN: SECURITY OFFICER
NORDEN SYSTEMS, INC ATTN: TECHNICAL LIBRARY	TECHNOLOGY DEVELOPMENT ASSOCIATES ATTN: R V BENEDICT
NORTHROP CORP ATTN: A BAHRAMAN	TELEDYNE BROWN ENGINEERING ATTN: G R EZELL
NORTHROP CORPORATION SYSTEMS DIVISION ATTN: E KING	TELEDYNE SYSTEMS CO, INC ATTN: R SUHRKE
PACIFIC-SIERRA RESEARCH CORP ATTN: H BRODE	TEXAS INSTRUMENTS, INC ATTN: T CHEEK
PENNSYLVANIA STATE UNIVERSITY 2 CYS ATTN: M JUPINA 2 CYS ATTN: P LANAHAN	TRW ATTN: M J TAYLOR
PHYSICON INC ATTN: MARK CHRISTOPHER	TRW INC ATTN: M J TAYLOR ATTN: R VON HATTEN ATTN: TECH INFO CTR,DOC ACQ
PHYSICON INC ATTN: MARION ROSE	TRW SPACE & DEFENSE SECTOR ATTN: DR D R GIBSON
R & D ASSOCIATES ATTN: D CARLSON	TRW SPACE & DEFENSE SECTOR SPACE & ATTN: D M LAYTON
RAND CORP ATTN: C CRAIN	UNISYS CORPORATION-DEFENSE SYSTEMS ATTN: P MARROFFINO
RAND CORP ATTN: B BENNETT	UNITED INTERNATIONAL ENGINEERING, INC ATTN: ED DONOVAN
RAYTHEON CO ATTN: JOSEPH SURRO	VISIDYNE, INC ATTN: C H HUMPHREY
RESEARCH TRIANGLE INSTITUTE ATTN: M SIMONS	FOREIGN
ROCKWELL INTERNATIONAL CORP ATTN: T YATES	FOA 2 ATTN: B SJOHOLM
ROCKWELL INTERNATIONAL CORP ATTN: YIN-BUTE YU	FOA 3 ATTN: T KARLSSON
S-CUBED ATTN: J M WILKENFELD	